Shaikh-Omar, Osama (2007) Recombinant expression of the Aryl Hydrocarbon Receptor. PhD thesis, University of Nottingham.

In the name of God

the most merciful the most gracious

RECOMBINANT EXPRESSION OF THE ARYL HYDROCARBON RECEPTOR

Osama Abdulrahman Shaikh-Omar, MPhil

Thesis submitted to the University of Nottingham

for the degree of Doctor of Philosophy

August 2007

ABSTRACT

Aryl Hydrocarbon Receptor (AhR) mediates drug and toxin action. The AhR proteins have been characterised in several mammalian species, and are soluble proteins found in various tissues. The AhR is normally found in the cytoplasm in a complex with 90 KDa heat shock protein (hsp90) and cellular chaperones such as ARA9 (AIP or XAP2) and p23. However, there has not been a systematic analysis of the proteins which chaperone the AhR ligand-binding domain (LBD). This work investigates the interaction between ligands and the AhR, the protein composition of the AhR ligand-binding domain (LBD) complex, by establishing translation of AhR LBD in reticulocyte lysate, which contains molecular chaperones such as hsp90, and p23 that stabilise the ligand binding form of AhR.

EGFP (Enhanced Green Fluorescent Protein) has been coupled to the mouse AhR $^{b-1}$ LBD, to enable fluorescence analytical techniques of ligand-binding to the AhR. The Glutathione S-Transferase (GST) affinity tag was fused to EGFP (GST-EGFP), then fused to AhR.LBD with one or two EGFP (GST-EGFP-AhR.LBD and GST-EGFP-AhR.LBD-EGFP) to enable rapid one-step purification of AhR fusion proteins, and associated chaperone proteins. Proteins were expressed in E.*coli* (BL21(DE3)plysS). The GST protein is soluble, and not fluorescent, and GST-EGFP and GST-EGFP-AhR.LBD-EGFP was soluble and fluoresecent. The GST-EGFP-AhR.LBD was an insoluble

fluorescent protein. Thus, the AhR proteins were purified from bacteria to test the specificity of the "pulldown" system under conditions which do not yield functional Ah Receptor.

The tagged AhR constructs were translated with [^{35}S]-methionine in reticulocyte lysate and translation products were ~36, 66, 84 and 109 kDa on SDS-PAGE. Reticulocyte lysate programmed with GST-EGFP-AhR.LBD and GST-EGFP-AhR.LBD-EGFP both bound ~800 d.p.m 2,3,7,8-[1,6-^{3}H]tetrachlorodibenzo-*p*-dioxin (a ligand for the AhR), while lysate programmed with GST.EGFP showed binding of ~15 d.p.m, indistinguishable from unprogrammed lysate. The AhR proteins were purified from reticulocyte lysate and subsequent pulldown experiments will enable proteomic analysis of the proteins associated with the AhR LBD.

ACKNOWLEDGMENTS

I would firstly like to thank my Almighty 'ALLAH' for giving me the courage and will to finish this work successfully.

This job would not have been possible without the assistance, support, and patience of many people. A thesis may have only one person's name on the cover, but it is the product of a various people.

I would like to thank my supervisors Dr Jeffery R. Fry and Dr David R. Bell for all their invaluable guidance, time and patience throughout my PhD. It has been a joy to work with you and I have learned a great deal from you both.

I wish to thank Mr Declan for his tireless help in order all stuffs through the practical work. Thanks to all members in Bell's lab including, Dr Jody Winter, Dr Tao Jiang, Dr Minqi Fan, Dr Mohammed Al-Anizy, Dr. Abdullah Al-khulaifi and Miss Rana Bazzi. My thanks must also go to the many people at the Biopolymer Synthesis and Analysis Unit particularly Jones and Kevin for allowing me to work in their laboratory. Thanks to the numerous others whom I can not mention by name.

My deep thank and appreciations to my parent (Abdulrahman and Aisha), my brothers, my sisters and my all family in-low for their prayers, encouragements and supports.

I am pleased to thank my wife, Hanady, and my children: Wesam, Bassam and Retaj for their help, patience, understanding and love during my study.

Last but not least, I have to extend my gratitude to Umm Al-Qura University for funding all my study, especially Professor A. Sultan. I should also thanks many people in the Saudi Cultural Bureau specially Mr. A. Al-Nasir, the cultural attaché, and my supervisor there Mr. Latef Ali.

This thesis is dedicated to:

My Mum,

Dad, &

Wife

LIST OF CONTENTS

LIST OF FIGURES

LIST OF TABLES

ABBREVIATIONS

A	Adenine
AA	Amino acid
AhR	Aryl hydrocarbon receptor
AIP	AhR interaction protein
Amp	Ampicillin
ARNT	Aryl hydrocarbon receptor nuclear translocator
ATP	Adenosine triphosphate
bHLH	Basic helix-loop-helix
bp	Base pair
BSA	Bovine serum albumin
C	Cytosine
CPR	Cytochrome P450 reductase
CYP	Cytochrome P450
cDNA	Complementary DNA
dATP	Deoxy adenosine triphosphate
DMSO	Dimethyl sulphoxide
DNA	Deoxyribonucleic acid
dNTP	Deoxy nucleotide triphosphate
DTT	Dithiothreitol
dTTP	Deoxy thymidine triphosphate
EDTA	Ethylenediaminetetraacetic acid

EGFP	Enhanced green fluorescent protein
ER	Oestrogen receptor
FCS	Fluorescence correlation spectroscopy
FRET	Fluorescence resonance energy transfer
G	Guanine
GR	Glucocorticoid receptor
GST	Glutathione S-transferase
HAH	Halogenated aromatic hydrocarbons
Hsp90	Heat shock protein 90
IPTG	Isopropyl-β-D-thiogalactopyranoside
Kb	Kilo base
kDa	Kilo dalton
LB	Luria-bertani broth
LBD	Ligand binding domain
Leu	Leuthine
Met	Methionine
mRNA	Messenger RNA
OD	Optical density
P23	An Hsp90-associated protein
P450	Cytochrome P450
PAH	Polycyclic aromatic hydrocarbon
PAGE	Polyacrylamide gel electrophoresis
PBS	Phosphate buffered saline
PCBs	Polychlorinated biophenyls

PCR	Polymerase chain reaction
PMSF	Phenylmethylsulfonylfluoride
PR	Progesterone receptor
RNA	Ribonucleic acid
SDS	Sodium dodecyl sulphate
T	Thymine
TAE	Tris-glacial acetic acid-EDTA buffer
TBE	Tris-boric acid-EDTA buffer
TBS	Tris-buffered saline
TCAOB	Tetrachloroazoxybenzene
TCDD	2,3,7,8-tetrachlorodibenzo-p-dioxin
TEMED	N, N, N, N,-tetramethylethylenediamine
Tris	Tris(hydroxymethyl)methylamine
TTBS	Tween-TBS
UHP	Ultra high purity
UV	Ultra violet
XAP2	The hepatitis virus X protein-associated protein 2

CHAPTER 1

1. INTRODUCTION

1.1 Overview

Humans and animals are exposed daily to environmental contaminants and carcinogens such as pesticides, herbicides or dioxins in the atmosphere, water, or nutrients. Some of these compounds are possibly toxic, and must be controlled or eliminated. The main purpose of the metabolism of these toxic chemicals in the body is to make these chemicals more water soluble and more easily excreted in urine or bile (Gram 1994). Some toxic chemicals, including some lipophilic drugs, are impervious to metabolism and will accumulate in cells and tissues (Gibson and Skett 1994). Once they accumulate in cellular membranes they can cause cell damage or even death. It is assumed that these compounds singly or in combination may induce a variety of toxic effects and diseases in both human and animals (Poland and Knutson 1982). For example Immunosuppression, cleft palate, and tumour promotion in animals and chloracne, immunosuppression and possibly cancer and heart diseases in humans could be caused (Birnbaum 1994). Halogenated aromatic hydrocarbons (HAHs) such as 2,3,7,8-tetrachlorodibenzo-p-dioxin (TCDD or dioxin), polychlorinated biphenyls (PCBs), chlorinated dibenzofurans (CDFs)

and many other environmental contaminants exert their pharmacological and toxicological effects by the activation of a protein called Aryl hydrocarbon receptor (AhR) (Hahn 1998; Whitlock *et al.* 1996). However, protective mechanisms against these compounds initiate induction of Cytochrome P450 to enhance detoxification. Initially, it was observed that polycyclic aromatic hydrocarbons such as carcinogens 3- methylcholanthrene (3-MC) and benzo-a-pyrene are typical inducers of several P450 proteins particularly CYP1A1, CYP1A2 and CYP1B1 (Kimura *et al.* 1989). The environmental contaminant 2,3,7,8-tetrachlorodibenzo-p-dioxin (TCDD or dioxin) is a much more potent inducer than 3-MC (Poland and Knutson 1982). Later Poland and his workers showed the existence of a mouse liver protein termed Aryl hydrocarbon receptor (AhR), which bound TCDD (Poland *et al.* 1986).

1.2 Dioxins

1.2.1 What are Dioxins?

Dioxin is a general term that describes a group of chlorinated organic chemicals with related chemical structures. Some have detrimental properties, depending on the number and position of chlorine atoms in their chemical structure (Poland and Knutson 1982). One of the most harmful dioxins is 2,3,7,8-tetrachlorodibenzo-p-dioxin (TCDD). Some polychlorinated biphenyls (PCBs), which have similar properties, are considered "dioxin-like" (Safe 1986). Dioxins are a group of toxic persistent organic chemicals that stay in the

environment for a long time. Dioxins are not intentionally produced, but are released into the environment as an outcome of burning chlorine-based chemical compounds with hydrocarbons and as a by-product of other chemical processes (Hankinson 1995).

1.2.2 Chemical Structure of Dioxins

The chlorinated dibenzo-p-dioxins are a class of compounds that are called "dioxins". The dioxin nucleus consists of two oxygen atoms joining two benzene rings. Chlorine atoms can be attached to eight different places on the molecule of dioxin, numbered from one to eight (Tschirley 1986). The number and arrangement of the chlorine atoms results in a set of 75 various dioxin combinations of chlorine and hydrogen are possible and resulting dibenzo-p-dioxin derivatives are called congeners. Chlorine increases the stability of these compounds and chlorines in positions 2,3,7 and 8 are especially important because they increase the toxicity of the congeners. The physical, chemical and toxic properties of dioxins are determined by the number and position of the chlorine substituents (Walker 2001). TCDD, a one of the most toxic dioxins, contains four chlorine atoms attached at position 2, 3, 7 and 8 as shown below in Figure 1-1.

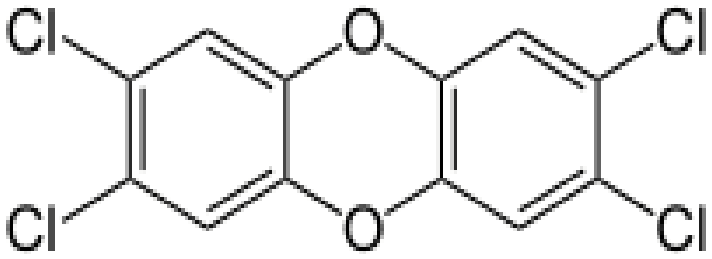

Figure 1-1 Chemical structure of the most toxic dioxin; 2,3,7,8 tetrachlorodibenzo-*p*-dioxin (TCDD). The TCDD molecule is composed of two benzene rings connected by a double oxygen bridge and contains four chlorine atoms two on each benzene ring at position of 2, 3, 7 and 8.

1.2.3 Sources and Fate of Dioxins in the Environment

Dioxins are known to occur naturally and are also produced by human activities. They are not synthesized for commercial purposes, but arise as trace contamination in the synthesis of several commercial products. They are formed by human activities from burning of many materials containing chlorine, such as *e.g.* plastics, wood treated with pentachlorophenol (PCP), pesticide manufacturing, other polychlorinated chemicals (PCBs), and even bleached pulp and paper. Cigarette smoke, home-heating systems, and exhaust from cars also carry tiny amounts of dioxins. They are also naturally produced from for example forest fires and volcanoes (Poland and Knutson 1982).

It has been established that extremely chlorinated isomers are often degraded more slowly than other isomers, suggesting that their accumulation is

attributable to their deficiency of degradation (Hutzinger *et al.* 1985). The processes that degrade dioxins are not understood, but density may be influenced by microbial degradation and volatilization (Vanden Heuvel and Lucier 1993). Transport of particulate bound dioxins in the soil occurs mainly by wind corrosion, although it may occur in cases of flooding and dredging. Leaching is not a potential culprit due to the hydrophobic nature of dioxins (half life is greater than 10 years in soil) and their low water solubility (Tschirley 1986). Dioxins enter the food chain when animals consume contaminated plants (Poland and Knutson 1982). They are fat-soluble accumulating in the fat and in the liver of humans and animals. This can increase their impact on humans and may cause a variety of health problems such as lymphomas, lung and breast cancers (Holloway 1994; Warner and McArthur 2001). Children are passed substantial body burdens by their mothers, although breast feeding increases the child's body burden. Breast fed children normally have considerably higher dioxin body burdens than non breast fed children until they reach 10 years old (Peterson *et al.* 1993).

1.2.4 Toxicity of Dioxins and AhR

2,3,7,8-Tetrachlorodibenzo-*p*-dioxin (TCDD) is the most toxic of the chlorinated congeners. Other dioxin congeners are given a toxicity valuation from 0 to 1, where TCDD is equivalent to 1. This toxicity valuation is called the Toxic Equivalence Factor (TEF). TEFs are consensus values because of the impracticality of testing all congeners of TCDD with a suite of toxicity tests

(Safe 1986). TEFs for mammalian species are the most relevant for human risk calculations (Vanden Berg *et al.* 2006).

Exposure to TCDD and its congeners produces a wide spectrum of toxic effects, e.g. cancer, teratogenesis, porphyria, dysplasia, thymic involution, etc. The toxic response depends on the dose of the toxin, the duration of exposure, species, strain, age, and sex of the animals (Poland and Knutson 1982). Differences in the accumulation of chemicals within different tissues of an animal can frequently give rise to differences in toxicity (Poland and Knutson 1982). However, the considerable difference in sensitivity to TCDD can not simply be explained by metabolic effects. It has been found that the whole body half life for TCDD only differs 3-fold between the guinea pig and hamster, while the differences in toxicity are 1000-fold (Schwetz *et al.* 1973).

Studies of the reproductive effects resulting from potential human exposure to TCDD are inconclusive. Data on male workers who applied agricultural sprays of 2,4,5-Trichlorophenoxyacetic acid (2,4,5-T) or who produced TCDD-contaminated materials are consistent with the animal data which indicate no reproductive effects in males from TCDD exposure (Smith *et al.* 1981; Townsend *et al.* 1982). TCDD is not genotoxic because TCDD does not covalently bind DNA, RNA or protein (Poland and Glover 1979), but it is a very strong tumour promoter (Pitot *et al.* 1980).

Dioxins are absorbed primarily through dietary consumption of fat, as this is where they accumulate in animals and humans. In humans, the extremely chlorinated dioxins are stored in fatty tissues and are neither promptly metabolized nor excreted. In humans, the estimated elimination half-life for highly clorinated dioxins (4-8 chlorine atoms) in adults is roughly 7.8 years (Geyer *et al.* 2002). It is thought that dioxins with few chlorines, which thus contain hydrogen atoms on adjacent pairs of carbons, can more readily be oxidized by cytochrome P450. The oxidized dioxins are therefore more readily excreted rather than stored for long periods (Poland and Knutson 1982). One feature of TCDD toxicity is that the majority of the toxic effects of dioxins are not observed until weeks following the exposure. It is possible that the adverse effects are the result of gene expression in target cells, which may account for the delayed toxic responses (Denison *et al.* 2002). In addition to acute toxicity, TCDD has capacity to cause cancer by acting as a tumour promoter. TCDD promotes the growth and transformation of already initiated cancer cells (Pitot *et al.* 1980).

The responses to TCDD are mediated by the binding of TCDD to a cytosolic receptor called Aryl hydrocarbon receptor (AhR). The modification in transcription of various genes (CYP1A1, CYP1A2 and epidermal growth factor receptor) by TCDD is believed to be an important step in the carcinogenic process and is correlated with changes in carcinogenic risk (Lucier 1993). In addition to mediating the responses to dioxins, AhR may also be involved in

cellular differentiation and may activate pathways important for cellular growth thus increasing the danger of tumours (Pitot *et al.* 1980).

1.3 Aryl hydrocarbon Receptor (AhR)

The aryl hydrocarbon receptor (AhR, Ah receptor or dioxin receptor) mediates most of the diverse biochemical, biological, and toxicological effects of TCDD and related proteins (Landers and Bunce 1991; Poland and Knutson 1982). The AhR is a protein within the cell that binds to aryl hydrocarbons forming a complex that moves into the nucleus of the cell. In the nucleus, this complex controls the onset of a series of biotransformation processes for the excretion of hydrocarbon compounds. AhR binds with halogenated aromatic hydrocarbons, including dioxins and polychlorinated biphenyls (PCBs), which can induce changes in gene expression, affecting cell growth, form and function. This is the reason why these chemicals can be carcinogenic or teratogenic (Poland and Knutson 1982). The following sections will discuss current understanding of the Ah receptor.

1.3.1 Identification of Ah Receptor

The responses of dioxin, related halogenated hydrocarbons compounds and polycyclic aromatic hydrocarbons were not the result of a direct reaction of the toxin. The Ah receptor is a basic helix-loop-helix protein (see below) that mediates the toxic effects of the TCDD (Poland and Knutson 1982). Various

environmental pollutants, agricultural chemicals, and drugs are known to act as ligands for the AhR. Polyhalogenated aromatic hydrocarbons such as TCDD and coplanar polychlorinated biphenyls, polycyclic aromatic hydrocarbons for instance 3-MC are representative powerful ligands (Bergander *et al.* 2003; Mimura and Fujii-Kuriyama 2005). Overall, analyses indicate that the AhR is a protein present in all living vertebrate groups, thus helping the study of dioxin toxicity and AhR role (Hahn *et al.* 1997). Cytosolic AhR has high affinity for non-halogenated polycyclic aromatic hydrocarbons (PAHs). The AhR was discovered using the potent P450 inducer dioxin, a chemical that enhanced the metabolism of PAHs (Poland and Knutson 1982).

1.3.2 Expression of Ah Receptor

The Aryl hydrocarbon receptor is a soluble intracellular protein present in most organs and cells that shows high affinity specific binding to certain planar aromatic compounds, such as polycyclic aromatic compounds (e.g., 3-MC) and halogenated aromatic compounds (e.g., TCDD). AhR was found in the cytosolic fractions of rat liver, lung, thymus, and kidney with much lower concentrations in testis, brain, and skeletal muscles (Carlstedt-Duke *et al.* 1979). Northern blotting analysis has been used to examine expression of human AhR in placenta, lung, heart, pancreas, and liver at high levels, while brain, kidney, and skeletal muscles show less expression (Dolwick *et al.* 1993b). Also, although a high affinity binding species was detected in two species of insects *Drosophila melanogaster* and the bollworm *Heliothis Zea*

(Bigelow *et al.* 1985), this finding has not been repeated. Dioxins are high affinity ligands for mammalian AhR, but no dioxin-binding proteins have so far been identified in invertebrates (Hahn 2002).

The AhR is found in various invertebrate species. Interestingly, recent studies establish that *Drosophila* AhR and *Caenorhabditis elegans* AhR (AhR-1) have no activity to bind foreign or endogenous chemicals as ligands. Although the protein has no ligand-binding activity, these AhRs heterodimerize with Arnt, binding to DNA with sequence the same as XRE, and activating transcription (Emmons *et al.* 1999; Powell-Coffman *et al.* 1998).

1.3.3 Molecular Structure of the Ah receptor

The AhR protein contains several domains critical for function and is classified as a member of the basic helix-loop-helix/Per-Arnt-Sim (bHLH/PAS) family of transcription factors (Fukunaga *et al.* 1995; Burbach *et al.* 1992). A basic-helix-loop-helix (bHLH) is a protein structural motif that characterizes a family of transcription factors. Its motif structure is characterized by two α helices joined by a loop (Lodish *et al.* 2004). One helix is typically smaller and due to the flexibility of the loop, allows dimerization by folding and packing against another helix. The larger helix typically contains the DNA binding regions (Chaudhary *et al.* 1999). The bHLH motif is located in the N-terminal of the protein. The basic-region is involved in the binding of the transcription factor

to DNA and the helix-loop-helix region can facilitate protein-protein interactions (Lodish *et al.* 2004) (Figure 1-2).

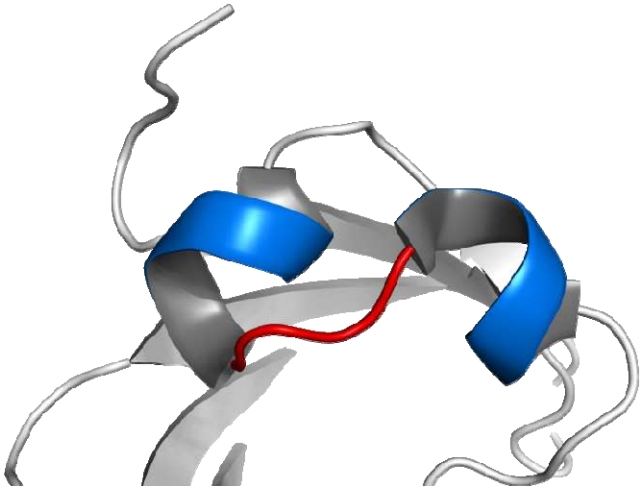

Figure 1-2 Basic helix-loop-helix (bHLH) structural motif of the AhR protein. Two α helices (blue) connected by a loop (red). This diagram has been taken form Wikimedia Commons.

The PAS represents the first letters of the three members of the family: the *Drosophila* Period clock protein (PER) (Crews *et al.* 1988), the vertebrate Aryl hydrocarbon receptor nuclear translocator (ARNT) (Hoffman *et al.* 1991), and *Drosophila* Single-minded protein (SIM) (Crews *et al.* 1988). These three proteins play an important role in the regulation of circadian rhythms, activation of the xenobiotic response, and fate determination, respectively (Korkalainen *et al.* 2004). The PAS domain of the AhR is the ligand binding domain (LBD), which contains two imperfect sequence repeats of about 50 amino acids (PAS-A and PAS-B) and is considered to act as an interactive surface for heterodimer or homodimer formation such as AhR and ARNT

complex. The PAS domain has recently been found in a wide variety of proteins such as AhR, ARNT, SIM and hypoxia-inducible factor (HIF-1α) (Gu *et al.* 2000 and Gorvo *et al.* 2007). The PAS-B domain of the AhR has the function of binding xenobiotic ligands (Dolwick *et al.* 1993a). The ligand binding domain of AhR is located in the sequence of amino acids 230–431 overlapping in part with the PAS-B region, and also with the binding site for Hsp90, which keeps AhR structurally competent to bind a ligand (Coumailleau *et al.* 1995). The AhR protein has a single transcriptional activation domain (TAD) in its COOH-terminus (C-terminus) (Figure 1-3). This TAD in the AhR contains glutamine and hydrophobic residues and acidic amino acids (Jain *et al.* 1994). Finally, a Q-rich domain is located in the C-terminal region of the AhR protein that involves in co-activator recruitment and transactivation (Kumar *et al.* 2001).

The AhR proteins have been characterised in several mammalian species, and are soluble proteins found in various tissues (Bayney *et al.* 1989; Gonzalez and Fernandez-Salguero 1998). There are some substantial variations in the structure of the AhR among species and among strains within species (Poland *et al.* 1987). The human and mouse AhRs show 100% amino acid identity in their NH_2-terminus (N-terinus), 97% in the HLH, and 87% in the PAS domain, whereas the C-terminus of these three proteins have 60% identity between human and mouse, 61% between human and rat, and 79% between rat and mouse (Schmidt and Bradfield 1996). The molecular size of AhR also shows a variation between species. It is 95 kDa in mouse, 101 kDa in chicken, 103 kDa

in guinea pig, 104 kDa in rabbit, 106 kDa in rat, 106 kDa in human, 113 kDa in monkey and 124 kDa in hamster (Poland and Glover 1987).

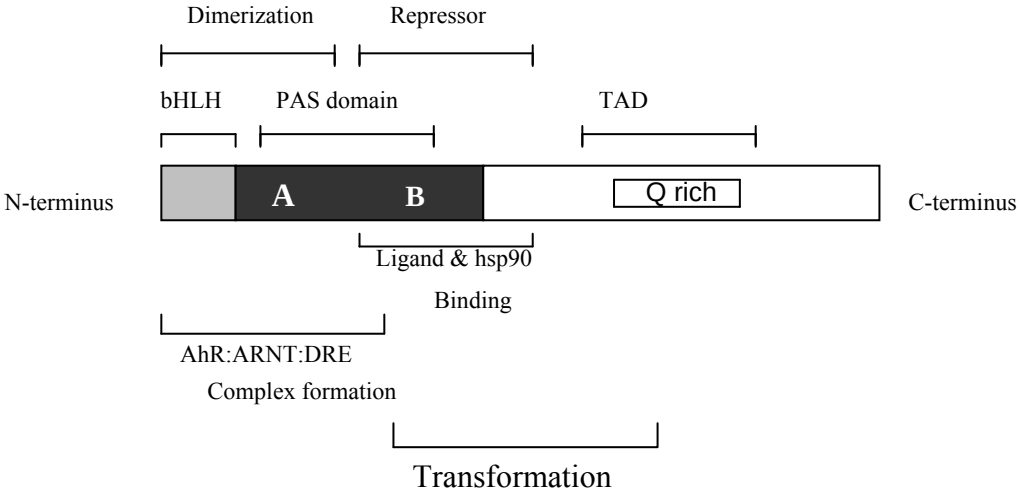

Figure 1-3 Schematic representation of functional domain of AhR. The grey area represents the bHLH region, the black area is the PAS domain and the region marked TAD indicates the transactivation domain. The region marked Dimerization represents bHLH and PAS sequences required for AhR-ARNT dimerization and also for DNA binding. The region marked Repressor indicates the area of Hsp90 interaction, the region marked PAS domain indicates the ligand-binding. This diagram was modified from (Schmidt and Bradfield 1996).

1.3.4 Mechanism of Action of Ah Receptor

AhR is a member of the basic helix-loop-helix/PAS family (Gu *et al.* 2000). In the presence of a ligand, AhR and its dimerization partner, the aryl hydrocarbon receptor nuclear translocator (ARNT) protein, form a heterodimeric transcription factor that binds dioxin responsive elements (DREs) on DNA. The AhR/ Arnt protein complex influences the expression of

a diverse set of genes that are involved in toxicity and other regulatory responses (Hankinson 1995).

Drug metabolising enzymes CYP1A1 and CYP1B1 are regulated through the ligand-activated AhR. These enzymes function to metabolise and excrete incoming xenobiotics (Shimada *et al.* 1996). Moreover, these enzymes play a central role in the activation of a variety of environmental carcinogens and mutagens such as TCDD (Tatemichi *et al.* 1999). Thus, induction of Cytochrome P450 enzymes has been used as a model system to understand the mechanism of action of AhR ligands.

Unliganded AhR resides in the cytoplasm, where it interacts with hsp90 and the X-associated protein 2 (XAP-2) that is part of a protein chaperone system involved in steroid-inducible and TCDD inducible signalling (Ma and Whitlock 1997; Pratt and Toft 1997). The protein-protein interaction occurs in the region of the PAS B domain of AhR. Following ligand binding the AhR undergoes a conformational change and translocates to the nucleus. Once nuclear translocation has occurred, hsp90 is released from the AhR, either at the translocation phase or after dimerisation with another bHLH partner, such as aryl hydrocarbon nuclear translocator (ARNT). This heterodimeric AhR/ARNT complex binds to its specific DNA recognition site, the dioxin responsive elements (DREs) located upstream of the CYP1A1 and CYP1B1 genes and promotes their transcription (Schmidt and Bradfield 1996) (Figure 1-4). These CYP enzymes are involved in the metabolism of a range of

xenobiotics. Indeed these enzymes play a central role in the activation of a variety of environmental carcinogens and mutagens (Marcus 1990).

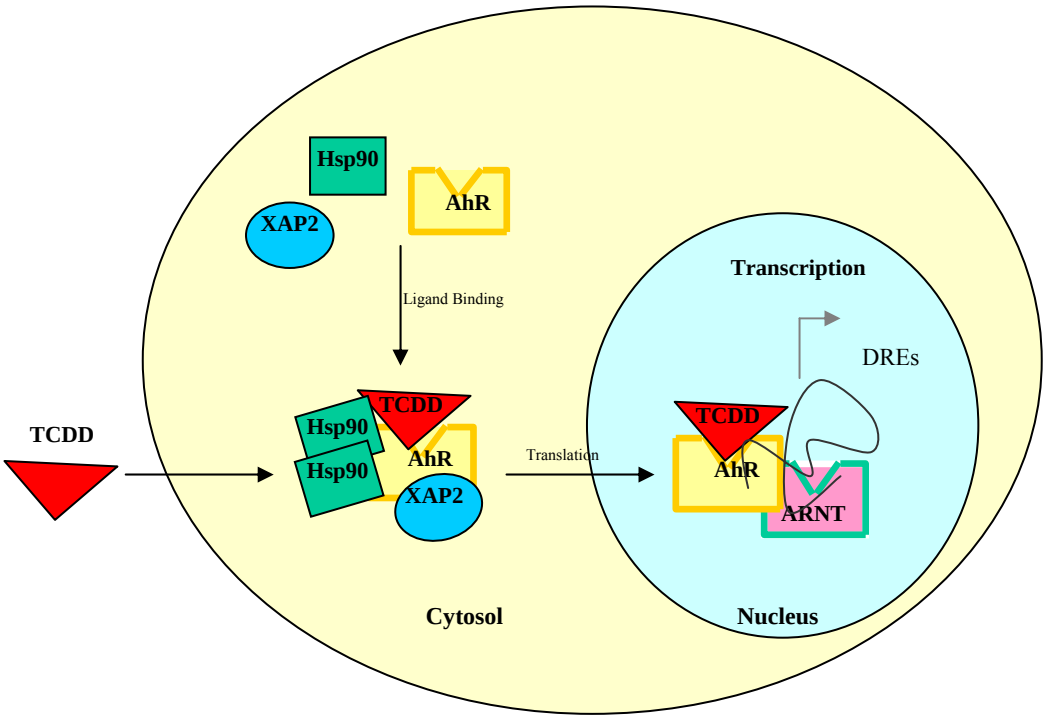

Figure 1-4 The mechanism of action of Aryl hydrocarbon receptor (AhR). The AhR is found in the cytoplasm bound to hsp90 and XAP2 chaperones. Upon binding dioxin (TCDD) the AhR enters the nucleus and exchanges its chaperones for ARNT. Then AhR-ARNT complex binds to the TCDD responsive elements (DREs) resulting in transactivation of the target genes. This diagram has been adapted from (Gu *et al.* 2000).

In general, activation of the AhR signalling pathway comprises several stages starting with translocation following ligand binding, then binding with nuclear factors, transactivation of gene transcription and degradation (Rowlands and

Gustafsson 1997). However, the biochemical and molecular mechanism by which the AhR signalling pathway is activated is yet to be demonstrated.

1.4 Molecular Chaperones and AhR

Protein folding, activation, and degradation in the cell require the action of a diverse group of factors known as molecular chaperones. Molecular chaperones are found in every organism and in most subcellular compartments. There are many different families of chaperones; each family acts to aid protein folding in a different way. In bacteria like *E. coli*, many of these proteins are highly expressed under conditions of high stress, for example, when placed in high temperatures. Some of the AhR bound proteins have been identified whereas others are still unknown. The unliganded AhR is found in a complex with other proteins including the 90-kDa heat shock protein (Hsp90) (Perdew and Poland 1988), a 23-kDa co-chaperone protein (p23) (Kazlauskas *et al.* 1999) and a 37-kDa X-associated protein (XAP-2) also known as ARA-9 or AIP (Bell and Poland 2000; Ma and Whitlock 1997). Some of these molecular chaperones are described in more detail below.

1.4.1 Heat Shock Proteins (Hsp)

Heat shock proteins which have been classified by molecular weight size in kilodaltons (kDa) of family members, are Hsp100, Hsp90, Hsp70, Hsp60, Hsp40, and the small Hsp family (typically 20 to 25 kDa). The function of

Hsps was unidentified, but previous studies have defined that major Hsps are central components of the molecular chaperone/protein folding machinery (Gerner and Schneider 1975). Hsp70, Hsp40, and Hsp60 family members play significant roles in nascent chain folding (Hartl 1996). Hsp70 members are also major components in membrane translocation processes. The small Hsps have important functions in disaggregation or degradation of misfolded complexes (Gething 1997), but it is not yet clear how important they are for nascent chain folding. Hsp90 may also have a role in nascent chain folding, but it is most notable for its numerous associations with important regulatory proteins (Pratt and Toft 1997). Hsp100 family members play an important role in thermotolerance in yeast (Lindquist and Kim 1996). The exact function of each of the families and its individual members is being actively investigated in many laboratories.

1.4.1.1 Heat Shock Protein 90 (Hsp90)

The Heat shock protein 90 (Hsp90) is one of the most abundant molecular chaperones, representing up to 2% of total cellular protein (Lai 1984; Richter and Buchner 2001). It has a direct role in the regulation of intracellular signalling pathways in unstressed cells (Pratt *et al.* 2004). Most studies on Hsp90 have focused on its role in maintaining soluble receptors in a conformation that is capable of ligand binding (Buchner 1999; Pratt and Toft 1997). Hsp90 protein is necessary for eukaryotic viability, and acts as a classic molecular chaperone by preventing aggregation and maintaining the

indigenous conformation of proteins in cells under various stress conditions (Richter and Buchner 2001). Hsp90 is required both for maintaining the dioxin receptor in a non-DNA binding and a ligand binding conformation (Pongratz *et al.* 1992). The role of Hsp90 is assisted and regulated by a number of accessory proteins acting as chaperones and co-chaperones (Pratt and Toft 2003). For example, Hsp70 and Hsp40 chaperones and the co-chaperones Hip and Hop (Hsp organization protein), p23, AHA1 and immunophilins (Sullivan *et al.* 1997). Previous experiments suggest that Hsp90 also plays a role in establishing the specific conformation of the p53 tumour suppressor protein (Blagosklonny *et al.* 1996). Hsp90 may be important for proper folding of AhR.LBD and for the regulation of the nuclear localization of the AhR (Whitelaw *et al.* 1995). Some proteins including steroid hormone receptors, AhR, serine, threonine, and tyrosine kinases, and telomerase are known to require Hsp90 in order to function (Richter and Buchner 2001). The steroid hormone receptors are among the best-characterized Hsp90 client proteins and have served as useful model proteins for studying the Hsp90 chaperone complex. In addition to Hsp90, several cofactor proteins are needed for the proper regulation of steroid hormone receptor signalling pathways. Before ligand interaction, AhR exists in a complex with Hsp90 proteins and co-chaperones. The helix-loop-helix and the PAS-B domains of AhR are directly linked with Hsp90, and this interaction serves to regulate AhR function (Perdew and Bradfield 1996). It was once thought that Hsp might be just a type of stabilizer for the AhR, which had to be removed before interaction with dioxin. Recently, it appears that Hsp90 may serve both to repress the

fundamental ability of the receptor to bind to DNA, and to act as a molecular chaperone which maintains the AhR protein in an optimal configuration for ligand binding. It has been suggested that upon ligand binding by the Hsp90/AhR complex, there is a further association with another heat shock protein molecule, Hsp50 (Nebert *et al.* 1993). Neither Hsp90 nor Hsp50 is part of the nuclear complex. AhR signalling was used as a reporter of Hsp90 chaperone function under various conditions in cells (Cox and Miller 2003). The relationship of AhR with a dimeric form of Hsp90 is a requirement for the receptor to acquire its ligand-binding activity (Ingemar 1963).

1.4.2 Hsp90-associated Protein (p23)

The p23 protein is an abundant Hsp90-associated protein, was first identified in association with steroid receptors (Smith *et al.* 1990) and was later shown to be a major component of Hsp90 complexes (Johnson and Toft 1994). It is thought that p23 interacts with target polypeptides that are indirectly associated via Hsp90. However, *in vitro* folding assays have shown that p23 itself can act as a molecular chaperone that binds independently to proteins and prevents them from aggregating (Bose 1996). There are three p23 proteins, yeast p23 (sba1p) (Fang *et al.* 1998) and the two human p23 proteins (p23 and tsp23). Sba1p was indistinguishable from human p23 in assays of seven intracellular receptor activities in both animal cells and in yeast; in contrast, certain effects of tsp23 were specific to that homolog (Freeman *et al.* 2000).

Maturation of AhR to a functional state is mediated through a procedure that is thought to effect the p23 co-chaperone (Kazlauskas *et al.* 2001) and an immunophilin protein called the hepatitis B virus protein X associated protein 2 (Xap2) (Meyer and Perdew 1999) by two mechanisms. First, in the absence of ligand, the Hsp90/AhR complex was associated with the XAP2 to mediate cytoplasmic retention of the AhR. Second, upon exposure to ligand, the p23-associated hsp90 complex mediates interaction of the AhR with subsequent nuclear translocation of the AhR (Kazlauskas *et al.* 1999). The p23 protein associates with the N-terminal nucleotide-binding site of Hsp90. The interaction of p23 with Hsp90 is dependent upon the presence of ATP (Chadli 2000). Previous studies demonstrated that p23 was needed for efficient AhR signalling (Cox and Miller 2002). It seems likely that p23 is involved in the regulation and stabilization of the ligand binding conformation of steroid receptors. Hsp90 may keep the receptor in a mature conformation. The steps leading to the maturation of the Hsp90/AhR complex involve several other factors, including a 23 kDa protein, p23 co-chaperone (Freeman *et al.* 2000; Pratt and Toft 1997).

1.4.3 X Protein-associated Protein (XAP2)

The hepatitis virus X protein-associated protein 2 (XAP2), also known as ARA9 (AhR-associated protein 9) (Carver and Bradfield 1997) or AIP (AhR interacting protein) (Ma and Whitlock 1997a), was initially discovered through

its ability to interact with the X protein of hepatitis B virus (Kuzhandaivelu *et al.* 1996). Ma and Whitlock used a yeast two-hybrid system to clone and identify the XAP2 protein (approximately 37-kDa) that interacts with the AhR (Ma and Whitlock 1997). This protein has been reported to increase the transcriptional action of the AhR, although the mechanism of activity has not been elucidated (Freeman *et al.* 2000). XAP2 interacts with AhR through the PAS-B domain and reduces receptor degradation, influences nuclear translocation, and enhances signalling of AhR. Two proteins (Cpr7 and Cns1) from *S. cerevisiae* that display sequence similarity to XAP2 have also been shown to enhance AhR signalling (Miller 2002). XAP2 is expressed in all tissues that have been examined, and is predominantly found in cytoplasm (Carver *et al.* 1998; Ma and Whitlock 1997). In mammalian cells and yeast, XAP2 has been found to associate with Hsp90. Some unliganded cellular receptors such as the glucocorticoid receptor (GR) have been demonstrated to exist in multiprotein complexes containing an Hsp90 dimer and other proteins. Chemical cross-linking studies of the untransformed GR were used to demonstrate that it was composed of Hsp90 and a polypeptide of 50 to 55 kDa (Bresnick *et al.* 1990; Rexin *et al.* 1988). The 50 to 55-kDa protein was later demonstrated to be an FK506-binding protein, now referred to as the immunophilin FKBP52 (also known as Hsp56, p59, and FKBP59) (Tai *et al.* 1992). CyP40 is a immunophilin present as one of several components of mature unactivated complexes of the glucocorticoid and progesterone receptors (Owens-Grillo *et al.* 1995). Following binding of ligand to the untransformed GR, the GR is then converted to a DNA binding form which binds to specific

glucocorticoid responsive elements (GREs) sequences in target gene promoters (Brian *et al*. 1998). CyP40, FKBP51 and FKBP52 belong to a distinct class of proteins which display an N-terminal immunophilin-like domain with overlapping regions for immunosuppressant drug interaction and isomerase activity, together with a conserved C-terminal tetratricopeptide repeat (TPR) domain proposed to mediate protein-protein interaction (Ratajczak *et al.* 1993; Nair *et al.* 1997). In vitro folding assays have shown that CyP40 and FKBP52 can function as molecular chaperones, similar to Hsp90 and Hsp70, by holding substrate proteins in a partially folded conformation (Freeman *et al.* 1996; Bose *et al.* 1996). Biochemical studies show that tetratricopeptide repeat TPR regions of FKBP59 are required for binding to Hsp90 (Radanyi *et al.* 1994). More studies have proposed that FKBP59 or CyP-40 interacts with TPR in the glucocorticoid receptor·Hsp90 complex (Owens-Grillo *et al.* 1996). Also, previous studies state that immunophilin FK506-binding protein (FKBP) 52 (FKBP52) do not interact directly with the AhR and were not detected in AhR complexes along with hsp90 by immunoblot or silver stain analysis (Chen and Perdew 1994; Meyer and Perdew 1999; Prokipcak *et al.* 1989). The ATP-bound conformation of Hsp90 is necessary for p23 binding (Sullivan *et al.* 1997). Likewise in rabbit reticulocyte lysate, XAP2 interaction with the AhR complex is favoured by the presence of ATP (Bell and Poland 2000).

Two functional roles of the XAP2 have been established. Firstly, XAP2 enhances the transcriptional action of the AhR. This has subsequently been shown to be a result of increased AhR stability (LaPres *et al.* 2000). Secondly,

XAP2 is capable of modulating the subcellular localization of the AhR. The endogenous AhR was found to localize to both cytoplasm and nucleus, but when XAP2 was overexpressed in COS-1 cells the AhR was redistributed to the cytoplasm (LaPres *et al.* 2000; Ma and Whitlock 1997; Meyer *et al.* 2000). This redistribution of the AhR to the cytoplasm is blocked by antibiotic (*e.g.* geldanamycin) (Kazlauskas *et al.* 2000).

1.4.4 Other Associated Chaperones

The Hsp90 chaperone activity has been shown to require other proteins, such as Hip, Hop, and Hsp70 (Bukau and Horwich 1998). Protein kinases, such as Raf-1 and pp60v-src, have also been demonstrated to require Hsp90 for appropriate function (Buchner 1999). Steroid hormone receptors (SHRs) that expect hsp90 for formation into mature complexes include the progesterone (PR), oestrogen (ER), and glucocorticoid receptors (GR) (Pratt and Toft 1997). Dittmar and Pratt described that rabbit reticulocyte lysate which is used for cell-free protein translation contains a multiprotein chaperone system that assembles steroid receptors into a complex with Hsp90. The hormone binding domain (HBD) of glucocorticoid receptor must be bound to Hsp90 to have a steroid binding conformation (Dittmar *et al.* 1996). Freeman also reported that Hsp90-associated co-chaperone p23 has been shown to modulate the function of a number of steroid hormone receptors such as the glucocorticoid and progesterone receptors show increased stability and higher capacity to bind hormone when complexes are associated with p23 (Freeman *et al.* 2000).

Steroid receptors initially associate with Hsp70 and Hop chaperones (Murphy *et al.* 2003) where Hsp90 plays a crucial role as a central organizer assisted by Hsp40. Followed by early complex loaded with Hsp90 the intermediate complex (Hsp70- Hop- Hsp90) is formed. This three-protein complex is shown to translate the non-steroid binding into steroid binding (Dittmar *et al.* 1996). However, to generate the final activated complex, Hop and Hsp70 have to exchange with one of the immunophilin proteins and p23 to form a mature complex (Richter and Buchner 2001).

The glucocorticoid receptor (GR) localises in the cytosol complexed with a variety of proteins including Hsp90, Hsp70 and FKBP52 (FK506-binding protein 52) (Pratt *et al.* 2006). The endogenous glucocorticoid hormone diffuses through the cell membrane into the cytoplasm and binds to the GR leading to release of the heat shock proteins. The resulting activated form of GR has two principle mechanisms of action (Buckingham 2006; Hayashi *et al.* 2004). First, a direct mechanism of action called transactivation that involves homodimerization of the receptor, translocation into the nucleus, and binding to specific DNA responsive elements activating gene transcription. Second, transrepression, an indirect mechanism of action involving other transcription factors such as NF-kB or AP-1 and is capable of transactivating target genes in the absence of activated GR.

1.5 Protein Folding

Proteins are synthesized as sequences of linear amino acids (primary structure). Protein folding is the physical process by which protein molecules take on a three-dimensional shape known as a "fold" (Bruce *et al.* 2002). The tertiary structure is vital for the protein to function correctly (Jeremy *et al.* 2002). However, inactive proteins are produced when proteins do not fold correctly (misfold). It is believed that several diseases result from the aggregation of misfolded proteins.

Molecular chaperones have been defined as proteins that bind to and stabilize another protein by controlled binding and release, facilitating its correct fate in vivo: be it folding, transport to a particular subcellular compartment, or disposal by degradation (Hartl 1996). Chaperones do not determine the tertiary structure of the folding proteins, but assist them to discover their structure more efficiently. A few chaperones behave as true catalysts by increasing the rate of protein folding but the majority act by preventing incorrect interactions during protein-folding (Csermely *et al.* 1998). For example, Hsp90 can behave as a molecular chaperone to prevent the accumulation of unstable protein conformers. It may also be possible that Hsp90 has a stabilizing effect on the proteins that it associates with (Welch and Brown 1996). Moreover, Hsp90 has been shown to function under cell free conditions as a molecular chaperone that facilitates the folding of various proteins (Jakob and Buchner 1994).

1.6 Enhanced Green Fluorescent Protein (EGFP)

1.6.1 Green Fluorescent Protein (GFP)

Green Fluorescent Protein (GFP) is a naturally fluorescent gene product of the jellyfish *Aequorea aquorea*. In 1955, Davenport and Nicoll reported that the light producing cells of *Aequorea aquorea* fluoresced green when irritated with ultraviolet light (Davenport and Nicol 1955). Later, Shimomura and co-workers tried to isolate the protein, depending on this observation, but they described a protein from jellyfish that emitted blue light in the presence of Ca^{2+} ions (Shimomura *et al.* 1961). Then in 1991, Zimmer reviewed that Davenport and Nicol observed that a protein extract from the jellyfish produced green fluorescence (Davenport and Nicol 1955). The first measurements of the fluorescence spectrum of aequorin and the fluorescence spectrum of GFP were reported by Johnson in 1962. Wild-type GFP has two excitation peaks, a major one at 395 nm and a smaller one at 475 nm (blue) and its emission peak wavelength is at 509 nm (green) (Garret and Johnson 1962) (Figure 1-5). The protein responsible for the fluorescence is called green fluorescent protein (GFP). The GFP is a bioluminescent protein and is a 27 kDa protein of 238 amino acids in length that was originally isolated from jellyfish *Aequorea victoria*. It has been expressed in bacteria, yeast, plants, zebrafish, and in mammalian cells (Chalfie *et al.* 1994; Inouye and Tsuji 1994). GFP is used as a cell lineage tracer, reporter of gene expression and as a fusion tag to monitor

protein localization within living cells (Chalfie and Kain 1998). GFP can function as a protein tag as it tolerates N- and C-terminal fusion to a broad variety of proteins.

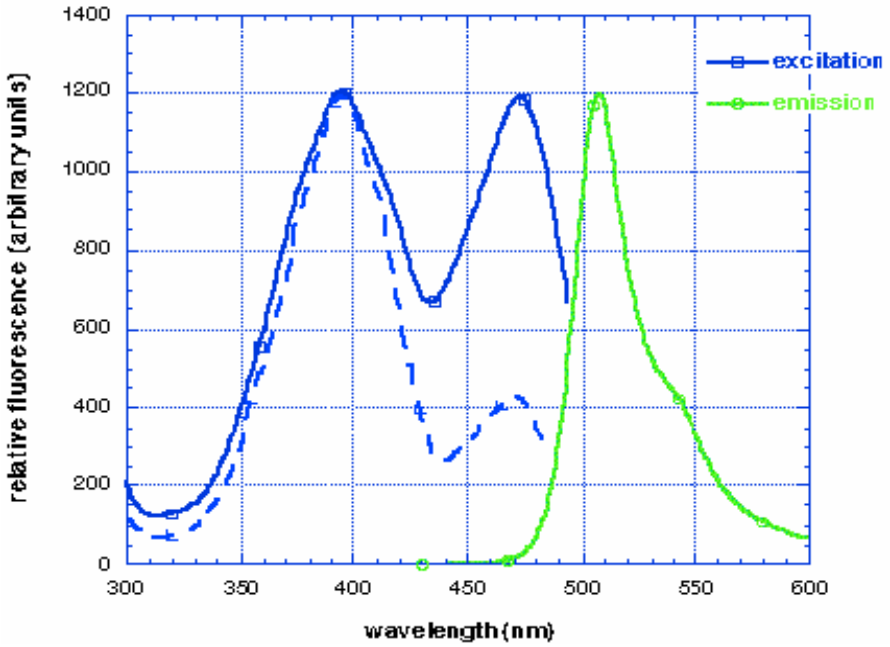

Figure 1-5 The excitation and emission spectra of *Aequorea aquorea* GFP. The GFP emits green light (absorbance maximum at 509 nm) when excited with blue or UV light (absorbance maximum at 395 nm and minimum at 475 nm). The picture has been taken from (Siemering *et al.* 1996).

Zhang and colleagues have constructed a GFP variant, which contains chromophore mutations that make the protein fluoresce 35– fold brighter than wild-type GFP, and is codon-optimized for higher expression in mammalian cells. These changes in the GFP coding sequence provide an enhanced GFP (EGFP) that is a powerful tool for the visualization of tagged proteins and transfected cells (Zhang *et al.* 1996) and is easily detected by fluorescence microscopy or flow cytometry in living cells. The GFP portion folds efficiently

and becomes fluorescent when GFP fusion protein is translated *in vitro* under standard conditions, (Kahn *et al.* 1997).

1.6.2 Crystal Structure of GFP

Although GFP was first crystallized in 1974 (Morise *et al.* 1974) and diffraction patterns reported in 1988 (Perozzo *et al.* 1988), the structure was first solved in 1996 independently by (Ormo *et al.* 1996). The structure of GFP is an 11 stranded β-barrel with an α-helix running up the axis of the cylinder (Figure 1-6). The chromophore in GFP, consisting of residues 65-67 (Ser, Tyr, and Gly), is attached to the α-helix and is almost completely buried in the centre of the cylinder, which has been called a β–can (Brejc *et al.* 1997; Palm *et al.* 1997). The proposed formation of the chromophore is illustrated in Figure 1-6.

Wavelength shifts of the absorbance of the chromophore happen with a change in protonation. The anionic form has an excitation maximum at 475 nm while the protonated or neutral forms have a maximum at 395 nm. The emission of the wild type protein has a maximum at 509 nm (Garret and Johnson 1962). Many mutations have been investigated as a way of changing the wavelengths of the chromophore, the folding properties, and the temperature sensitivity (Cody *et al.* 1993). Tsien classified GFP mutations into several classes according to the changes in the chromophore. With all of the mutations, GFP's intrinsic ability to fold decently has been established (Tsien and Prasher 1997).

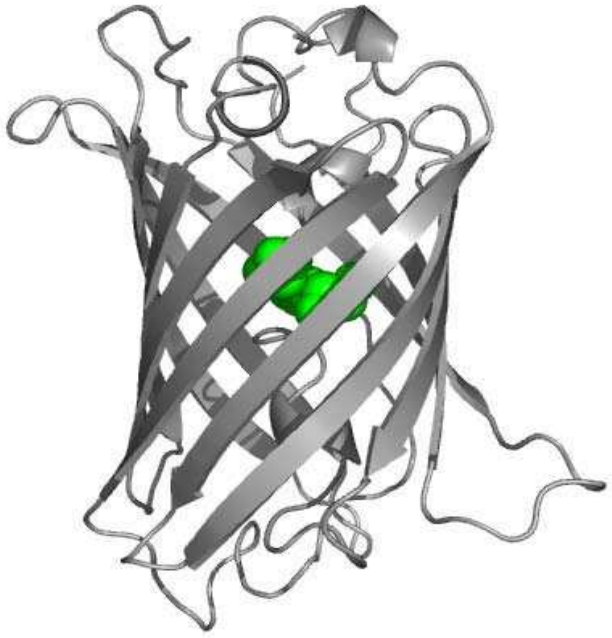

Figure 1-6 Three-dimensional structure of GFP, showing 11 β-strands forming a hollow cylinder through which is threaded a helix bearing the chromophore, shown in ball-and-stick representation.

1.7 Aims of the Thesis

Aryl hydrocarbon receptor (AhR) is a soluble intracellular protein that regulates induction of the cytochrome P450 enzymes CYP1A1, CYP1A2 & CYP1B1. The AhR also mediates toxic effects of halogenated aromatic hydrocarbons (HAHs) such as 2,3,7,8-tetrachlorodibenzo-p-dioxin (TCDD). There are several fusion proteins and domains that have been successfully expressed in *E. coli (*Dyson *et al.* 2004). For example glutathion-S-transferase (GST) (Smith and Johnson 1988), the maltose binding protein (MBP) (Bedouelle and Duplay 1988; di Guan *et al.* 1988), and the Z-domain from

protein A (Nilsson *et al.* 1987), which were developed as affinity fusion proteins, have been shown to increase solubility in some cases. Also previous studies show that the GFP was highly soluble when expressed in *E. coli* (Crameri *et al.* 1996; Waldo *et al.* 1999; Pedelacq *et al.* 2006). However, the AhR fails to yield functional ligand-binding protein when expressed in bacteria (Coumailleau *et al.* 1995, D R Bell, unpublished data). But functional AhR can be expressed in the rabbit reticulocyte lysate system (Dolwick *et al.* 1993a), which contains molecular chaperones such as hsp90, and p23 that are required for folding into the ligand binding form of AhR. However, there has not been a systematic analysis of the proteins which chaperone the AhR.LBD. This work aims to identify these proteins and thereby characterise the folding pathway that the AhR.LBD requires for functionality.

The overall goal of this study is to characterise the structure and function of the Ah receptor and its ligands. Therefore, the aims and objectives of this study were:

- To make an AhR construct that consisted of Glutathione S-transferase (GST), coupled to EGFP (enhanced green fluorescent protein) and the mouse AhR^{b-1} LBD to form GST-EGFP-AhR.LBD. To do that, this construct needed to be designed by Vector NTI 7 software and the construct was then made practically using cloning techniques.
- To express AhR LBD in bacteia (*e.g.* BL21(DE3)pLysS), which is the most easy and cheap system used to assay the products.

- To establish translation of AhR LBD in the rabbit reticulocyte lysate system in order to make protein.
- To consider whether AhR protein is functional when AhR binds to TCDD, e.g. by TCDD-binding assay.
- To purify the fusion proteins and any associated chaperone protein using GST affinity tags.
- To identify the AhR associated chaperones by MS-MS sequencing of the fragments.
- To characterise the folding pathway that the AhR.LBD requires for functionality.

CHAPTER 2

2. MATERIALS AND METHODS

2.1 Materials

2.1.1 Chemicals and Consumables

All reagents used were Analytical or Ultrapure grade. The chemicals used throughout the work such as Ammonium acetate, bovine serum albumin, phosphoric acid, TEMED, SDS, Tween 20, ethidium bromide, Bromophenol blue, DTT and PMSF were all obtained from Sigma. NaCl, NaOH, HCl, Phenol, methanol, glacial acetic acid and chloroform were purchased from Fisher Scientific UK Limited. Glycerol was provided from Courtin & Warner. EDTA, glucose, ethanol and ammonium sulphate were from BDH Laboratories Supplies. L-Methionine [^{35}S] (1175 C/mmol) was from MP Biomedicals. 2,3,7,8-Tetrachloro [1,6-^{3}H] dibenzo-p-dioxin (27.7 C/mmol) was from Eagle Picher Pharmaceutical Service, USA. IPTG and glycine were obtained from Melford. *Spodoptera frugiperda* (Sf9) cells were purchased from Invitrogen. Rat liver cytosol proteins were a kind gift from Miss Rana Bazzi in D.R. Bell's laboratory (Nottingham). QIAquick gel extraction kit, miniprep and maxiprep DNA purification kits were purchased from Qiagen Ltd. Bulk GST Purification

Module was from Pharmacia. MicroSpin GST purification Module was purchased from Amersham Biosciences Ltd. Amicon Ultra Centrifugal Filter Devices was provided from Millipore Corporation. μMACS Tag Isolation Kits were obtained from Mitenyi Biotec. S.Tag Rapid Assay kit and His-Bind Resin chromatography were purchased from Novagen. Hoechst 33258 dye was from NanoDrop Technologies.

Consumables such as universal and eppendrof tubes, tips and gloves were obtained from Sterilin, Pechiney Plastic Packaging, SARSTEDT and Ansell Limited. All the consumables, equipments and glassware were sterilised by autoclaving followed by overnight incubation in a hot air oven to ensure the elimination of any DNA or micro-organisms.

2.1.2 Enzymes and Antibodies

All enzymes were supplied with the appropriate reaction buffer. *BamHI, EcoRI, BstBI, Csp45* and *XbaI* were provided from Promega. *BglII, HindIII, SalI, SpeI, NheI, NotI,* RNase Inhibitor was from Amersham Biosciences. *T4* DNA ligase was purchased from New England BioLabs. Shrimp alkaline phosphatase was from USB Corporation. Lysozyme was from Sigma.

Ampicillin, chloramphenicol, kanamycin and tetracycline were all obtained from Sigma Chemical Co. Goat Anti-Rabbit IgG conjugated secondary antibodies were from Amersham Biosciences.

2.1.3 Oligonucleotide Primers Used

Oligonucleotides were synthesised by John Keyte of the Biopolymer Synthesis and Analysis Unit, School of Biomedical Sciences, University of Nottingham.

Primer's Name	Primer's Sequence (5` to 3`)	Primer's Orientation
T7 terminator	ACGATCAATAACGAGTCGCCACC	antisense
T7 promoter	TAATACGACTCACTATAGGGCGA	sense
Sp6	GTATTCTATAGTGTCACCTAAAT	antisense
oso1	CACTACCTGAGCACCCAGTCCGCCCTGAGC	sense
oso2	TCTACAAATGTGGTATGGCTGATTATGATC	antisense
oso3	CCGGTGATGACGACGACAAGAG	antisense
oso4	GATGGTGAGCACGGGCGAGGAGCTGTTCACC GGGG	sense
oso5	AAGGGAGAGAAAGGGCTGGAGATCTCGTAC AACACAG	antisense

Table 2-1 Oligonucleotide primers used for sequencing of the GST-constructs. The first five primers were used to identify sequence and orientation of the fusion inserts. The last two primers (oso3 and oso4) were used for PCR for GST-EGFP-AhR.LBD-EGFP construct. The *Eco*RI and *Bam*HI start codon appeared in underlined in the beginning of oso3 and sos4 primers. The table also shows the name and orientation of each primer.

2.1.4 Solutions, Buffers and Media

Tryptone, Agar and Yeast Extract were purchased from Difco Laboratories. Tris-base was provided from Gibco-BRL. Sterilization of all solutions buffers, media and ultrapure water (Select PURITE from PURITE Ltd) was achieved by autoclaving (20 minutes, 120 °C and 1 bar). Thermolabile solutions were sterilised by filtration through 0.2 µm filters.

2.1.5 Structure of pFAST.BAC HTc-AhR LBD Vector

The vector pFAST.BAC was used for transposition of the AhR construct into bacmid DNA. A fragment of the b-1 allele of the mouse AhR, containing residues 228-416, as described in Bell and Poland, 2000, was previously subcloned into the *BamHI* site of either pFAST.BAC HT b vector by Dr. D.R. Bell (Nottingham). This clone was used for subsequent subcloning. Figure 2-1 shows the structure of pFAST.BAC-AhR228 vector.

The presence of the AhR constructs in pFAST.BAC could be confirmed by restriction digest with *BamHI* as described in Section 2.2.2.5.

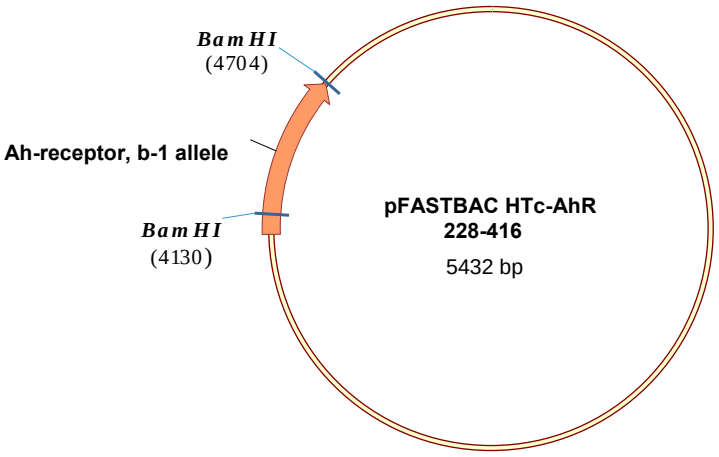

Figure 2-1 Diagram of pFASTBAC HTc-AhR 228-416 vector. Mouse Ah receptor b-1 allele was inserted into pFASTBAC HTc vector down stream of virus polyhedrin promoter. The red filled arrow shows the orientation of the AhR 228-416. The positions of *BamHI* site in pFASTBAC HTc and in AhR 228-416 were labelled. The fragment of digestion with *BamHI* for sense is 574bp.

2.1.6 Bacterial Strains and Cloning Vectors

Stratagene provided *E. coli* strains, JM109 cell and XL-2 Blue competent cells. Bacterial strains BL21(DE3) and BL21(DE3) plysS were purchased from Novagen or Promega. pEGFP-C2 vector was obtained from CLONTECH. pGEM5 vector was purchased from Promega. pET41b DNA vector was purchased from Novagen.

2.1.7 Image Processing Materials

Agarose, NuPAGE Bis-Tris gels with MES or MOPS buffer, Tricine gels and 5X LDS loading buffer were provided from Invitrogen. 30% acrylamide/bisarylamide was from Severn Biotech Ltd. Coomassie Brilliant Blue G was from Aldrich. Coomassie Brilliant Blue R-250 was obtained from ICN Flow. 3MM paper was obtained from Whatman. PVDF membrane was from Amersham. Marvel was from Premier International Foods (UK). X-ray film was manufactured by Fuji and obtained from Amersham. Developer and fixer replenisher were obtained from Ilford (Kodak GBX). 1, 4-Dioxane, SDS6H-1VL marker and molecular weight marker were from Sigma. 1Kb plus DNA ladder was obtained from Invitrogen. 1Kb DNA step ladder was from Promega.

Nonlinear regression (curve fit) for ligand binding and Sf9 cell growth were performed using GraphPad Prism version 4.00 (GraphPad Software, San Diego California USA) or SigmaPlot.

2.2 Methods

2.2.1 Cell Culture

All cell manipulations were performed under aseptic conditions in a class II Microbiological Safety Cabinet complying with B.S. 5726 (WALKER Safety Cabinets Ltd). All items used in the hood were either purchased in a sterile form or were sterilised by high pressure and temperature (autoclaving) before use. All consumables and glassware were sterilised by autoclaving followed by overnight incubation in a hot air oven. Before placing in the hood all items were sprayed with 70% ethanol.

2.2.1.1 Spodoptera Frugiperda (Sf9) Cell Line

Insect cells offer several advantages when compared to mammalian cells including lower media costs and production of high levels of recombinant proteins. Sf9 is a *Spodoptera frugiperda* cell line, and is probably the most common cell line used for baculovirus expression vector system (BEVS) applications. The Sf9 cell line was originally cloned in 1985 (Smith *et al.* 1985) from the parent cell line, IPLB-SF21 AE2, which was derived from ovarian tissue of the fall armyworm *Spodoptera frugiperd*a (Vaughn *et al.* 1977).

2.2.1.2 Cell Culture Procedure

Cells were grown at 27 ^{o}C in an incubator (SANYO INCUBATOR *CFC FREE*). Confluence of monolayer cells, estimated by light microscopy, was 3-4 days for Sf9 cells in 25 cm² flask. For harvesting, cells were washed twice with Sf-900 II Serum-Free medium (Life-Technologies) and dislodged from the surface using a solution containing 0.05 % (w/v) tyrpsin and 0.2 % (w/v) EDTA or using a sterile cell scraper. The cells were counted in a haemocytometer chamber (Weber Scientific International Ltd) before reseeding in a plastic flask at the appropriate density of 5-6 X 10^5 cells. A vital stain (0.4% trypan blue solution) was used to distinguish viable and nonviable (dead) cells. The haemocytometer and coverslip were thoroughly cleaned and wiped both with 70% alcohol before use. The coverslip was moistened and placed centrally over the counting area and across the grooves. An aliquot of the cell suspension was transferred into an eppendorf and diluted 1:1 in trypan blue (0.4% (w/v) Trypan blue in PBS). The mixed cell solution was added into the junction between chamber and the coverslip. The viable and nonviable cells in the same 1mm^2 area were counted under a light microscope at low magnitude. The number of viable cells/ml was calculated using the following equation:

$$\text{Viable cells/ml} = \frac{\text{total number of viable cells counted}}{\text{number of 1mm}^2\text{ areas counted}} \text{ X dilution factor X}10^4$$

When a new batch of cells was required, cell vials were removed from liquid nitrogen and thawed rapidly to 37 °C in a water bath under aseptic conditions. The cells were transferred to a sterile 25-cm^2 flask containing 5ml of normal media which is a Sf-900 II Serum-Free medium with 4.5gl^{-1} glucose supplemented with 6mM L-glutamine, 1% (w/v) non-essential amino acids, 10% (v/v) foetal calf serum and 60 μgml^{-1} gentamicin. . This suspension was centrifuged for 2 minutes at 5000 x g. The supernatant containing dimethyl sulphoxide, DMSO, (toxic material) was removed. The cells were re-suspended in 5ml normal media. The cells were then incubated at 27 ˚C for 2-3 hours to adhere to the surface of the plastic flask.

The medium was then removed and the cells were fed with fresh medium to reduce the DMSO concentration even further. The next morning the medium was replaced with fresh medium. Finally, the cells were placed in the incubator for growth.

2.2.1.3 Virus Plaque Assay

2.2.1.3.1 Overview

The plaque assay can be used to purify virus or to determine viral titres in plaque-forming units per ml, so that known amounts of virus can be used to infect the cells during subsequent experimental work. In this assay, monolayer

cells were infected with a low concentration of virus and only isolated cells were infected. Overlays of agarose keep the cells stable and limit the spread of the virus. When each infected cell produces virus and lyses, only the immediate surrounding cells become infected. Then areas of clearing are produced. These areas are called plaques, and each plaque represents a single infecting virus. Therefore, isolating individual plaques may purify clonal virus populations. The infectious potency of a stock of baculovirus can be determined by examining and counting plaque formations.

2.2.1.3.2 Virus Plaque Assay

A monolayer culture of Sf9 cells was prepared. After 48 hours a cell suspension of 5 to 6 X 10^5 density was made. 2 ml of this cell suspension were transferred to each well of a 6-well culture plate. After cell attachment to the culture plate, the medium was removed from the wells and replaced with 1 ml of virus dilutions (10^{-6}, 10^{-7} and 10^{-8}). The plate was then transferred to a rocking platform and slowly rocked for at least a few hours.

In order to prepare a plaquing overlay, 4% of autoclaved agarose (low gelling temperature) was mixed with medium (1:3) in a sterile hood. The media were removed from all wells and replaced with 2 ml of plaquing overlay mixture. The plate was then transferred to a humidified storage box and incubated for 4-5 days at 27 ˚C.

Plaques were stained by adding 1 ml neutral red/ PBS (1:19) solution to each well. The plate was incubated at 27 ˚C in the dark room for 2 hours. The solution was aspirated and the plate was inverted overnight at room temperature. The next day, plaques were counted and the titre was calculated. Baculovirus plaques were generated by the infection of Sf9 cells with individual baculovirus particles. Uninfected Sf9 cells surrounding the plaque were stained pink with neutral red.

2.2.2 General DNA Techniques

DNA cloning has four main stages: a method for generating DNA fragments, a reaction that joins these DNA fragments to a vector, introducing the recombinant DNA into a host cell where it can replicate and a method of selecting for a clone of recipient cells. In this study positive bands that identified in DNA gels were extracted and purified using a QIAquick gel extraction (Qiagen Ltd) kit following the manufacturers' instructions.

2.2.2.1 Alkaline Lysis (Crude Preparation)

Alkaline lysis is a method for isolating plasmid DNA. Bacterial colonies were inoculated in 5 ml LB broth containing an appropriate antibiotic and incubated with shaking overnight at 37 ºC. One ml of bacterial culture was transferred into a clean 1.5 ml eppendorf tube and centrifuged at 14000 x g for 1 minute in a bench top centrifuge. The supernatant was decanted and the cell pellet was

resuspended in 100 µl of solution I (50 mM glucose, 25 mM Tris-HCl pH 8, 10 mM EDTA and RNase A (100 µg/ml)). To this, 200 µl of solution II [200 mM NaOH, 1% SDS], was added to each eppendorf tube and the solutions were mixed by inversion 4-6 times. 150 µl of ice-cold solution III (5 M potassium acetate, 1.5% glacial acetic acid) was then added to each eppendorf and mixed immediately by inversion 4-6 times and then placed on ice for 5 minutes. The samples were then centrifuged at 14000 x g for 5 minutes at 4 ºC. The supernatant was transferred to a new eppendorf tube and extracted with an equal volume of phenol/chloroform and then centrifuged at 14000 x g for 2 minutes at 4 ºC. The aqueous layer was transferred to a new eppendorf and the DNA was precipitated by addition of 1/10 volume of 7.5 M ammonium acetate and 2 volumes of 100% ethanol. The sample was mixed gently and then incubated at -20 ºC for an hour. The tube was then centrifuged at 14000 x g for 20 minutes at 4 ºC. The supernatant was decanted and the pellet was washed with 70% ethanol and centrifuged at 14000 x g for 5 minutes at 4 ºC. The supernatant was removed and the pellet was allowed to air-dry for 5 minutes. The plasmid DNA pellet was then resuspended in 50 µl sterile UHP water and stored at -20 ºC.

2.2.2.2 Qiagen Miniprep of Plasmid DNA

Purified plasmid DNA can be obtained by using QIAprep Spin Miniprep kit (Qiagen). The procedure followed the manufacturer's instructions. 1 ml was taken from the 5 ml of overnight culture of *E. coli* in LB broth containing

appropriate selective antibiotics. This was then transferred to an eppendorf tube and spun down at 14,000 x g for 1 minute using a bench top centrifuge. The pellet was resuspended in 250 µl of Buffer P1 before 250 µl of Buffer P2 was added. The tube was then gently inverted 4-6 times. 350 µl of Buffer N3 was added into the tube and immediately mixed by inversion 4-6 times. The mixture was then centrifuged at 14,000 x g for 10 minutes. The supernatant was transferred to the QIAprep spin column. This column was centrifuged at 14,000 x g for 1 minute and the flow-through was discarded. The column was then washed by adding 0.75 ml of Buffer PE and centrifuged for 1 minute. The flow-through was discarded and the spin column was centrifuged for an additional 1 minute to remove any residual wash buffer. Then the QIAprep column was placed in a clean 1.5 ml microcentrifuge tube. To elute DNA, 50 µl of sterile UHP water was added to the centre of the column. Finally, to collect the plasmid DNA, the column was allowed to stand for 1 minute at room temperature before 1 minute of centrifugation.

2.2.2.3 Sequence of Plasmid DNA

In order to send a DNA sample for sequence analysis, the concentration of the plasmid DNA was measured using either the Hoechst dye assay and a CARY Eclipse Fluorescence spectrophotometer (VARIAN Australia PTY Ltd.) or determining the optical density of the DNA at 260 nm using a SUPER Aquarius (CE9500) Spectrophotometer. Qiagen purified DNA was sent to the Biopolymer Synthesis and Analysis Unit, School of Biomedical Sciences,

University of Nottingham. The sequencing reaction uses a Perkin Elmer ABI Prism 373A Fluorescent automated DNA sequencer and a method based on the Sanger Dideoxy Chain Termination Method (Sanger *et al.* 1977). Sequencing was performed using universal primers in both forward and reverse directions.

2.2.2.4 Qiagen Maxiprep of Plasmid DNA

Maxipreps of DNA were made to generate a large amount of purified plasmid or construct DNA that can be used in further manipulation experiments. A QIAGEN Plasmid Maxi Kit (Qiagen) was used to prepare large amounts of plasmid DNA. The technique is comparable to that used for minipreps of DNA described in section 2.2.2.2. The preparation is performed on a large scale, starting with 500 ml of culture media and yielding approximately 0.5 ml of DNA in sterile UHP water. The QIAGEN maxipreps were performed using the manufacturers' instructions.

2.2.2.5 Restriction Digest

Typically a restriction digest would take place in a reaction volume of 20 µl in an eppendorf tube. The optimal buffer for the restriction enzyme was chosen according to the manufacturer's manual. The restriction digest mixture contained 0.2-1 µg of DNA, 2 units of restriction enzyme, 2 µl of the appropriate 10 X restriction enzyme buffer and H_2O to a final volume of 20 µl. This reaction mixture was incubated at 37 °C for 1-2 hours to cut the vector or

plasmid. Then digestion products were analysed on a 0.8% agarose gel by electrophoresis (see below).

2.2.2.6 Agarose Gel Electrophoresis

DNA fragments were analysed by gel electrophoresis. 2.5 µl of 10 X loading buffer (0.25% Bromophenol blue, 50% glycerol, 0.25% xylene cyanol FF, prepared in 1 X TBE (0.045 M Tris-Borate, 0.001 M EDTA (pH 8.0)) was added to 20 µl of digestion reaction. DNA molecules were separated in a 0.8% agarose-TAE (0.04 M Tris-acetate, 0.001 M EDTA (pH 8.0)) containing 0.2-0.4 mg of ethidium bromide. The agarose mixture was warmed in a microwave until the agarose was molten, then poured into the appropriate gel casting mould containing a well forming comb and allowed to set at room temperature. After solidification the gel was placed in the electrophoresis tank and immersed in the 1 X TAE running buffer. The samples were then loaded into the wells formed by the comb and run by electrophoresis at 100 volts for about 60 minutes, using a POWER PAC 3000 machine from the Bio-Rad Laboratories.

The approximate size of the DNA products was estimated by comparison to DNA size markers, molecules of known size, which were electrophoresed alongside the samples. DNA bands were visualised by illumination with an UV trans-illuminator and photographed.

2.2.2.7 Phosphatase Treatment of DNA

In order to prevent linearised cloning vector from re-circularizing, shrimp alkaline phosphatase (SAP) was used to remove the 5'-terminal phosphate from double-stranded DNA. In an eppendorf tube, to the 50 µl of restriction digested DNA, 5 µl of 10 X shrimp alkaline phosphatase buffer (USB) (200 mM Tris-HCl (pH 8.0), 100 mM $MgCl_2$) and 1 µl of SAP enzyme (USB) were added. The reaction was incubated at 37 °C for 30 minutes and SAP enzyme was inactivated by heating at 65 °C for 15 minutes. The final solution could then be used for further manipulations such as ligation.

2.2.2.8 Ligation of DNA

DNA fragments were ligated into vectors (e.g. pGEM5 or pET41b) by the action of the enzyme *T4* DNA ligase. An optimal ratio of vector to insert DNA should be determined when performing ligation reaction. Therefore, the vector and insert DNA are in a 1;1, 1:3, 1;9 or etc. ratio. The reaction took place in a total of 10 µl volume in an eppendorf tube. In case of 1:1 ratio, 1 µl of vector DNA, 1 µl of insert DNA, 2 µl of T4 ligase buffer, 1 µl of *T4* ligase (1U/µl) and H_2O to a final volume of 10 µl. The tube was vortex mixed and then centrifuged briefly to keep the mixture at the bottom of the tube. The mixture was incubated overnight at 4 °C or for 2 hours at room temperature. The

solution was kept to be used for transformation of competent cells using electro-competent cells or calcium chloride-competent cells as required.

2.2.2.9 Transformation

2.2.2.9.1 Preparation of Calcium Chloride Competent Cells

A single colony of *E.coli* cells (*e.g.* JM109) from a freshly streaked LB agar plate was picked and inoculated into a 5 ml LB (Luria-Bertani) broth culture that contained the appropriate selective antibiotic (none for JM109). The culture was grown overnight in an incubator at 37 ºC with vigorous shaking (240 rpm). A 50 ml culture of LB broth with appropriate selective antibiotics was inoculated with the 5 ml of fresh overnight bacterial growth. The mixture was incubated on the shaker (240 rpm) for 2-3 hours at 37 ºC or until an OD 600 of 0.6 was reached. The culture was placed on ice for 15 minutes and then centrifuged at 4000 x g for 15 minutes at 4 ºC. The supernatant was discarded and the pellet resuspended in 50 ml of ice-cold sterile 0.1 M $CaCl_2$. Suspended cells were again centrifuged and resuspended 4 times as before. The cells were then pelleted once more, the supernatant discarded and the final pellet resuspended in 2 ml of sterile 0.1 M $CaCl_2$, 10% glycerol. The cells were placed in 200 µl aliquots and stored at -80 ºC.

2.2.2.9.2 Transformation of DNA into Calcium Chloride Competent Cells

To thaw the competent cells, an aliquot was incubated on ice for 20 minutes. Then about 1 µl of the ligation reaction was added to 100 µl of the competent cells (bacterial cells treated with calcium chloride to make them porous and able to take up DNA) and mixed thoroughly. The mixture was incubated on ice for 30 minutes. Following this, cells were treated to heat shock for 90 seconds at 42 ^{o}C and then returned immediately into ice for 2 minutes. In order to maximise the transformation efficiency, 1 ml of LB broth was added to the competent cells and they were incubated in a water bath at 37 ^{o}C for 45 minutes. 200 µl of the incubated competent cells were added to a previously prepared LB plate, which contained the appropriate selective antibiotics. This plate was incubated at 37 ^{o}C in an incubator overnight to allow for colony formation.

2.2.2.9.3 Preparation of Electro-competent Cells

A single colony of E.coli cells from a freshly streaked LB agar plate was picked and treated as in section 2.2.2.9.1, except that after the first centrifugation step the pelleted cells were resuspended in 50 ml of ice-cold sterile Ultra High Purity (UHP) water. Following the final centrifugation at 4000 x g for 15 minutes at 4 ºC the pellet was resuspended in 2 volumes of

sterile ice-cold water. The cells were then placed on ice until use for electrotransformation.

2.2.2.9.4 Transformation of DNA into Electro-competent Cells

This method of transforming is more efficient than that of chemical transformation but is very sensitive to high salt concentrations, which may affect the transformation process. An aliquot of competent cells was thawed and 1 µl of the ligation reaction was added to 70 µl of the competent cells and mixed thoroughly. The mixture of DNA and cells were placed in a 1 mm gap electroporation cuvette and electroporated with a voltage of 1.8 KV using an *E.Coli* Pulser electroporator (from Bio Rad Laboratories). The cells were immediately resuspended in 1 ml of LB broth and allowed to recover at 37 °C for 45 minutes. Then about 100 µl of the electroporated competent cells were (screened on) added to an LB plate, which contained the appropriate selective antibiotics. Selection of the transformed cells was obtained by growing the electroporated cells overnight at 37 ^{o}C.

2.2.2.10 Purification of DNA

2.2.2.10.1 Extraction of DNA from Gel

Sometimes DNA needed to be recovered from the agarose gel using QIAquick Gel Extraction Kit (Qiagen Ltd.). Instead of the UV trans-illuminator, a Dark

Reader (from Clare Chemical Research) was used to detect the band. This is because the Dark Reader uses visible light and causes less damage to the DNA than the UV trans-illuminator. The DNA band was then excised using a clean scalpel, placed in an eppendorf tube and weighed. This excised gel fragment was then treated with 3 volumes of buffer QG. The tube was incubated at 50 °C with mixing for 10 minutes or until the gel fragment was dissolved. Then 1 volume of isopropanol was added to the sample and mixed. To purify the DNA, the sample was applied to the QIAquick column and centrifuged for 1 minute at 14,000 x g. The flow-through was discarded and 0.75 ml of buffer PE (wash buffer) was added to the column and spun for 1 minute. The flow-through was discarded and the spin column was centrifuged for an additional 1 minute to remove any residual wash buffer. Then the QIAprep column was placed in a clean 1.5 ml eppendorf tube. To elute the DNA, 30 µl of sterile UHP water was added to the centre of the column. Finally, to collect the DNA, the column was allowed to stand for 1 minute at room temperature before 1 minute of centrifugation.

2.2.2.10.2 Phenol/Chloroform Extraction of DNA

Phenol/chloroform (1:1) was used to remove protein contamination from DNA solutions. One volume of phenol/chloroform mixture was added to the nucleic acid sample. The mixture was vortexed thoroughly into an emulsion for 1 minute and then centrifuged at 14000 x g for 5 minutes in a bench top centrifuge at 4 °C. Two separated layers (phenolic and aqueous) and an

interface were obtained. The aqueous layer contains the nucleic acids whereas the interface layer contains the contaminant proteins. The aqueous layer was taken carefully into a clean eppendorf tube.

2.2.2.10.3 Ethanol Precipitation of DNA

Ethanol precipitation was used to obtain clean DNA from a solution. Nucleic acids were precipitated by adding two volumes of 100% ice-cold ethanol and 1/10 volume of 7.5 M ammonium acetate or 3 M sodium acetate, pH 5.2. The solution was mixed and placed at –20 °C for an hour. The tube was then centrifuged at 14000 x g in a microfuge for 20 minutes at 4 °C. The supernatant was decanted and the pellets were washed with 2 volumes 70% ice-cold ethanol and centrifuged at 14000 x g for 5 minutes. The supernatant was discarded and the pellets were then air-dried for 5 minutes to remove any remaining ethanol. The pellets were dissolved in sterile UHP water.

2.2.2.11 Quantification of DNA

2.2.2.11.1 Spectrophotometric Measurement

To determine the amount of DNA in solutions, readings were taken at wavelengths of 260 and 280 nm. The ratio between the readings at 260 and 280nm provides an estimate of the purity of the nucleic acid. A pure preparation of DNA has an OD_{260}/ OD_{280} value of approximately 1.8.

A 5 µl aliquot of DNA solution was diluted in 1 ml of UHP water (1:200) and transferred into a crystal cuvette. The absorbance of this solution was measured at 260 nm in a spectrophotometer. A solution containing 50 µg of double-stranded DNA has an absorbance of 1 at 260 nm, which means A_{260}=1=50µg/ml of double-stranded DNA. The concentration of DNA = 50 x 200 x A_{260}

2.2.2.11.2 Hoeschst 33258 Dye Assay

The Hoechst 33258 dye assay is a fluorescent nucleic acid stain for quantitating double-stranded DNA (dsDNA). The assay is very sensitive and accurate with minimal consumption of sample. A further advantage is that the assay is not affected by proteins and other contaminants because the dye only gives a signal when bound to dsDNA.

The solutions for this assay were first prepared as follows:

10 X TNE Buffer

70 ml of distilled water, 20 ml 1M Tris Base, 10 ml 0.2M EDTA and 70 ml 5M NaCl were mixed the thoroughly on a stir plate and 1 M HCl was used to titrate the 10 X TNE buffer (pH of 7.4). The solution was transferred to a graduated cylinder and adjusted to a final volume of 200 ml using distilled water.

DNA stock solution (100 µg/ml) was prepared by diluting 10 µL of stock DNA preparation (10 mg/ml) with 990 µl of 1 X TNE solution to a final concentration of 100 µg/ml.

Hoechst dye stock (10 mg/ml) was diluted 50,000 fold in two stages to obtain a final concentration of 0.2 µg/ml:

The Hoechst stock (10 mg/ml) was diluted 100 fold by mixing 495 µl of 1 X TNE with 5 ul of the 10 mg/ml stock that was filtered with a 0.45 µm filter and stored at 4 ºC in the dark. Then the Hoechst dye was diluted 500 fold by adding 4.99 ml of 1X TNE to 10 µl of 0.1 mg/ml stock Hoechst dye that was prepared fresh before each assay as lower dye concentrations will aggregate over time.

Working Solution		Volume (µl) of 1X TNE	Final DNA concentration in Hoechst Dye assay
10mg/ml DNA Salmon stock (µl)	Distilled Water (µl)		
0	5	995	0 µg/ml
0.5	4.5	995	50 µg/ml
1	4	995	100 µg/ml
2	3	995	200 µg/ml
4	1	995	400 µg/ml
5	0	995	500 µg/ml

Table 2-2 Protocol for preparing Low-range standard curve.

After preparation of all the solutions above, a low range assay (50-1000 µg final DNA concentration) was chosen for the standard curve at excitation 350

nm and emission 450 nm. For running the standard curve, a Quartz cuvette was used and the fluorometer was zeroed at these conditions using distilled water as a blank. Briefly, 1 ml of the Hoechst reagent (1 mg/ml) was added to each standard curve sample containing DNA stock solution (10 mg/ml) and the unknown sample concentrate. The working assay solution was prepared fresh prior to each assay by adding 5 µl working solution and 5 µl of sample. The samples incubated in the dark for 5 minutes and the reading was then taken using the Fluorescence spectrophotometer. The concentration of DNA was determined using the standard curve.

2.2.2.12 Polymerase Chain Reaction (PCR)

The Polymerase Chain Reaction (PCR) is a popular technique for amplifying a specific region of DNA sequence. The PCR usually consists of a series of 20 to 35 cycles. The PCR is carried out in three steps (Figure 2-2), and requires several basic components include oligonucleotide primers, deoxyribonucleotides (dNTPs), $MgCl_2$ and Taq DNA polymerase.

The first step is DNA denaturation ; in this step the double stranded DNA molecules are denatured to form single stranded DNA, which acts as templates in the next step. The second step is annealing,that uses oligonucleotide primers which when attach by base-paring to a single stranded templates act as the start point for complementary strand synthesis in the DNA molecules. The last step

is extension that creates an additional copy of the DNA, thus doubling the number of copies of DNA each cycle (Mullis *et al.* 1986).

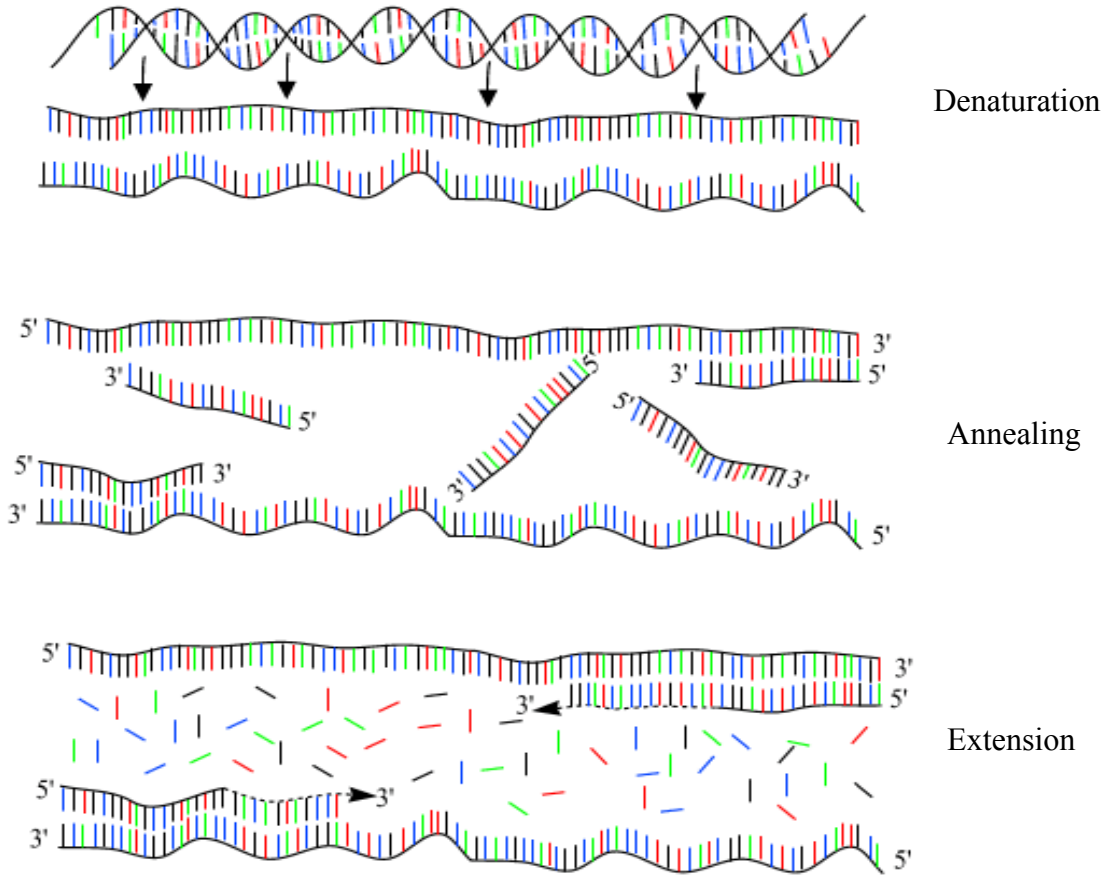

Figure 2-2 Schematic drawing of the PCR cycle. Each PCR cycle consists of three steps: Denaturing, Annealing and Extension. The two resulting DNA strands make up the template DNA for the next cycle. Therefore, doubling the amount of DNA duplicated for each new cycle.

2.2.3 Protein Methodologies

2.2.3.1 Expression of Proteins in BL21(DE3)PLysS *E.coli* Cells

A fresh colony was picked from a plate of BL21(DE3)plysS (Novagen) bacteria and inoculated in 50 ml of 1% glucose LB broth containing Kanamycin (30 mg/ml) and Chloramphenicol (34 mg/ml). The culture was incubated at 37 ºC with shaking (240 rpm) overnight. The incubated culture was diluted with 250 ml of 1% glucose LB broth containing the same antibiotics and incubated with shaking (240 rpm) for approximately 3 hours at 37 ºC until an OD 600 nm of 0.6 was reached. 3 ml of this culture was transferred into a clean universal tube and stored at -20 °C as a sample of un-induced bacteria. 300 µl of 1M IPTG was added to the remaining culture. The cultured cells were then divided into three; 100 ml were incubated at 37 °C with shaking (240 rpm) for 1 hour, 100 ml were incubated at 30 °C with shaking (240 rpm) for 3 hours and 100 ml were incubated at 25 °C with shaking (240 rpm) overnight. After induction, 1 ml of each the three induced cultures was transferred into a clean eppendorf tube and stored at -20 °C as samples of induced cells. The remainder of the cultures were then centrifuged at 4000 x g for 20 minutes at 4 °C. The pellets were each resuspended in 10 ml of 0.1M NaCl, 50 mM Tris pH 8 per gram of bacteria. Lysozyme was added to a concentration of 1 mg/ml and incubated for 1 hour at 4 °C. Also, 1 µl of 0.1 M PMSF (protease inhibitor) per 1 ml of the suspension or other inhibitors as

required were added. Then the cells were lysed by sonication for 8 bursts of 30 seconds and placed immediately on ice for 30 seconds. The sonicated cells were then centrifuged at 4000 x g for 30 minutes at 4 °C. The supernatant was decanted into a fresh tube and stored at –20 °C as induced total cell supernatant. The pellets were resuspended in 8 M urea, 100 mM Tris-HCl (pH 8) and stored at –20 °C until use. The suspension was centrifuged at 4000 x g for 20 minutes at 4 °C. The supernatant was decanted into a fresh tube, labelled as supernatant of insoluble proteins, and centrifuged twice at 4000 x g for 20 minutes in a JA2-21 rotor to remove any particulate material. The supernatant was then poured into a fresh tube and stored at –20 °C until use. The protein concentration was then determined as described in section (2.2.3.2). Proteins were then analysed on denaturing Polyacrylamide gel electrophoresis.

2.2.3.2 Bradford Protein Assay

To determine the concentration of protein samples the coomassie blue method of Bradford (Bradford and Williams 1976) was used. 5X Bradford dye was prepared by dissolving 100 mg of Serva blue G-250 in 50 ml 95% ethanol, and 100 ml of 85% phosphoric acid. The solution was completed by bringing the volume to 1 litre with deionised water. A standard curve was made using bovine serum albumin (BSA) between 0 and 100 µg, freshly prepared from a 1 µg/µl stock solution of BSA. For each sample, duplicate aliquots were diluted to a volume 20 µl. 1X Bradford dye reagent was prepared and filtered through 3MM paper (Whatman). 1 ml of 1X Bradford reagent was added to each

sample, and the samples were then vortexed and incubated at room temperature for 5 minutes. The absorbance of the samples was measured at 595 nm in polystyrene cuvettes. The protein sample was measured in the same way as the BSA standards. The concentration of protein was determined using the standard curve. Non-linear regression analysis in Prism 4.0 software was used to calculate the unknown sample concentrations.

2.2.3.3 *In Vitro* Transcription and Translation System

Rabbit reticulocyte lysate is a commonly used model system for studying the regulation of protein synthesis at the level of translation because of its lack of interfering transcriptional effects (Heminger *et al.* 1997).

The procedure was performed using the TNT Coupled Reticulocyte Lysate kit from Promega according to the manufacturer's instructions. 1 µg of GST (G), GST-EGFP (GG), GST-EGFP-AhR (GGA) and GST-EGFP-AhR-EGFP (GGAG) recombinant DNAs were used as templates for transcription with T7 polymerase followed by translation in the presence of L-[^{35}S] methionine. Firefly luciferase (approximately 61 kDa) was used as a positive control. An amino acid mixture minus methionine and also an amino acid mixture minus leucine (added after 60 minute incubation) were used in this reaction. After addition of all the components, the 25 µl reactions were gently mixed and incubated for 90 min at 30 °C. Proteins were resolved by SDS-PAGE and autoradiographed.

2.2.3.4 Autoradiography

Proteins were autoradiographed using Fujifilm Fluorescent Image Analyzer FL-A-2000 and storage phosphor imager. The phosphor Imager applies Imaging Plate (IP) technology as a radioactive energy sensor that comprised designed phosphors that trap and store the radiation energy. The stored energy is stable until scanned with a laser beam that releases the energy as luminescence.

2.2.3.5 SDS-Polyacrylamide Gel Electrophoresis (SDS-PAGE)

SDS-PAGE depends on the separation of proteins according to their molecular weight under denaturing conditions. A negative charge is produced by binding of sodium dodecyl sulphate (SDS) to the amino acid chain of the protein and consequently, the proteins are separated according to their molecular weight size.

SDS-PAGE was performed using an Xcell SureLock Mini-Cell Kit (Invitrogen) for commercial gels or a BIO-RAD Mini-PROTEAN II Cell electrophoresis kit for home made one. Resolving and stacking gel mixtures were premade separately by adding the following components and stored at 4 °C until required, with the exception of TEMED and 10% APS (to start the

polymerisation), which were added to the required gel volume on the day of use immediately prior to pouring into the gel plate (see table 2-3).

Components	Resolving (10 ml)			Stacking (10 ml)
	8% Gel	10% Gel	12% Gel	5%
H_2O	4.6	4.0	3.3	6.8
30% Acrylamide\ bisacrylamide (37.5:1)	2.7	3.2	4.0	1.7
1.5M Tris (pH 8.8)	2.5	2.5	2.5	1.25
10 % SDS	0.1	0.1	0.1	0.1
10 % ammonium persulfate (APS)	0.1	0.1	0.1	0.1
TEMED	0.006	0.004	0.004	0.01

Table 2-3 Composition of resolving and stacking gel mixtures (10 ml each). The following tables were used to calculate the volume of each component required to make a certain percentage and volume of gel.

The gels were left to polymerise for about an hour. The stacking gel component of the gel was made immediately prior to electrophoresis and was applied to the top of the resolving gel with a well comb which was inserted at the top of the gel plate. The gel was left to polymerize for 30 minutes. The completed gel running apparatus was then placed into its gel tank and its reservoirs were filled with the appropriate amounts of electrophoresis buffer (25 mM Tris-HCl (pH 8.3), 250 mM Glycine, 0.1% SDS (w/v)). Protein samples were prepared by mixing with 1 M DTT and 5X loading buffer (250 mM Tris-HCl (pH 6.8),

0.5 M DTT, 10% SDS (w/v), 0.5% Bromophenol Blue dye (w/v), 50% glycerol (v/v)) and denatured by heating for 10 minutes at 70 °C. Electrophoresis was carried out using 120 volts for 90 minutes until the bromophenol blue dye reached the bottom of the gel. The gel was fixed in 1% glycerol, 7% methanol and 7% acetic acid for 10 minutes to prevent the gel from cracking during drying and dried under vacuum. Dried gels could be used to obtain autoradiographs quantified in the phosphor imager. Alternatively, the gel was stained with Coomassie blue stain solution and dried.

2.2.3.6 Staining of SDS-PAGE

2.2.3.6.1 Coomassie Brillant Blue Staining

Coomassie blue R-250 was used for staining polyacrylamide agarose gels after electrophoresis to visualise the resolved protein bands. Before use, it was filtered through Whatman 3MM paper to remove any undissolved particles. After electrophoresis, the gel was immersed in coomassie blue staining solution (0.25 g coomassie R-250, 90% methanol: water (1:1 v/v), 10% glacial acetic acid) for at least one hour with gentle agitation. The staining solution was decanted and could be reused. The gel was washed with destain solution, which consisted of 30% methanol and 10% glacial acetic acid. The gel was destained with several changes of destaining solution until bands could be visualised clearly and dried.

2.2.3.6.2 Silver Staining

Silver Stain Plus (from Bio-Rad Laboratories) is a quick, simple system for detecting proteins or nucleic acids in polyacrylamide gel after electrophoresis. Proteins and nucleic acids can be visualized in 1 hour. Silver Stain Plus is 30-50 fold more sensitive than Coomassie Blue R-250 dye and will detect nanogram quantities of protein and DNA.

5 ml of silver complex solution, 5 ml reduction moderator solution and 5 ml image development reagent were added to 35 ml of deionised water. Immediately before use 50 ml of the development accelerator solution was added quickly. The staining solution was added to the staining vessel. The gel was placed in the staining vessel and stained with gentle agitation for approximately 20 minutes or until the desired staining intensity was reached. The gel was placed in 5% acetic acid to stop the staining reaction. The gel was rinsed in high purity water for 5 minutes and dried.

2.2.3.6.3 SYPRO Ruby Protein Gel Staining

SYPRO Ruby protein gel stain (Sigma) is a highly sensitive, ready-to-use fluorescent stain for the detection of proteins separated by polyacrylamide agarose gel electrophoresis. To visualise the resolved protein bands, SDS-PAGE gel was immersed in SYPRO Ruby stain and incubated for 4 hours to

overnight with gentle agitation. The gel was covered with aluminium foil before, during, and after staining steps to protect the stain from light. The staining solution was decanted and the gel was washed with destain solution, which consisted of 10% methanol and 7% glacial acetic acid. The gel was destained with 3-4 changes of destaining solution for 1 hour each with gentle agitation. The gel was placed directly on transilluminator for photographing using Versa Doc Imaging System Model 1000 from BIO-RAD.

2.2.3.7 Drying of SDS-PAGE

A gel dryer, such as Model 583 Gel Dryer, BIO-RAD was used in this method. Firstly, a sheet of filter paper was placed on the porous gel support plate. A sheet of dry cellophane was placed on the filter paper. The gel was placed onto Whatman 3MM filter paper and covered with a plastic wrap. Then a gel dryer was used to apply a vacuum with heat at 80 ºC for 90 minutes.

2.2.3.8 Determination of EGFP Fluorescence

50 µl of bacterial lysate or 5 µl of reticulocyte lysate was diluted in distilled water to a final volume of 500 µl. Then a fluorescence emission scan (without polarisation) was measured to determine the optimal wavelengths. The scan was done for G as a control with no EGFP and GG, GGA and GGAG that have EGFP which has emission intensity between 488 and 509 nm. Results were analysed by measuring the intensity of the emission for each expressed protein.

Fluorescence of total protein and fluorescence per unit of protein were calculated.

2.2.3.9 S.Tag Rapid Assay for *In Vitro* Synthesized Proteins

The S.Tag System is a protein tagging and detection system based on the interaction of the S.Tag peptide with ribonuclease S-protein. This specific binding is of high affinity and allows convenient detection and purification of any protein fused with the S.Tag sequence (Kim and Raines 1993).

For each set of samples, a blank without added target protein and the S.Tag Standard included in the kit were run in parallel. 10 µl of S.Tag Grade S-protein, 40 µl of 10 X S.Tag assay buffer and 2 µl of sample lysate were added to H_2O to a final volume of 400 µl. This reaction mixture was incubated at 37 °C for exact 5 minutes. The reaction was stopped by adding 100 µl of cold 25% TCA and then vortexed and placed on ice for exact 5 minutes. The tubes were centrifuged at 14,000 x g for 10 minutes. The absorbance of the supernatants at 280 nm was measured. The amount of S.Tag protein in the sample was calculated using the following equation:

Tube 3 A_{280} / 2 µl × 0.1 pmol S.Tag Standard / Tube 2 A_{280} = pmol/µl.

Tube 2: contains S.Tag standard translation reaction.

Tube 3: contains a sample lysate.

2.2.3.10 GST Purification

The glutathione S-transferase (GST) gene fusion system is a system for the expression, purification and detection of fusion proteins produced in *E.coli*. Fusion proteins are purified from bacteria lysates by affinity chromatography using Glutathione Sepharose 4B contained in GST Purification Modules. First, specific filters called 30 kDa Aminco Ultra-4 centrifugal filter devices which allow glutathione that has low molecular weight to pass through and retain larger molecular weight proteins, was used.

2.2.3.10.1 Filtration with a 30 kDa Aminco Ultra-4 Filter Spin Column

200 µg of bacterial extract fractions or 10 µl of rabbit reticulocyte lysate reaction were diluted with 500 µl of mixed buffer (2 mM ATP, 50 mM KCl, 10 mM Tris (pH 7.5), 5 mM $MgCl_2$ and 10 mM sodium molybdate (pH 7.5)). The mixture was applied into the 30 kDa Aminco Ultra-4 filter spin column and spun at 4000 x g for approximately 25 minutes or until 100 µl of filtered solution remains in the Aminco Ultra-4 filter spin column. Then the pass through solution was discarded and 400 µl of mixed buffer were added and centrifuged as before. The filtration step was repeated three times before adding the final 100 µl of filtered solution to 50 µl of a 50% slurry of glutathione beads for subsequent purification.

2.2.3.10.2 Bulk GST Purification Module

The lysed bacteria were thawed slowly on ice. 50 µl of a 50% slurry (for each 1.33 ml of original slurry add 1 ml of 1 X PBS) of glutathione Sepharose 4B beads (Pharmacia) were added to 200 µg of bacterial lysate and mixed gently for 10 minutes at room temperature. The mixture was washed three times with 1 ml ice-cold 1 X PBS buffer then vortexed briefly and centrifuged at 500 x g for 30 sec at 4 °C to remove unwanted bacterial proteins. Then fusion proteins were eluted with 50 µl elution buffer which contained Reduced Glutathione (10 mM GSH and 50 mM Tris) by centrifugation for 5 minutes to sediment the beads and then the supernatant was transferred to a clean tube. Finally, the proteins were run on gel and the gel was stained with coomassie blue stain.

2.2.3.10.3 MicroSpin GST Purification Module

200 µg of bacterial lysate was added to a glutathione sepharose 4B micro-spin column and mixed gently for 10 minutes at room temperature. The column was washed three times with 600 µl ice-cold 1X PBS buffer and centrifuged at 3000 x g for 1 minute at 4 °C to wash the matrix. Then 100 µl of reduced glutathione elution buffer was added and the elution solution was collected in a clean tube by spinning at 3000 x g for 1 minute at 4 °C.

2.2.3.10.4 His.Bind Resin Chromatography

Affinity chromatography is a method of separating biochemical mixtures, based on a specific interaction such as that between antigen and antibody, enzyme and substrate, or receptor and ligand. His-Bind Resin is used for rapid one-step purification of proteins containing a His-Tag sequence by metal chelation chromatography. The His-Tag sequence binds to Ni^{2+} cations, which are immobilized on the His-Bind resin. After unbound proteins are washed away, the target protein is recovered by elution with imidazole.

100 µl of resin slurry was added to a 1.5 ml microcentrifuge tube and centrifuged at 500 × g to remove the excessive Ni^{2+}. The resin was charged and equilibrated by the following sequence of washes. For each wash step appropriate buffer was added, the tube inverted several times to mixed and centrifuged for 1 minute at 500 × g. The resin was washed two times with two volumes sterile deionized water, three times with two volumes of 1 X charge buffer and two times with two volumes of 1 X binding buffer. Next, the lysate was added to the microcentrifuge tube containing the prepared resin. The mixture was mixed gently by inversion several times and incubated for 5 minutes on ice. After centrifuge for 1 minute at 500 × g, the supernatant was discarded. Then resin was washed three times with three volumes 1 X binding buffer followed by two times with three volumes 1 X wash buffer. Finally, the bound protein was eluted with 1 X elute buffer.

2.2.3.10.5 µMACS Epitope GST Protein Isolation Kits

The procedure followed the manufacturer's instructions. 50 µl Anti-GST MicroBeads was added to the lysate to magnetically label the epitope-tagged target protein. The mixture was mixed well and incubated for 30 minutes on ice. After the µMACS column was placed in magnetic field of the µMACS Separator, 200 µl of Lysis Buffer was applied on the µ column. The incubated mixture of cell lysate and MicroBeads was run through the µMACS column. The µMACS column was washed four times with 200 µl wash buffer-1 followed by 100 µl wash buffer-2. Then 20 µl of pre-heated 95 °C hot elution buffer was applied to the µMACS column and incubated for 5 minutes at room temperature. Finally, immunoprecipitated proteins were collected by applying 50 µl of pre-heated 95 °C hot elution buffer to the µMACS column. The eluted proteins were analyzed by SDS-PAGE.

2.2.3.11 Immunoblotting

Western blotting is a method, which transfers the proteins from the gel to an immobilizing membrane using an electric field. Antibodies can detect specific immobilised proteins on PVDF membrane and therefore enables further characterization.

2.2.3.11.1 Western Blotting

10-15 μg of protein samples were resolved by SDS-PAGE gel as described in section 2.2.3.5 and then transferred onto Polyvinylidene Difluoride (PVDF) membrane (MILLIPORE Immobilon Transfer Membrane). The gel was transferred onto two pieces of 3MM Whatman blotting paper. Then 7x10 cm PVDF membranes were pre-wetted by immersing in 100% methanol for 5 minutes and then wetted with 1X transfer buffer (25 mM Tris-HCl, 192 mM glycine, 20% methanol (v/v), 0.1% SDS w/v) for 10 minutes. A piece of PVDF membrane was then placed carefully on the top of the gel. Another two Whatman papers were placed on the membrane to sandwich the gel and the membrane in an electroblotting cassette. Any air bubbles between layers were removed using gentle pressure. The cassette was closed and placed into the transfer tank, which was filled with 1 X transfer buffer, and the transfer was performed at 90 volts for 1 hour.

When transfer was completed, the PVDF membrane was blocked in blocking solution (10% marvel (w/v)) non-fat dried milk in TBS (20 mM Tris base, pH 7.5, 500 mM NaCl) for 1 hour with gentle agitation. After three 5 minutes washes with TTBS (TBS and 0.1% Tween-20), the blots were incubated with 40 ml of marvel-TTBS solution containing a mouse AhR primary antibody which was first incubated for 30 minutes at 4 °C 1:1 with a crude *Escherichia coli* extract to block non-specific protein binding at a dilution 1:1000 for one

hour with agitation. The blot was washed 5 times for 5 minutes with 1X TTBS solution. The blot was then incubated in 40 ml of marvel-TTBS solution containing 5 µl of Goat Anti-Rabbit IgG (H+L)-HRP Conjugate (BioRad) secondary antibody (to find locations where the primary antibody bound) at 1:10000 for one hour with agitation. The blot was then washed 5 times for 5 minutes with 1x TTBS solutions and developed with ECL Western blotting detection reagent (Amersham Biosciences). The mixture of detection reagent 1 and detection reagent 2 (1:1 v/v) was added to the top of the membrane for 1 minute at room temperature. Excess reagent was drained off. The membrane was wrapped in cling film. The blot was placed in the film cassette. A sheet of Hyperfilm ECL (Amersham Biosciences) was placed on top of the membrane in the dark room. The film was exposed for different lengths of time (0.5, 1.5, 5, and 15 minutes) and then the film was developed by 1X developer solution (Kodak GBX) for few seconds until bands appeared. The film was washed in water for 2-3 minutes and fixed in 1X fixer solution (Kodak GBX) until the film became clear.

2.2.3.12 [^{3}H]-TCDD Ligand Binding Assay

The functionality of AhR LBD can be determined and quantified by using an *in vitro* radioligand-binding assay. Since AhR is sensitive to temperature, the following procedures were carried out on ice or at 4 ˚C.

2.2.3.12.1 Setting up the Binding Assay Reaction

Ligand binding assays were made up to a final protein concentration of 5 mg/ml with BSA where appropriate, in 1.5 ml of ice-cold lysis buffer (MENG buffer (25 mM MOPS, pH 7.5, 0.02% (v/v) sodium azide, 1 mM EDTA and 10% (v/v) glycerol). Also, 7.5 µl of 200 nM [^{3}H] TCDD was added to 1.5 ml reaction to get a final concentration of 1 nM. The experiment was been carried out using a positive control, rat liver cytosolic (RLC) proteins that were prepared in D.R. Bell's laboratory (Nottingham).

Two groups of samples (total and non-specific) were dispensed in triplicate in aliquots of 200 µl. To each of the total binding tube that contains 1 nM [^{3}H] TCDD, 1 µl of solvent (*p*-Dioxane) was added. A parallel triplicate sample was set up at the same time for determination of non-specific binding. To these non-specific binding tubes that contain 1 nM [^{3}H] TCDD, a 1 µl of 40 nM TCAOB, non-radioactive competitor, was added. Then, the samples were mixed thoroughly by vortexing followed by a brief spin down. The samples were then incubated overnight at 4 ˚C.

2.2.3.12.2 Dextran-coated Charcoal Treatment

The following day, the sample was treated with charcoal-dextran to remove unbound and loosely bound ligands. To do this, 30 µl of dextran-coated

charcoal (6.7 mg charcoal/ml in MDENG buffer (25 mM MOPS, pH 7.5, 0.02% sodium azide, 1 mM EDTA, 2 mM DTT and 10% glycerol)) was added to each sample. The sample was mixed by vortexing, and incubated on ice for 10 minutes. The charcoal/dextran was pelleted by centrifugation for 10 minutes at 14,000 x g at 4 ˚C. 150 µl of supernatant was transferred from each sample into a scintillation vial containing 5 ml scintillation fluid. The sample was mixed vigorously with scintillation fluid before counting.

2.2.3.12.3 Determination of the Bound and Free Ligand

Radioactivity of [^{3}H]-TCDD was determined by liquid scintillation counting using a Packard Tri-carb Model 2100TR Liquid Scintillation Analyser. Specific binding was defined as the difference between total and non-specific binding. Data were collected as d.p.m values, then converted to nM as follows (Birdsall and Lazareno 1997; Hulme and Birdsall 1992):

$RL^* = B\ d.p.m / (V \cdot SA \cdot 2220)$ nM

Where *B* is the radioligand bound (d.p.m.) corrected for counter background, *V* is the volume of radioligand assayed (ml), *SA* is the specific activity of the radioligand (Curies/mmole), and 2220 is the conversion factor from d.p.m. to nanocuries.

CHAPTER 3

3. RESULTS

3.1 Virus Plaque Assay

3.1.1 Optimization of Virus Plaque Assay

The recombinant virus is purified by a plaque assay using *Spodoptera frugiperda* (*Sf*9) cell line. A plaque assay is a focus of cells originating from infection by an infectious particle and represented a clonal population. Once a culture is adapted to growth and culture condition it is essential to establish an optimum cell density for seeding the cells. To do plaque assay, cells must be in growth with viability of at least 90% from the total number of cells. The number of viable cells/ml can be calculated using the following equation:

$$\text{Viable cells/ml} = \frac{\text{total number of viable cells counted}}{\text{number of 1mm}^2\text{ areas counted}} \text{ X dilution factor X } 10^4$$

3.1.2 Optimization of the Plating Density

To perform transfection, important parameters that can affect the efficiency of the experimental results must be optimised. The most important of these are:

plating density of viable cells and the amount of DNA used. Serial densities (0.5×10^5, 1×10^5, 2×10^5, 3×10^5, 4×10^5 and 5×10^5) of Sf9 cells were used to obtain the best density of Sf9 cells with optimum incubation period possible to reach 80 – 90% confluence. Table 3-1 shows that 5×10^5 density needs only 3-4 days to be approximately 80-90% confluence.

Time	**Density of the Sf9 cells (cells/well)**					
	0.5×10^5	**1×10^5**	**2×10^5**	**3×10^5**	**4×10^5**	**5×10^5**
Zero hour	33	52	82	97	160	192
1 day	43	57	116	177	230	273
2 days	48	66	187	224	292	311
3 days	56	75	226	262	360	confluent
4 days	72	94	252	291	confluent	
5 days	118	134	321	confluent		
6 days	177	211	confluent			
7 days	239	276				
	confluent	Confluen t				

Table 3-1 Illustrates the results of experiments carried out to optimise the plating density of the cells. Sf9 cells growing in monolayer in 6-plate at serial density from 0.5×10^5 to 5×10^5 cells/well were used. The number of viable cells in a well were determined by using a haemocytometer in conjunction with a vital stain. A mixed of cell suspension and trypan blue was added into the junction between chamber and the cover slip. The viable and nonviable cells in the same $1mm^2$ area were counted under a light microscope. The number of viable cells/ml was calculated using the equation in section 3.1.1.

3.1.3 Optimization of Virus Titre

The optimal amounts of virus needed to infect the Sf9 cells need to be established through experimental work. Only three plaque assay experiments were performed. Two of them were contaminated while, one experiment gave average of 25 plaques at a dilution of 1 $x10^{-6}$ but no plaques were observed at dilutions of 1 $x10^{-7}$ and $1x10^{-8}$ in 5 days after seeding. Cytochrome P450 CYP4X1 is a baculovirus (a kind gift from Dr. Tao Jiang, School of Biology, University of Nottingham) was used for titering. The titre of virus was determine by plaque assay. The Plaque assay, can be used to determine viral titre in plaque-forming units per ml (pfu/ml), was calculated by using the following formula:

$$\text{Virus Titre (pfu/ml)} = \frac{1}{\text{dilution factor X number of plaques}} \text{ X } \frac{1}{\text{ml of inoculums /plate}}$$

According to the result of this experiment and by applying this formula,

The dilution factor was 1 $x10^{-6}$

The number of plaques was 25

The inoculums /plate was 2 ml

Therefore, the virus titre was 12.5 $x10^{-6}$ pfu/ml

3.1.4 Baculovirus Expression Vector System

Baculoviruses are powerful expression systems for the production of biologically active recombinant proteins. *Spodoptera frugiperda* (Sf9) cells have been the cell line of choice for the expression of recombinant proteins and virus production using baculovirus expression vector systems (BEVS) (Smith *et al.* 1985). It has been reported that the full-length AhR was expressed in insect cells and a fraction of the proteins are in soluble form (Chan *et al.* 1994). In this project, few experiments of virus plaque assay have been done but reliable results not yet reached. The baculovirus work on expression of cytochrome P450 CYP4X1 was abandoned, as the P450 constructs to be used did not yield spectrally-detectable cytochrome in either Sf9 cells or after bacterial expression (data not shown). But before doing virus plaque assay experiment plating density of the cells and duration of incubation were optimized. As can be seen in table 3-1, the starting plating density of 5 $x10^5$ needs 3-4 days to achieve approximately 80-90% confluence. Based on these results I classified this condition as the optimal one because the cells can be passaged twice a week. Consequently, this condition was used in the further experiments. Also, other factors such as the concentration of DNA used need to be optimized as described in section 3.1.3.

3.2 GST-constructed Plasmids

The current study was to investigate the interaction between the Aryl hydrocarbon Receptor (AhR) and its ligands, and the protein composition of the AhR ligand-binding domain (LBD). Translation of AhR.LBD has been established in rabbit reticulocyte lysate, which contains molecular chaperones that are necessary for protein synthesis and is known to produce functional AhR e.g. (Kazlauskas *et al.* 1999).

Towards this goal, four expression plasmids were constructed, based on pET41b plasmid containing a glutathione S-transferase (GST) Tag. The first expression plasmid was pET41b vector itself as a negative control expressing GST only. The second contained GST-EGFP as a fluorescence control. The other two plasmids constructed contained GST-tagged AhR.LBD with one or two EGFP fluorescent tags (GST-EGFP-AhR.LBD and GST-EGFP-AhR.LBD-EGFP). In this thesis, the four constructed plasmids will be called G, GG, GGA and GGAG respectively.

Figure 3-1 shows a cartoon of the proteins derived from these plasmids incorporating the following features: an N-terminal GST affinity Tag to facilitate purification of the protein of interest, and the gene for enhanced green fluorescent protein (EGFP), which is for detection of the presence of the fusion protein. The EGFP is fluorescent whereas, GST and AhR.LBD proteins are not.

		Predicted Mr (Da)
GST (**G**)		35 618
GST-EGFP (**GG**)		65 492
GST-EGFP.AhR.LBD (**GGA**)		83 818
GST-EGFP.AhR.LBD-EGFP (**GGAG**)	GST EGFP AhR.LBD EGFP	108 973

Figure 3-1 Schematic diagram of GST, GST-EGFP, GST-EGFP-AhR.LBD and GST-EGFP-AhR.LBD-EGFP constructs. Enhanced Green Fluorescent Protein (EGFP) is coupled to the mouse AhR b-1 Ligand Binding Domain (AhR.LBD), and AhR.LBD-EGFP fusion, or directly to the Glutathione S-transferase (GST) affinity tag.

3.3 Design of Constructs Using Vector NTI Suite 7

Initially, GST-EGFP-C2, GST-EGFP-AhR.LBD and GST-EGFP-AhR.LBD-EGFP plasmid constructs were designed using Vector NTI Suite 7 (Baxevanis and Ouellette 1998). Vector NTI is a software package for nucleic acid and protein manipulation. In this study Vector NTI is used to model manipulation and creation of some biological molecules, which are then made practically using cloning techniques (see below).

3.4 Production of the Constructs

3.4.1 T7-GST-EGFP-C2 Construct

It can be seen from Figure 3-2 that, the T7-GST-EGFP was constructed in two steps. In brief, an EGFP fragment was subcloned into pGEM5ZF vector and then into pET41b vector.

In the first step approximately 815 bp EGFP fragment of pEGFP-C2 vector was cut out with *NheI* and *XbaI* and ligated into the pGEM5ZF vector, which was first digested with *SpeI*. After that, putative subclone was digested with *SalI* to identify which way around the insert was. Two fragments of ~3013 (plasmid) and ~802 bp (EGFP) were seen (shown in Figure 3-3) as expected. Therefore, the subclone chosen contained the insert in the correct orientation.

Subsequently, pGEM5-EGFP was sequenced using sense SP6 and antisense T7 specific primers (Figure 3-4). From the alignment result in Figure 3-4 it can be seen that the clone was a 100% match for EGFP.

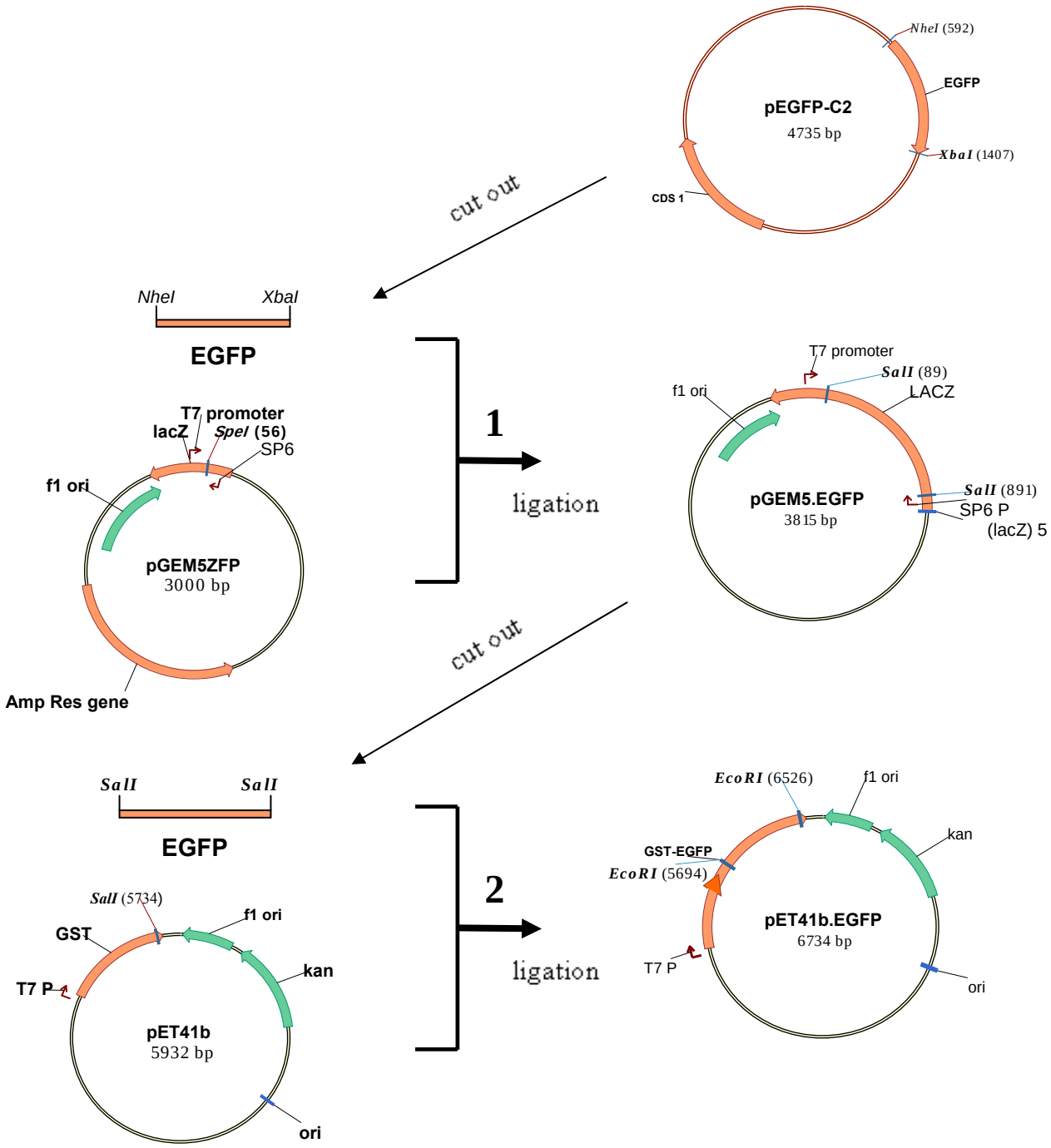

Figure 3-2 Sketch shows the cloning strategy of GST-EGFP. This strategy was divided into two stages. Stage 1 was subcloning EGFP into the *SpeI* site of the pGEM5ZF vector. Stage 2 was subcloning EGFP into the *SalI* site of the pET41b vector. The positions of some features in the vectors were labelled (red and grey filled part) include T7 promoter and terminator, SP6, ampicillin resistance gene (Apr), Kanamicin resistance (Ka), gene (Ori), Gentamicin resistance (GMr) and some site-specific transposition elements. The orientation of the AhR is shown with the arrow.

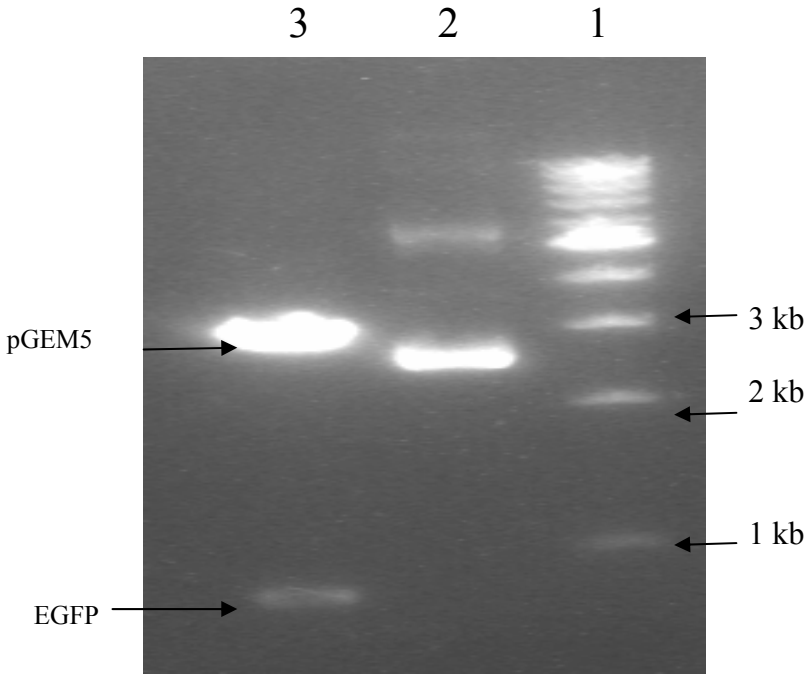

Figure 3-3 Characterisation of EGFP in pGEM5-EGFP plasmid. Lane 1 contained the 1kb size marker (Lifetech). Positions of 1, 2 and 3 kb for the marker are indicated on the right. Lane 2 contained uncut pGEM5-EGFP. Lane 3 contained cut pGEM5-EGFP with *SalI* as described in Materials and Methods section 2.2.2.5. DNA was separated on 0.8% agarose gel. The gel was stained using ethidium bromide and visualised using a UV transilluminator.

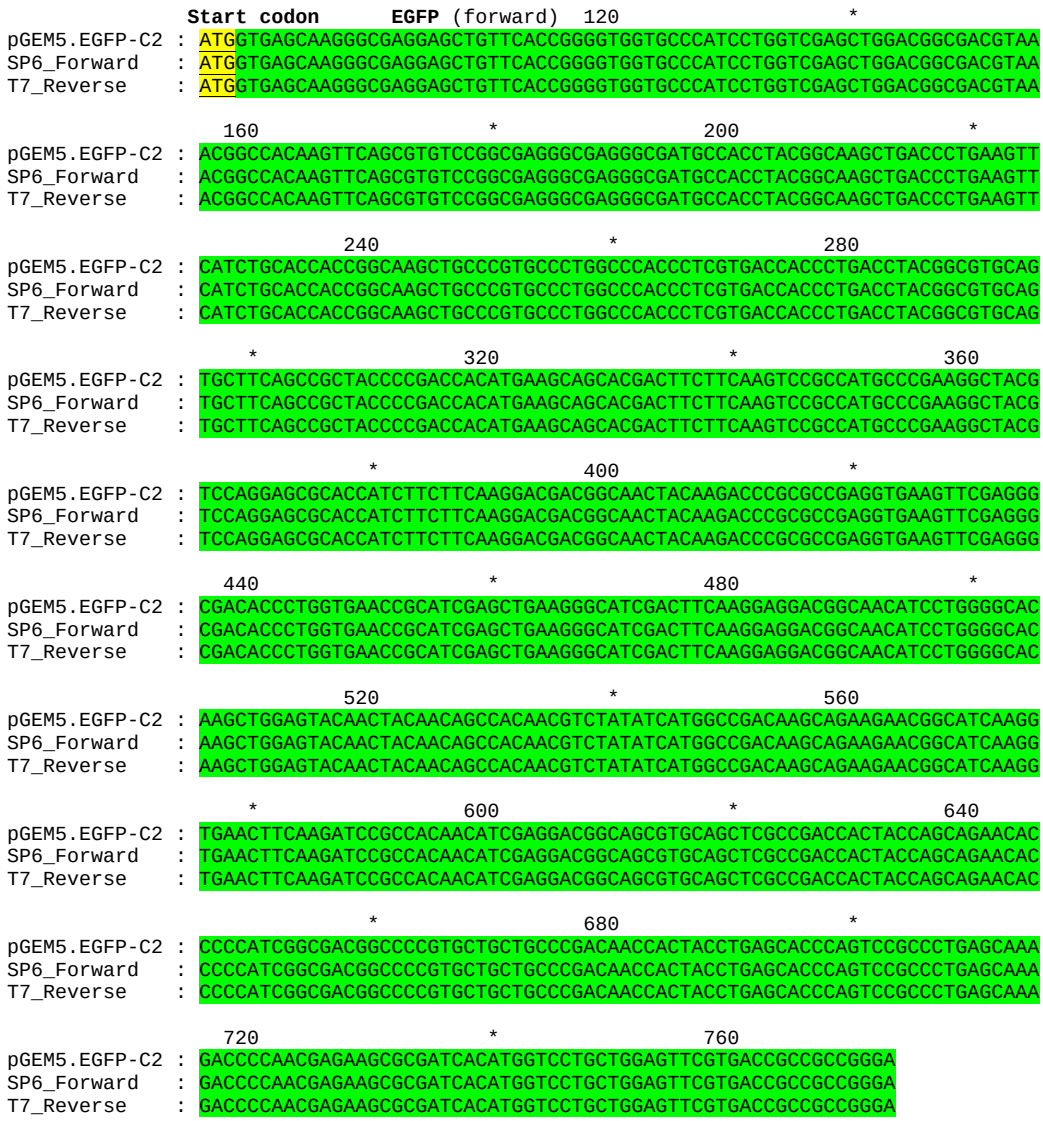

Figure 3-4 Alignment of EGFP insert and pGEM5-EGFP sequences. Alignment was created by alignX of Vector NTI program and displayed by GeneDoc program. The upper sequence ‘pGEM5-EGFP-C2’ is the matching sequence found in Vector NTI. The two lower sequences ‘SP6 Forward’ and ‘T7 Reverse’ are sequences of the insert (clone) in both directions. The start codon appeared in underlined and yellow colour. The EGFP matching area appeared in green colour.

The second stage was started when the ~802 bp EGFP fragment of pGEM5-EGFP-C2 plasmid in the Figure 3-3 was excised with *SalI* and subcloned into the *SalI* site of the pET41b expression vector.

The gel in Figure 3-5 shows two fragments, ~5902 bp (pET41b vector) and ~832 bp (EGFP) as expected after cut with *EcoRI* in order to check the orientation of EGFP insert in the pET41b vector. Also, to confirm that the insert was in the right orientation, sequencing was carried out using sense T7 terminator and antisense oso3 primers (Table 2-1) as shown in Figure 3-6. The sequence data confirmed that a pET41b-EGFP construct had been produced. This product was a 100% match for EGFP. Therefore, the final result was a construct of approximately 6734 bp pET41b-EGFP that could be used for further experiments.

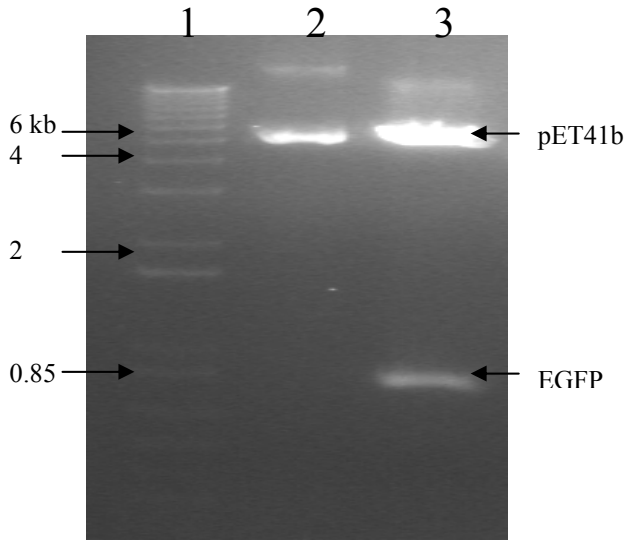

Figure 3-5 Characterisation of EGFP in pET41b-EGFP plasmid. Lane 1 contained the 1kb size marker. Positions of 0.85, 2, 4 and 6 kb for the marker are indicated on the left. Lane 2 contained uncut plasmid. Lane 3 contained cut plasmid with *EcoRI* as described in section 2.2.2.5. DNA was separated on 0.8% agarose gel. The gel was stained using ethidium bromide and read using a UV transilluminator.

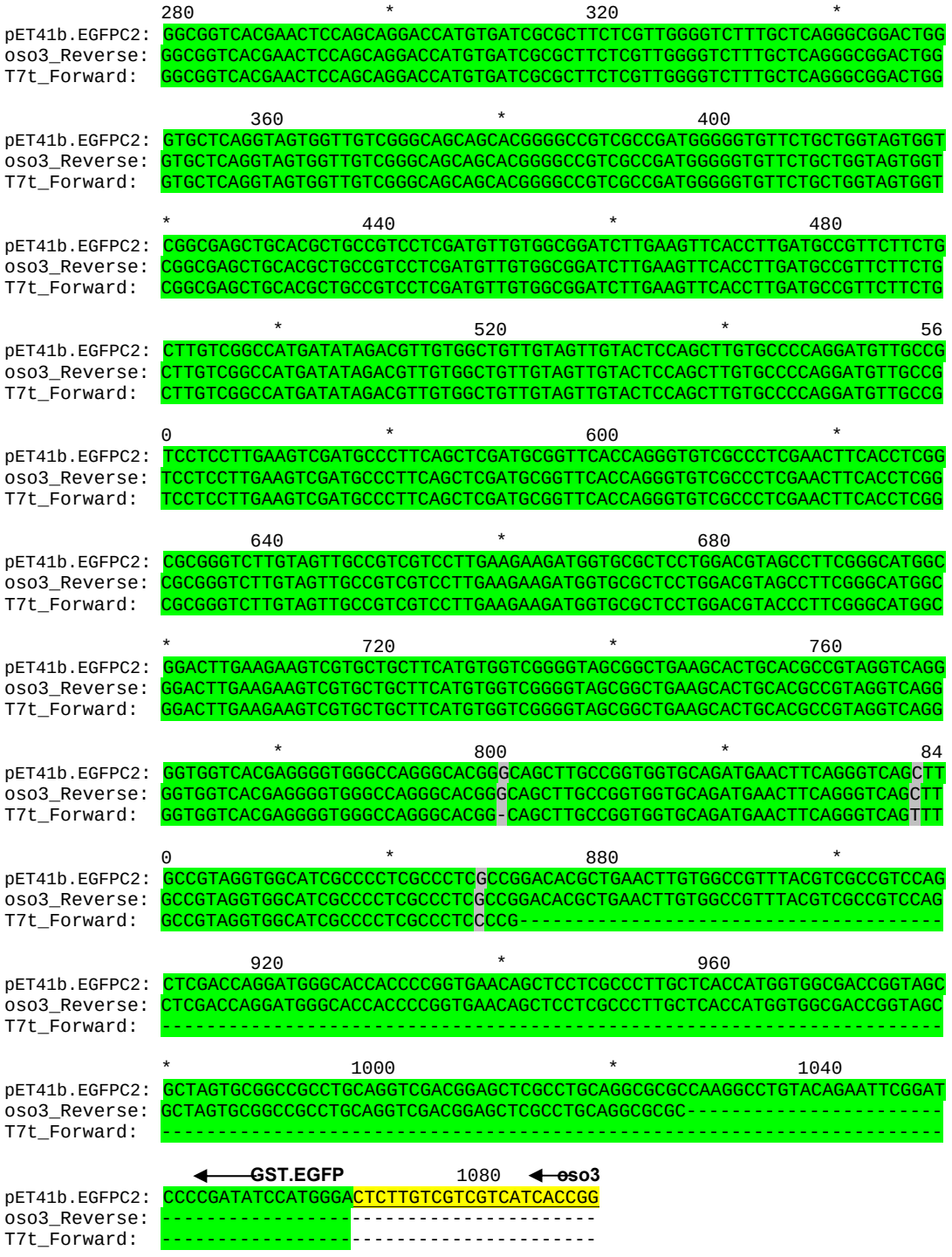

Figure 3-6 Alignment of EGFP insert and pET41b-EGFP sequences. Alignment was created by alignX of Vector NTI program and displayed by GeneDoc program. The upper sequence 'pET41b.EGFP-C2' is the matching sequence found in Vector NTI. The two lower sequences 'oso3 Reverse' and 't7t Forward' are sequences of the insert (clone) in both directions. The oso3 Reverse primer appeared in underlined and yellow colour. The EGFP was ligated in the reverse position and the EGFP matching area appeared in green colour. Not identical positions marked with grey.

3.4.2 GST-EGFP-AhR.LBD Construct

The GST-EGFP-AhR.LBD construct (Figure 3-1) was constructed in three stages. As can be seen in Figure 3-7, the EGFP was coupled to the AhR.LBD and then subcloned into the pGEM5 vector, before being subcloned into the pET41b vector.

The first stage was started with digestion of the AhR.LBD fragment from pFASTBAC HTcAhR 228-418 (section 2.1.5) using *BamHI* restriction enzyme as illustrated in Figure 3-8A. After that AhR 228-418 fragment was subcloned into the *BglII* site of the 5432 bp pEGFP-C2 expression vector. Figure 3-8B shows that *Csp45I* has been used in order to check the orientation of the AhR insert. Using gel electrophoresis, if the insert in the wrong orientation, there will be three bands of ~3067, ~2080 and ~162 bp. Whereas, if it is in the correct orientation, there will be three bands of ~2779, ~2080 and ~450 bp. The 450 bp fragment is the AhR.

In order to confirm the production of this stage, the AhR insert was sequenced using sense (oso1) and antisense (oso2) primers (Table 2-1). As shown in Figure 3-9, the sequence results demonstrate that the insert was in the correct orientation. Thus, the final result of this stage was a construct of pEGFP-AhR.LBD.

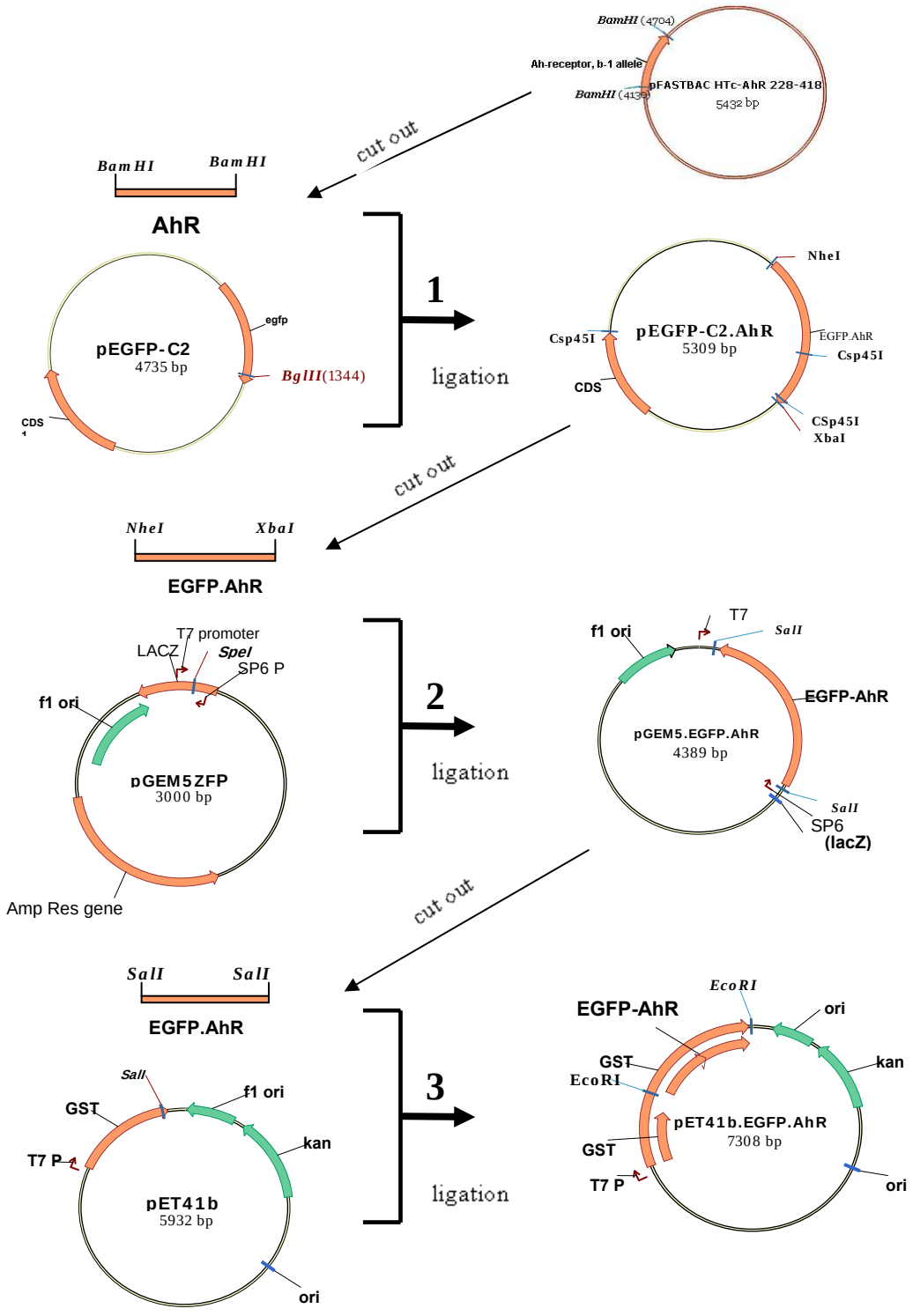

Figure 3-7 Sketch shows cloning strategy of GST-EGFP-AhR.LBD. This strategy was divided into three stages. Stage 1 was subcloning the AhR.LBD into the *BglII* site of pEGFP-C2 vector, stage 2 was subcloning the EGFP-AhR.LBD into the *SpeI* site of pGEM5 and stage 3 was subcloning EGFP-AhR.LBD into *the SalI* site of the pET41b vector.

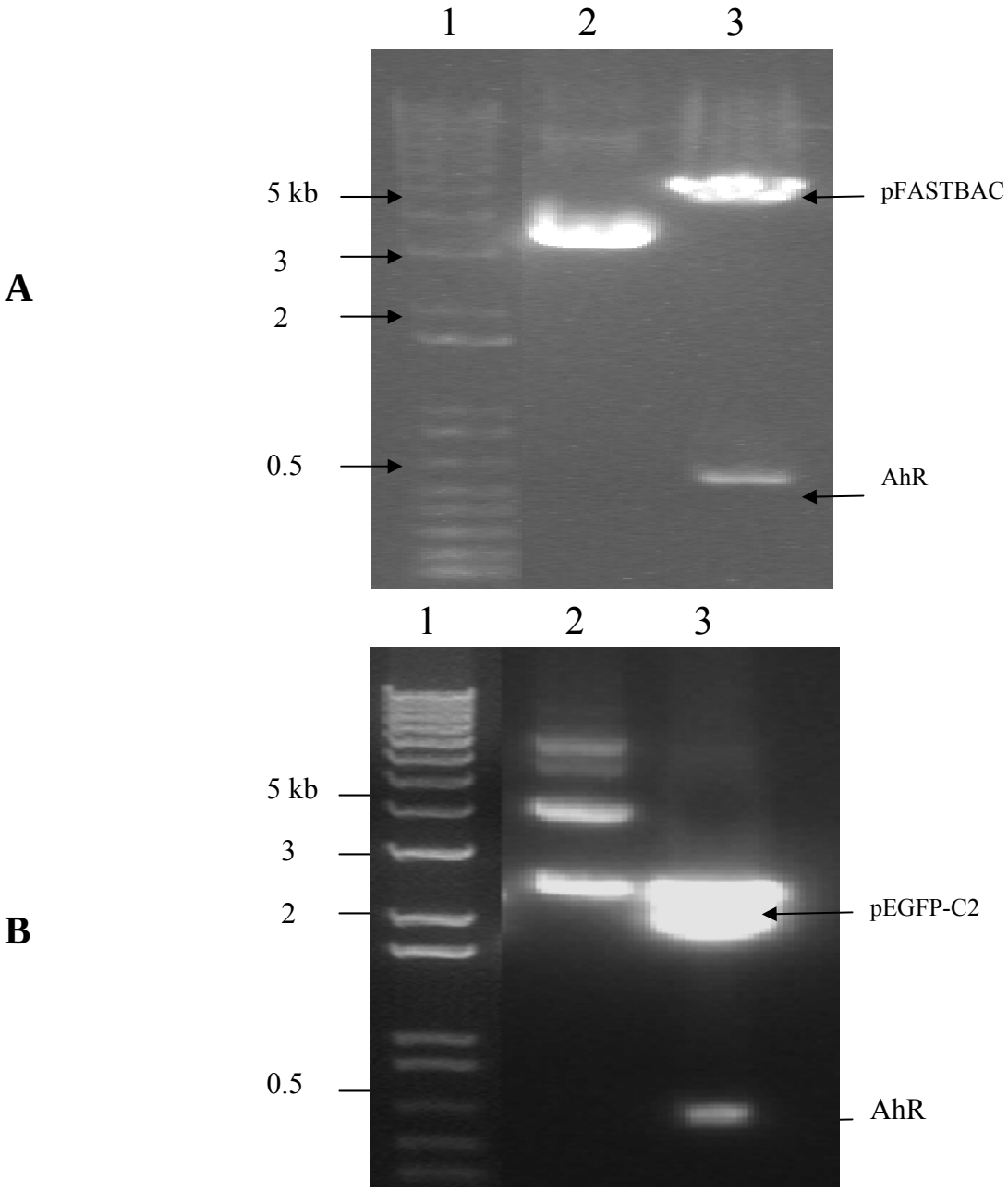

Figure 3-8A and B Restriction digestion of AhR.LBD insert. Lane 1 in Gels A and B contained the 1kb size marker. Positions of 0.5, 2, 3 and 5 kb for the marker are indicated on the left of each gel. In Gel A, Lanes 2 and 3 contain uncut and cut (*BamHI*) pFASTBAC HTcAhR 228-418, respectively. Gel B shows the results from digestion of pEGFP-AhR with *Csp45I*. Lane 2 contains uncut plasmid. Lane 3 contains pEGFP-AhR.LBD cut with *Csp45I* as described in section 2.2.2.5. DNA was separated on 0.8% agarose gel. The gel was stained using ethidium bromide and visualised using a UV transilluminator.

```
                4653  pEGFP-C2    *          AhR.LBD *      4760         *
pEGFP-AhR.LBD: ----------------------AGATCCTGGCAATGAATTTCCAAGGGAGGTTAAAGTAT
oso1_Forward : CTGTACAAGTCCGGCCGGACTCAGATCCTGGCAATGAATTTCCAAGGGAGGTTAAAGTAT
oso2_Reverse : CTGTACAAGTCCGGCCGGACTCAGATCCTGGCAATGAATTTCCAAGGGAGGTTAAAGTAT

                     4780         *      4800         *      4820         *
pEGFP-AhR.LBD: CTTCATGGACAGAACAAGAAAGGGAAGGACGGAGCGCTGCTTCCTCCACAACTGGCTTTG
oso1_Forward : CTTCATGGACAGAACAAGAAAGGGAAGGACGGAGCGCTGCTTCCTCCACAACTGGCTTTG
oso2_Reverse : CTTCATGGACAGAACAAGAAAGGGAAGGACGGAGCGCTGCTTCCTCCACAACTGGCTTTG

                     4840         *      4860         *      4880         *
pEGFP-AhR.LBD: TTTGCAATAGCTACTCCACTTCAGCCACCCTCCATCCTGGAAATTCGAACCAAAAACTTC
oso1_Forward : TTTGCAATAGCTACTCCACTTCAGCCACCCTCCATCCTGGAAATTCGAACCAAAAACTTC
oso2_Reverse : TTTGCAATAGCTACTCCACTTCAGCCACCCTCCATCCTGGAAATTCGAACCAAAAACTTC

                     4900         *      4920         *      4940         *
pEGFP-AhR.LBD: ATCTTCAGGACCAAACACAAGCTAGACTTCACACCTATTGGTTGTGATGCCAAAGGGCAG
oso1_Forward : ATCTTCAGGACCAAACACAAGCTAGACTTCACACCTATTGGTTGTGATGCCAAAGGGCAG
oso2_Reverse : ATCTTCAGGACCAAACACAAGCTAGACTTCACACCTATTGGTTGTGATGCCAAAGGGCAG

                     4960         *      4980         *      5000         *
pEGFP-AhR.LBD: CTTATTCTGGGCTATACAGAAGTAGAGCTGTGCACAAGAGGATCGGGGTACCAGTTCATC
oso1_Forward : CTTATTCTGGGCTATACAGAAGTAGAGCTGTGCACAAGAGGATCGGGGTACCAGTTCATC
oso2_Reverse : CTTATTCTGGGCTATACAGAAGTAGAGCTGTGCACAAGAGGATCGGGGTACCAGTTCATC

                     5020         *      5040         *      5060         *
pEGFP-AhR.LBD: CATGCTGCAGACATACTTCACTGTGCAGAATCCCACATCCGCATGATTAAGACTGGAGAA
oso1_Forward : CATGCTGCAGACATACTTCACTGTGCAGAATCCCACATCCGCATGATTAAGACTGGAGAA
oso2_Reverse : CATGCTGCAGACATACTTCACTGTGCAGAATCCCACATCCGCATGATTAAGACTGGAGAA

                     5080         *      5100         *      5120         *
pEGFP-AhR.LBD: AGTGGCATGACAGTTTTCCGGCTTCTTGCAAAACACAGTCGCTGGAGGTGGGTCCAGTCC
oso1_Forward : AGTGGCATGACAGTTTTCCGGCTTCTTGCAAAACACAGTCGCTGGAGGTGGGTCCAGTCC
oso2_Reverse : AGTGGCATGACAGTTTTCCGGCTTCTTGCAAAACACAGTCGCTGGAGGTGGGTCCAGTCC

                     5140         *      5160         *      5180         *
pEGFP-AhR.LBD: AATGCACGCTTGATTTACAGAAATGGAAGACCAGATTACATCATCGCCACTCAGAGACCA
oso1_Forward : AATGCACGCTTGATTTACAGAAATGGAAGACCAGATTACATCATCGCCACTCAGAGACCA
oso2_Reverse : AATGCACGCTTGATTTACAGAAATGGAAGACCAGATTACATCATCGCCACTCAGAGACCA

                     5200         *      5220         *      5240         *
pEGFP-AhR.LBD: CTGACGGATGAAGAAGGACGAGAGCATTTACAGAAGCGAAGTACGTCGCTGCCCTTCATG
oso1_Forward : CTGACGGATGAAGAAGGACGAGAGCATTTACAGAAGCGAAGTACGTCGCTGCCCTTCATG
oso2_Reverse : CTGACGGATGAAGAAGGACGAGAGCATTTACAGAAGCGAAGTACGTCGCTGCCCTTCATG
                                                                pEGFP-C2
                    5260         *      5280         *      5300       5309
pEGFP-AhR.LBD: TTTGCTACCGGAGAGGCTGTGTTGTACGAGATCTCCAGCCCTTTCTCTCCCTAAAT-
oso1_Forward : TTTGCTACCGGAGAGGCTGTGTTGTACGAGATCTCCAGCCCTTTCTCTCCCTAAATG
oso2_Reverse : TTTGCTACCGGAGAGGCTGTGTTGTACGAGATCTCCAGCCCTTTCTCTCCCTAAATG
```

Figure 3-9 Alignment of AhR.LBD insert and mouse AhR sequences. The AhR .LBD insert was cut with *BamHI* and subcloned into the *BglII* site of pEGFP vector. Alignment was created by alignX of Vector NTI program and displayed by GeneDoc program. The upper sequence 'pEGFP-AhR.LBD' was the matching sequence found in Vector NTI. The two lower sequences 'oso1 Reverse' and 'oso2 Forward' are sequences of the insert (clone) in both directions. The restriction sites for subcloning appeared in underlined and yellow colour. The AhR.LBD matching area appeared in blue colour.

The second stage involved excising ~1389 bp EGFP-AhR.LBD fragment from pEGFP-AhR.LBD-C2 using *NheI* and *XbaI* and ligated into the *SpeI* site of the pGEM5 vector. After that, putative subclones were digested with *SalI* to identify the orientation of the insert. It can be seen from Figure 3-10 that the digestion of pGEM5-EGFP.AhR.LBD gave two fragments of ~3013bp (plasmid) and ~1376 bp (the size of EGFP-AhR.LBD), as expected. That means the selected subclone contained the insert in the correct orientation. Subsequently, Figure 3-11 illustrates the results of pGEM5-EGFP-AhR.LBD sequencing. Match for EGFP-AhR.LBD using antisense SP6 primer shown relatively low identities only at positions marked with grey. These errors are at the beginning of the sequence run; inspection of the chromatogram shows that there are anomalous peaks present. These bands are a commonly encountered artefact of dye sequencing and are likely to be an artefact.

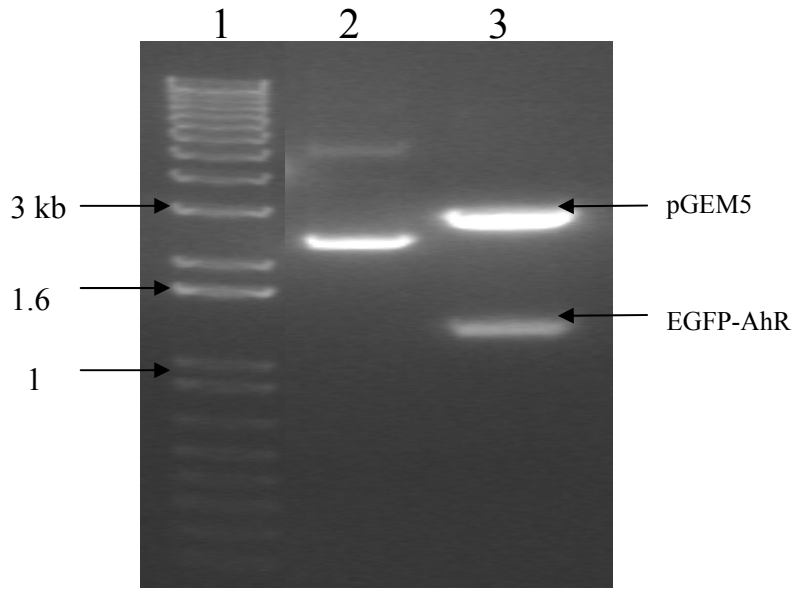

Figure 3-10 Characterisation of EGFP-AhR.LBD in pGEM5-EGFP-AhR.LBD plasmid. Lane 1 contained the 1kb size marker. Positions of 1, 1.6 and 3 kb for the marker are indicated on the left. Lane 2 contained uncut pGEM5.EGFP.AhR. Lane 3 contained cut pGEM5.EGFP.AhR with *SalI* as described section 2.2.2.5. DNA was separated on 0.8% agarose gel. The gel was stained using ethidium bromide and read using a UV transilluminator.

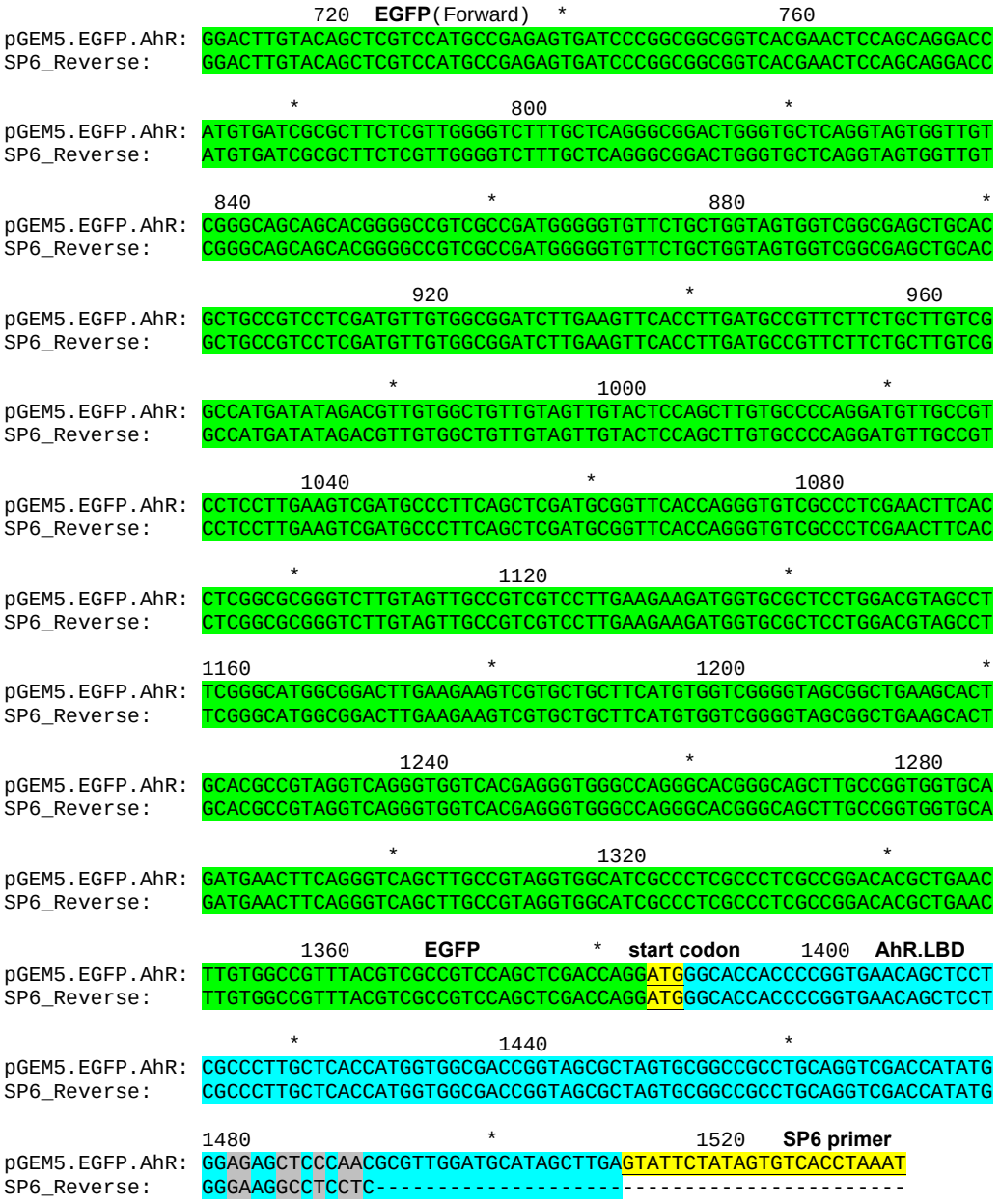

Figure 3-11 Alignment of EGFP-AhR.LBD insert and pGEM5-EGFP-AhR.LBD sequences. Alignment was created by alignX of Vector NTI program and displayed by GeneDoc program. The upper sequence 'pEGM5-EGFP-AhR' was the matching sequence found in Vector NTI. The lower sequence 'SP6_Reverse' was the sequence of the insert (clone) in one direction. Some differ in sequence results can be seen only at positions marked with grey. The SP6 primer and start codon appeared in underlined and yellow colour. The EGFP and AhR matching areas appeared in green and blue colour respectively. Not identical positions marked with grey.

Finally, the ~1376 bp EGFP-AhR.LBD fragment of pGEM5-EGFP-AhR.LBD was excised with *SalI* and ligated into pET41b that had been previously cut with *SalI*. The gel in Figure 3-12 shows two fragments ~5902 and ~1406 bp (the size of EGFP-AhR.LBD) when cut with *EcoRI* in order to check the orientation of the EGFP-AhR.LBD insert. Using an antisense T7 terminator primer for sequencing (as illustrated in Figure 3-13) confirmed that the EGFP-AhR.LBD insert was in the right orientation. This clone shown an error at positions marked with grey. These could be due to a commonly encountered artefact of dye sequencing because other direction sequence shows right matching at the same positions (as can be seen in Figure 3-6). Therefore, the final result was a construct of approximately 7308 bp pET41b-EGFP-AhR.LBD that could be used in subsequent experiments.

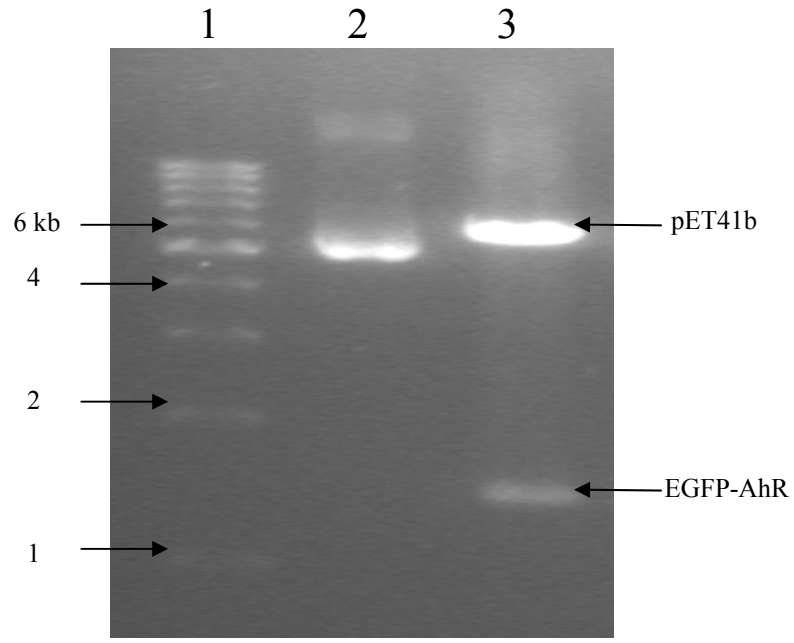

Figure 3-12 Characterisation of EGFP-AhR.LBD in pET41b-EGFP-AhR.LBD plasmid. Lane 1 contained the 1kb size marker. Positions of 1, 2, 4 and 6 kb for the marker are indicated on the left. Lane 2 contained uncut pET41b-EGFP-AhR.LBD. Lane 3 contained cut pET41b-EGFP-AhR.LBD with *EcoRI* as described section 2.2.2.5. DNA was separated on 0.8% agarose gel. The gel was stained using ethidium bromide and read using a UV transilluminator.

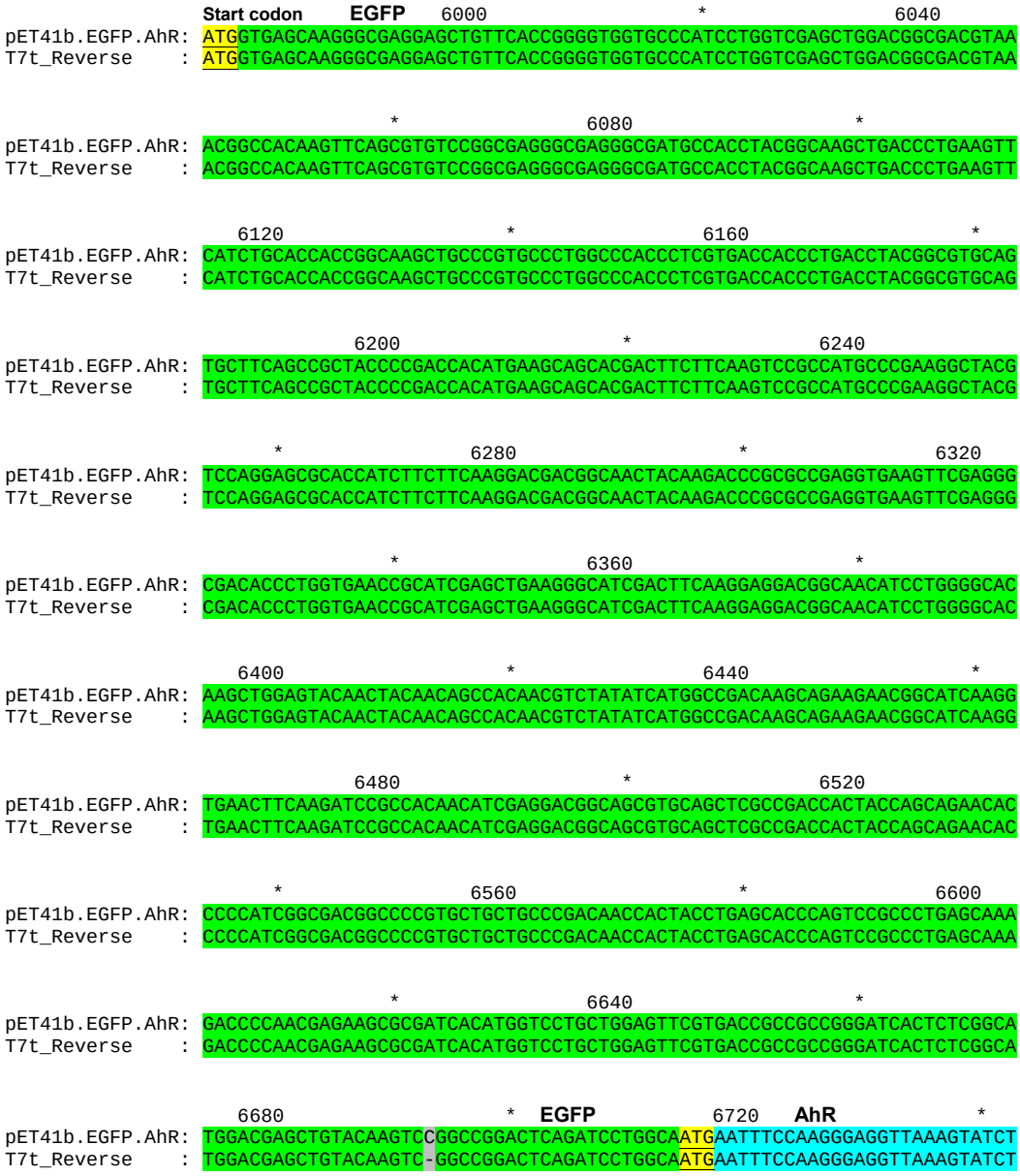

Figure 3-13 Alignment of EGFP-AhR.LBD insert and pET41b.EGFP.AhR.LBD sequences. The EGFP-AhR.LBD insert has cut with *SalI* and subcloned into the *SalI* site of the pET41b vector. Alignment was created by alignX of Vector NTI program and displayed by GeneDoc program. The upper sequence 'pET41b.EGFP.AhR.LBD' was the matching sequence found in Vector NTI. The lower sequence 'T7t_Reverse' was the sequences of the insert (clone) in one direction. The start codon site appeared in underlined and yellow colour. The EGFP and AhR were ligated in the reverse position and their matching areas appeared in green and blue colour respectively. Not identical position marked with grey.

3.4.3 GST-EGFP-AhR.LBD-EGFP Construct

This construct was made to study the interaction of two EGFP molecules separated by the AhR.LBD. This is to determine if ligand-binding affects the interaction of the two EGFP molecules.

Figure 3-14 represents the protocol for fusion of an additional EGFP onto the pET41b-EGFP-AhR.LBD construct. Addition of one more EGFP into the pET41b-EGFP-AhR.LBD construct was performed in our laboratory by Mr. Declan Brady (Nottingham). The pET41b-EGFP-AhR.LBD-C2 was used as a template for PCR, to remove the stop codon from the 3' terminus of the AhR LBD. The oligonucleotide sequences used for amplifying the AhR insert were oso4 and oso5 that were listed in table 2-1. The EGFP-AhR.LBD fragment was then subcloned into pGEM-T vector. After that, the putative subclone was cut with *EcoRI* and *BamHI* and subcloned into the *EcoRI and BamHI* sites of the pEGFP-N1 vector, thereby creating a fusion with the second EGFP. Finally, the whole EGFP-AhR.LBD-EGFP fragment was restricted with *EcoRI* and *NotI* and subcloned into the *EcoRI* and *NotI* sites of the pET41b vector. As can be seen in Figure 3-15 the pET41b-EGFP-AhR.LBD-EGFP-C2 fusion was digested with *NotI* and *EcoRI* in order to confirm the insert in the candidate pET41b clone. Subsequently, the pET41b-EGFP-AhR.LBD-EGFP was partially sequenced. Only single stranded sequencing was performed using

sense oso3 primer. Figure 3-16 shows that the result of the sequence, but the complete sequence of whole construct is not shown.

The sequence in Figure 3-16 shown an error at positions marked with grey. The reason behind that was described before on page 98.

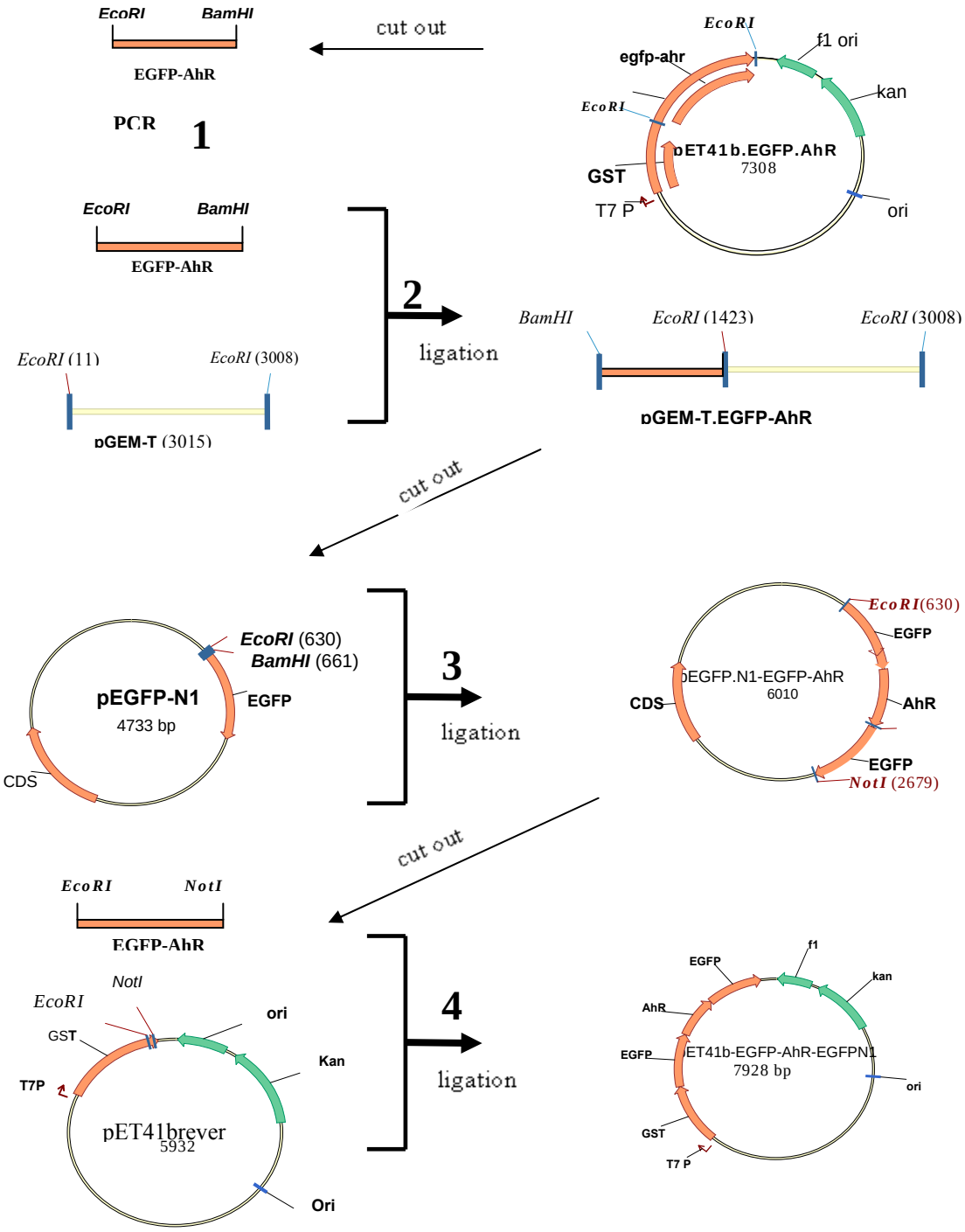

Figure 3-14 Schematic diagram shows fusion of EGFP into pET41b.EGFP-AhR.LBD construct. Addition of C-terminal EGFP into pET41b.EGFP-AhR.LBD construct consists of four stages. First, the EGFP-AhR.LBD fragment from pET41b.EGFP-AhR.LBD was excised with *EcoRI* and *BamHI*. Then the fragment was amplified by PCR, to introduce a C-terminal restriction site, followed by subcloning into pGEM-T vector. Third, the subcloned fragment was cut with *EcoRI and BamHI* and subcloned into the *EcoRI and BamHI* sites of pEGFP-N1 vector. Fourth, the EGFP-AhR.LBD-EGFP fragment was cut out with *EcoRI* and *NotI* before subcloning into *EcoRI* and *NotI* sites of pET41b vector.

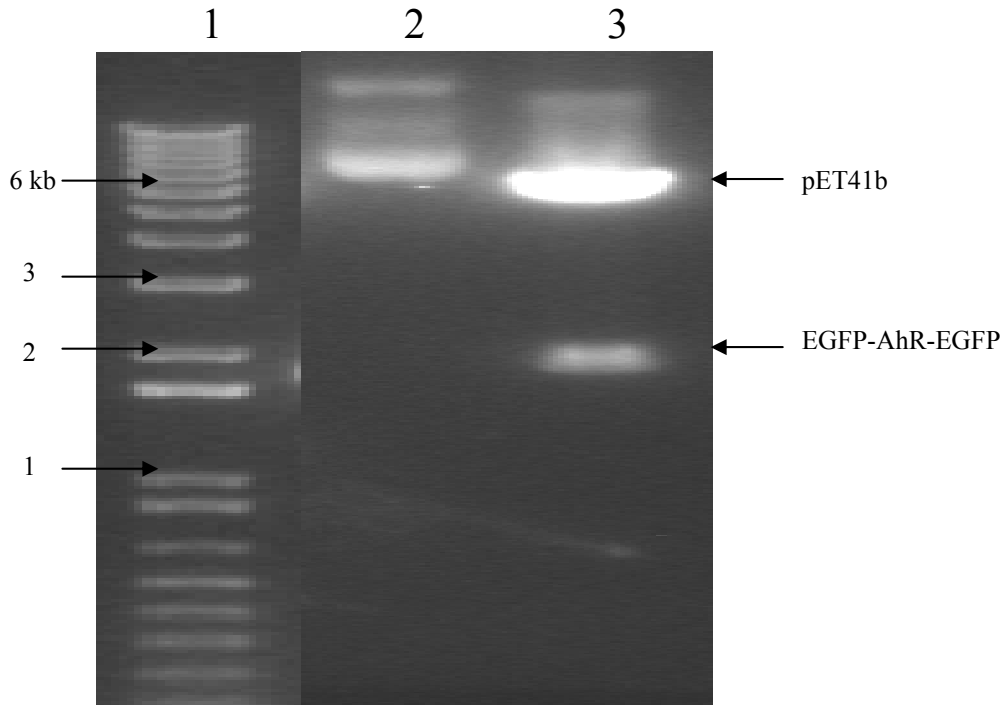

Figure 3-15 Characterisation of EGFP-AhR.LBD-EGFP in pET41b-EGFP-AhR.LBD-EGFP plasmid. Lane 1 was contained the 1kb size marker. Positions of 1, 2, 3 and 6 kb for the marker are indicated on the left. Lane 2 contained uncut pET41b-EGFP-AhR.LBD-EGFP. Lane 3 contained cut pET41b-EGFP-AhR.LBD-EGFP with *EcoRI* and *NotI* as described in section 2.2.2.5. DNA was separated on 0.8% agarose gel. The gel was stained using ethidium bromide and read using a UV transilluminator.

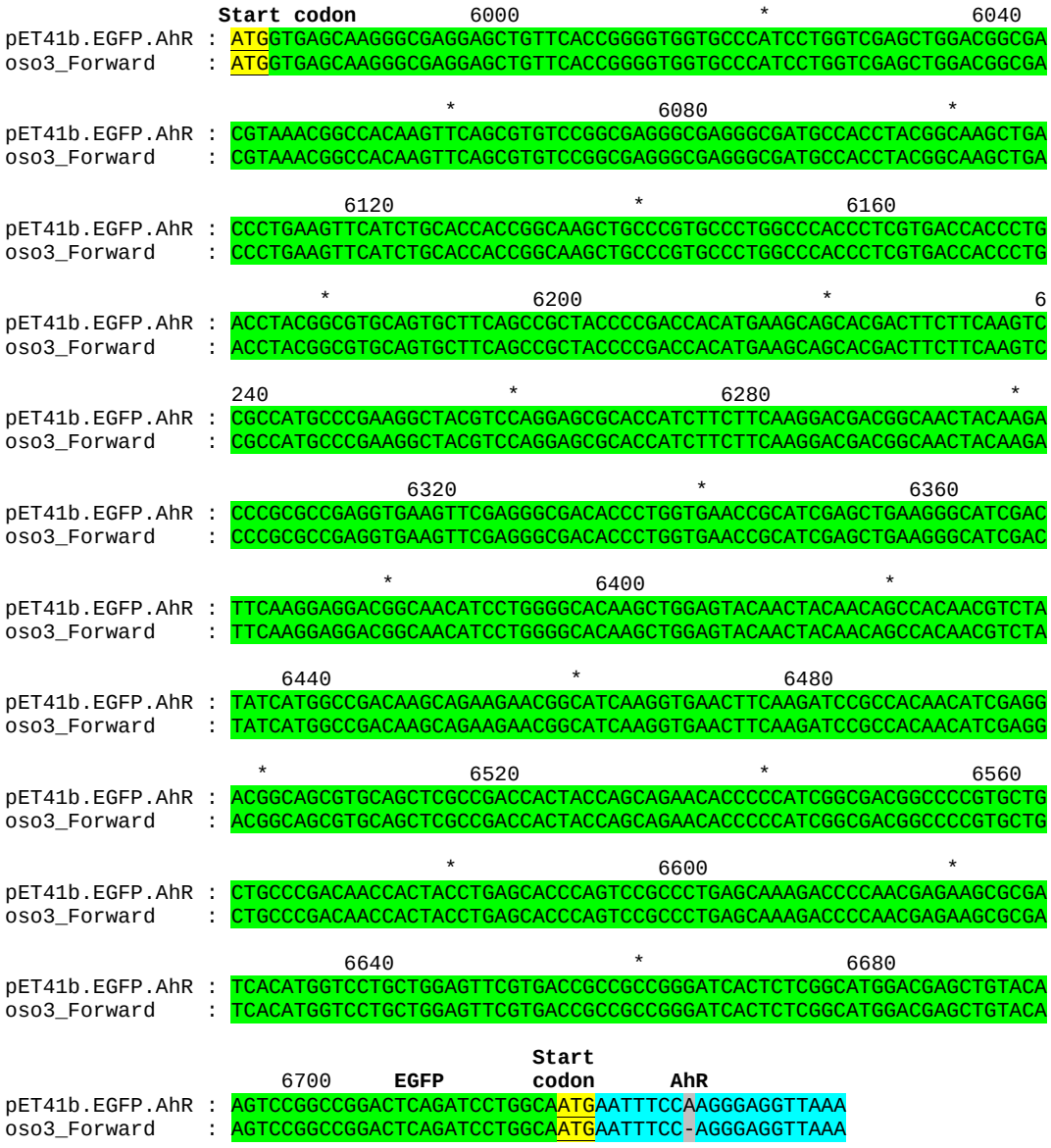

Figure 3-16 Alignment of EGFP-AhR.LBD-EGFP insert and pET41b-EGFP-AhR.LBD-EGFP sequences. Alignment of AhR.LBD insert and mouse AhR sequence. Alignment was created by alignX of Vector NTI program and displayed by GeneDoc program. The upper sequence 'pET41b-EGFP-AhR.LBD' was the matching sequence found in Vector NTI. The lower sequence 'oso3_Forward' was the sequence of the insert (clone) in one direction. The start codon appeared in underlined and yellow colour. The EGFP and AhR matching areas appeared in green and blue colour respectively. Not identical position marked with grey.

3.5 Expression of Recombinant Proteins

3.5.1 Expression of Recombinant Proteins in Bacteria

For expression of GST-fusion proteins, constructs in pET41b (GST, GST-EGFP, GST-EGFP-AhR.LBD and GST-EGFP-AhR.LBD-EGFP) were transformed into *E. coli* BL21(DE3)pLysS cells. These four recombinant proteins will be called G, GG, GGA and GGAG respectively. Initially, induction with 1 mM IPTG was carried out at 37 °C and 30 °C for 3 hours incubation, or at 25 °C overnight. Then the induced BL21(DE3)pLysS cells were harvested by centrifugation at 4,000 x g for 20 minutes at 4 °C and lysed by sonication for 8 bursts of 30 seconds at 4 °C. Lysed cells were centrifuged twice at 10,000 x g for 20 minutes in order to determine which of the expressed proteins were soluble and which were insoluble. Samples of the soluble (supernatant) and insoluble (pelleted) proteins from the three induction temperatures were loaded on an 8% SDS-PAGE gel alongside induced BL21(DE3)pLysS cells (without plasmid), uninduced cells and molecular weight marker. Figures 3-17A and B illustrates that G and GG proteins were visible in a coomassie-stained SDS-PAGE gel as a soluble proteins at the expected size of 36 and 66 kDa respectively. While Figure 3-18 shows that GGA and GGAG were visible as insoluble proteins at the expected sizes of 84 and 109 kDa, respectively. Therefore, measuring the fluorescence was undertaken as an independent and sensitive method of confirming the presence of the GG, GGA and GGAG proteins, which were difficult to recognize on SDS-PAGE.

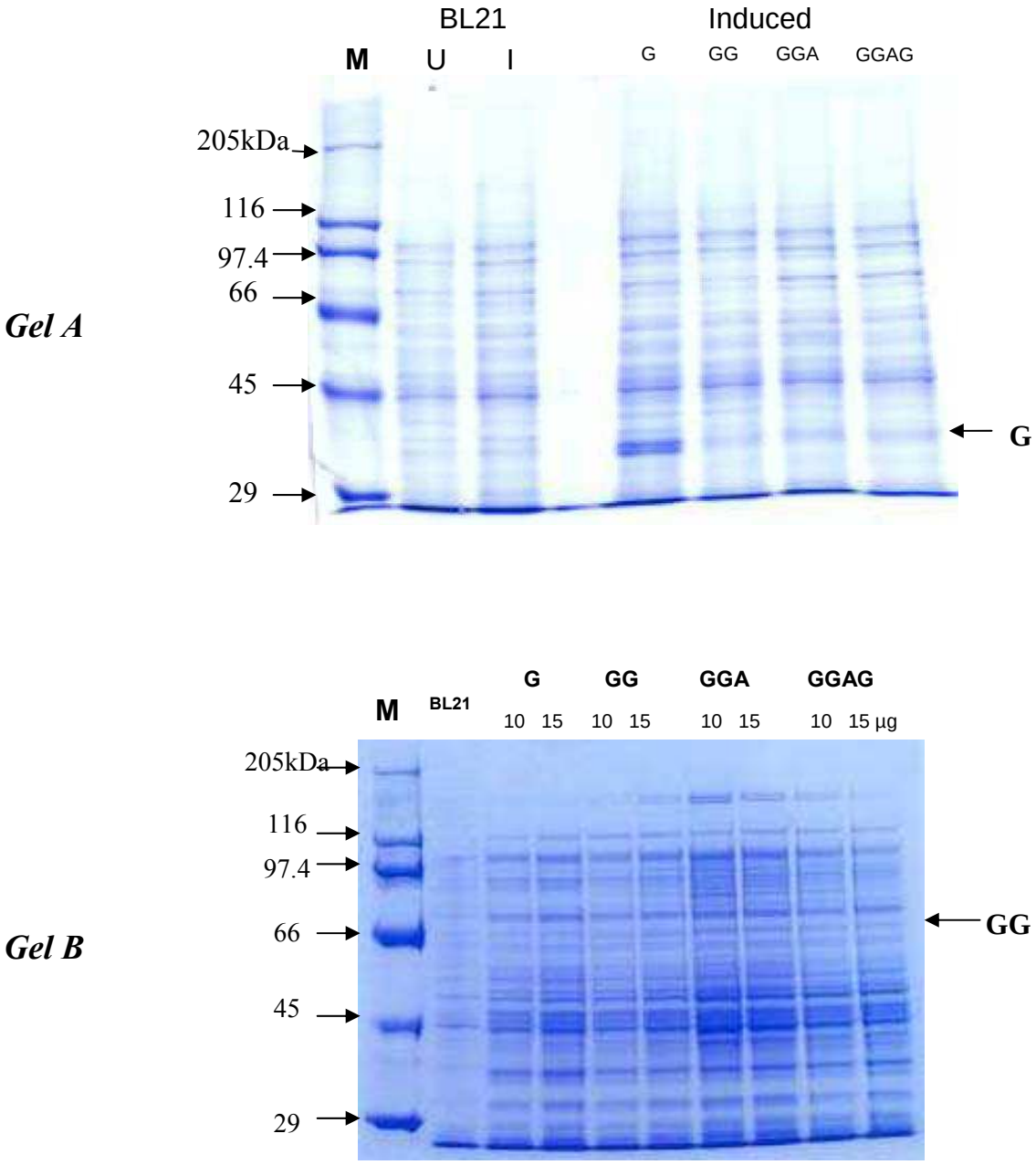

Figure 3-17A and B Electrophoresis of soluble bacterially-induced GST constructs at 30 °C. Plasmids were introduced into bacteria to produce proteins. Bacteria were lysed, and separated by centrifugation at 10000g for 20 minutes to yield supernatant (A and B) fractions. Proteins from these samples were separated on 8% SDS-PAGE and visualised by coomassie blue staining. Lane 1 in Gels A and B contained the 6H molecular weight marker; the position of the 29, 45, 66, 97.4, 116 and 205 kDa marker proteins is indicated on the left in kDa. Lane 2 in Gel A contained uninduced BL21 cells. Lane 3 in Gels A and B contained induced BL21 cells (without plasmid). Lanes 4, 5, 6 and 7 in Gel A contained induced G, GG, GGA and GGAG supernatants, respectively. Lanes 3 to 10 in Gel B contained induced supernatants G, GG, GGA and GGAG loading in double with 10 and 15 µg each respectively.

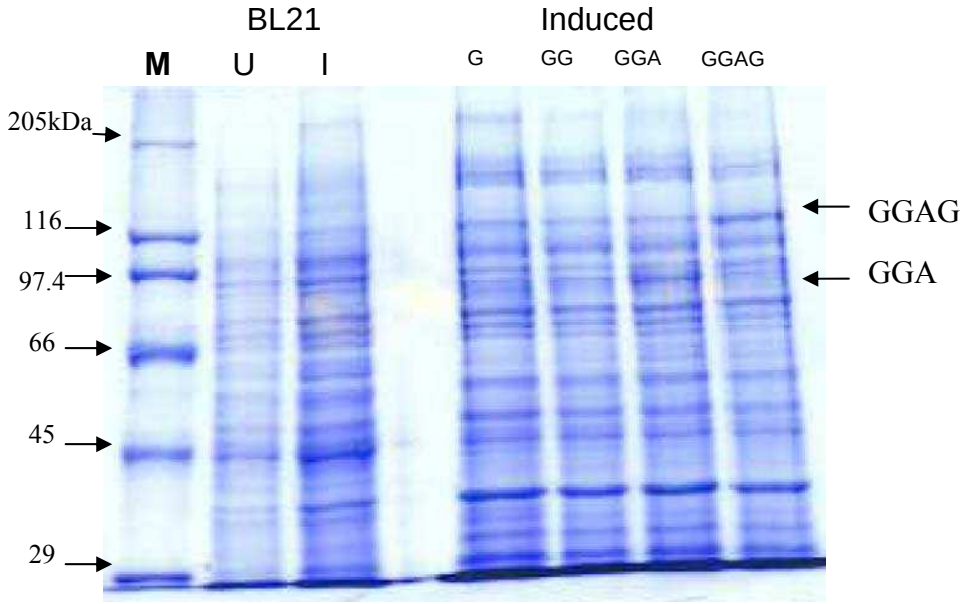

Figure 3-18 Electrophoresis of insoluble bacterially-induced GST constructs. Plasmids were introduced into bacteria to produce proteins. Bacteria were lysed, and separated by centrifugation at 10000g for 20 minutes to yield pellet fractions. Proteins from these samples were separated on 8% SDS-PAGE and visualised by coomassie blue staining. Lane 1 in the gel contained the 6H molecular weight marker; the position of the 29, 45, 66, 97.4, 116 and 205 kDa marker proteins is indicated on the left in kDa. Lane 2 contained uninduced BL21 cells. Lane 3 contained induced BL21 cells (without plasmid). Lanes 4, 5, 6 and 7 contained induced G, GG, GGA and GGAG 10000g pellets, respectively.

3.5.1.1 Fluorescence Detection of EGFP

A fluorescence emission scan was measured with excitation at 485 nm for EGFP, which emits with a peak at 509 nm. Total protein preparations from GG, GGA and GGAG inductions show peaks of fluorescence at about 509 nm, whereas total protein from the G induction shows much weaker fluorescence, with a peak at 530 nm (Figure 3-19). The fluorescence from G (GST only) is not showing EGFP fluorescence because it is not different from endogenous background (data not shown), and peaks at a different wavelength from the known wavelength of EGFP. Therefore, the fluorescence which was detected from GG, GGA and GGAG proteins demonstrated the presence of EGFP, since it is both more intense than that seen with bacterial protein controls (e.g. G), and has a peak emission wavelength which is different from the controls, and consistent with the known emission spectrum of EGFP (Johnson et al 1962). From the graphs in Figure 3-19A, B and C it may be seen that the induction of the recombinant constructs at 25 °C and 30 ºC produced higher levels of fluorescence per unit protein than at 37 ºC. From the fluorescence and electrophoresis results, it can be concluded that all four proteins were expressed but the amounts of the GG, GGA and GGAG were too low to be clearly seen on SDS-PAGE.

In order to determine if these proteins were soluble, fluorescence intensity was measured after centrifugation. The samples were spun at 10,000 x g for 10 minutes, followed by 240,000 x g for 30 minutes, to prepare a cytosolic

fraction. Fluorescence emission spectra of these soluble extracts show that the GG and GGAG extracts expressed soluble EGFP-based proteins (Figures 3-20A), since the control protein extract showed much reduced fluorescence, without a peak at 509 nm, and these samples had much greater levels of fluorescence, with a peak at 509 nm, corresponding to the emission peak of EGFP. While the GG and GGAG cytosolic extracts showed a significant fluorescence, the GGA cytosolic extract showed very little fluorescence at 509 nm, yet there was strong fluorescence in the insoluble GGA extract, showing that the GGA protein had been expressed and was insoluble (Figures 3-20B). Note that fluorescence intensity is in arbitrary units, and these can only be compared for samples assayed under identical conditions (excitation wavelength, slit width, photomultiplier tube voltage, etc). Thus all the samples in Figure 3-19 were assayed on the same day under identical conditions, but these are not necessarily identical to the conditions used for assay of the samples in Figure 3-20; thus the scales on these figures are not necessarily directly comparable.

Chart A

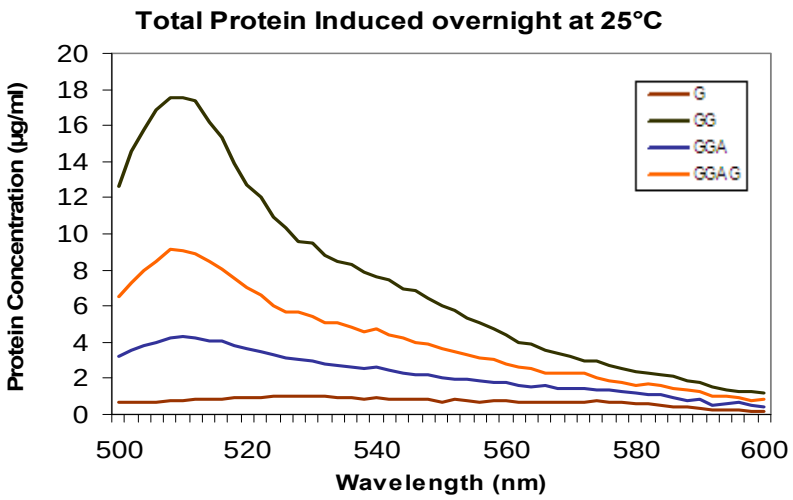

Chart B

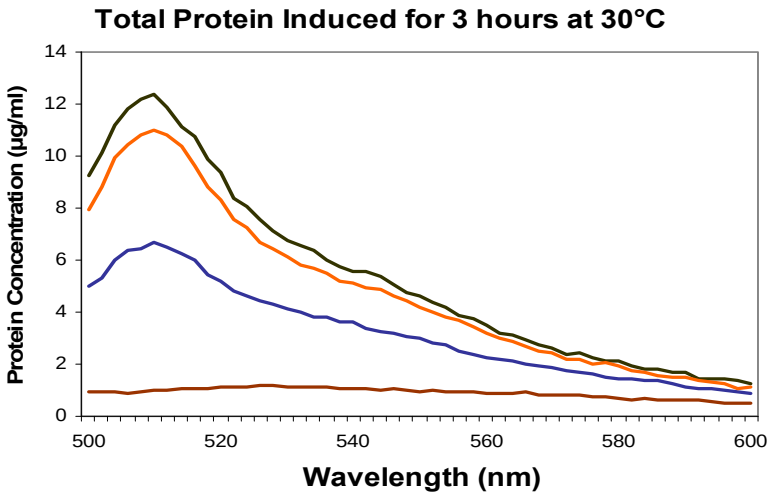

Chart C

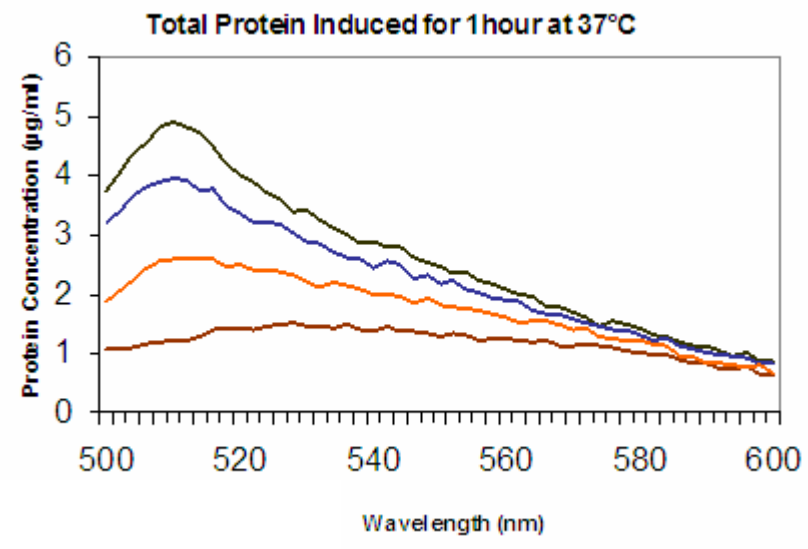

Figure 3-19A, B and C Fluorescence spectra from total protein of G, GG, GGA and GGAG total bacterial extracts. Total Bacterial extracts were performed on samples as described in Figure 3-16, and fluorescence emission spectra were obtained with excitation at 485 nm. Fluorescence emission is normalized to the protein concentration of the extract. Charts A, B and C show emission scans of total protein extracts induced at 25 °C, 30 °C or 37 °C, respectively.

Chart A

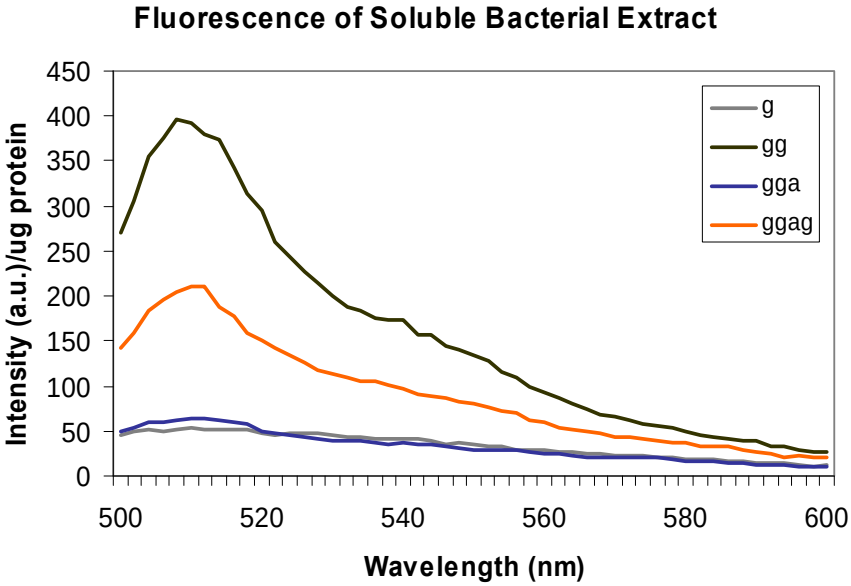

Chart B

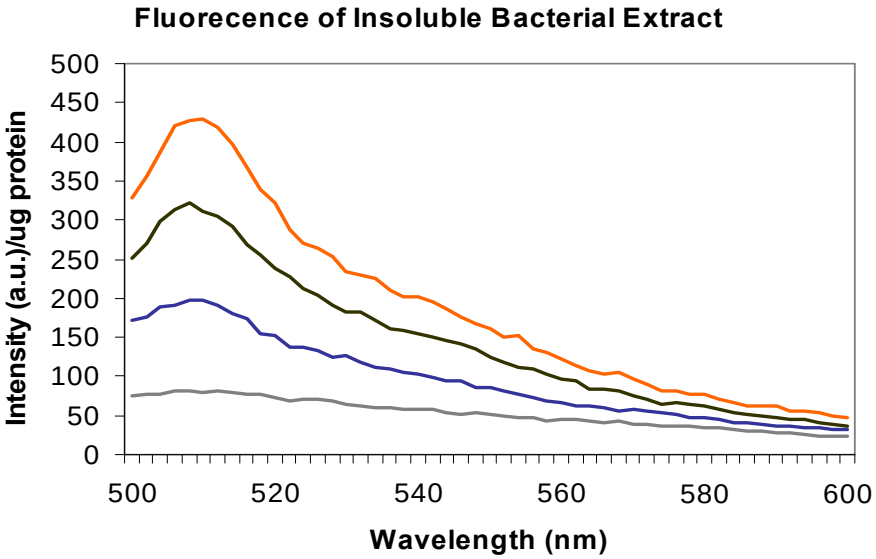

Figure 3-20A and B Fluorescence emission spectra of soluble and insoluble bacterial extracts. Samples were prepared as described in Figures 3-17 and 3-18, using bacteria induced at 30 °C. After cell lysis, the extracts were centrifuged at 10000g for 10 minutes, followed by centrifugation at 240000 x g for 30 minutes to yield a cytosolic supernatant. Samples were normalized using protein concentration. Chart A shows fluorescence of soluble bacterial extracts after two spins of the induced cultures. Chart B shows fluorescence of insoluble bacterial extracts after two spins of the induced cultures.

3.5.1.2 Detection of Recombinant AhR by Western Blotting

As the induced bands of recombinant AhR-containing soluble proteins were not detectable on SDS-PAGE, it was not possible to determine the molecular mass of the fluorescent proteins detected in Section 3.5.1.1. It is therefore important to determine if the fluorescent proteins were of the expected molecular mass, or if they represented proteolysis products containing EGFP alone. Western Blotting with ECL detection, a protein identification and quantification technique, was used with an antibody raised against amino acids 285-416 of the mouse AhR (Dr. Tao Jiang PhD Thesis). Figure 3-21 shows that the antibody fails to detect any immunoreactive bands in insoluble extract from BL21 bacterial cells, showing that the antibody fails to cross-react with bacterial proteins. The GG extract fails to show any cross-reacting bands, consistent with the low levels of expression of insoluble GG, and the lack of AhR protein, but the GGA and GGAG extracts showed immunoreactive bands of 84 and 109 kDa respectively; these are the expected size fragments, and this confirmed the presence of AhR in these bacterial extracts. The G extract also yielded a weak immunoreactive band at 36 kDa, the size of the G protein on SDS-PAGE. Although G should not be detected because it does not contain AhR sequences or sequence similarity, the G protein was produced at very high levels in the insoluble extract (Figure 3-21). The pET41 leader sequence has regions of similarity with the pRSET leader (used for the AhR antigen), and this low level similarity, coupled with the high level of expression of the GST protein, may explain the weak immunoreactivity against the G extract (Figure

3-22). However it is clear that this is weak immunoreactivity, since the antibody fails to detect the insoluble GG protein (which is present at higher levels than either GGA or GGAG), and therefore this cannot explain the much stronger immunoreactivity against the GGA and GGAG protein extracts.

Figure 3-23 shows Western Blot experiments, which were carried out to determine the amount of AhR in the GGA and GGAG samples. This was performed by constructing a series of standards using different amounts of the AhR antigen (amino acids 285-416 of the LBD)(1, 3, 10, 30 and 100 ng) and BL21 (extracts from *E.coli* cells only), G, GG, GGA and GGAG in the same gel. This experiment showed the estimated concentration of AhR in both GGA and GGAG recombinant proteins to be about 0.8% of the total proteins.

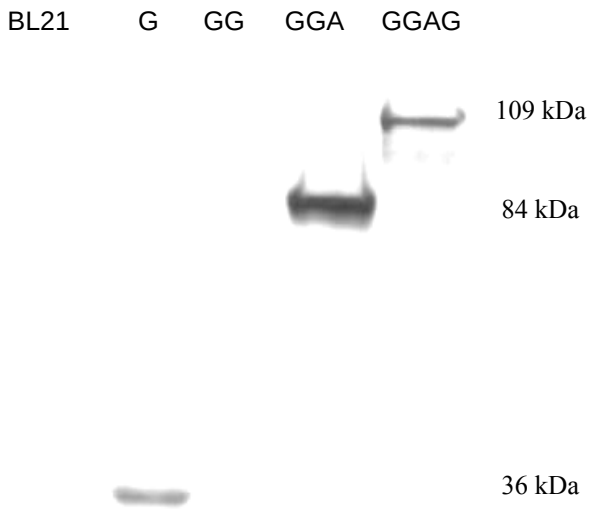

Figure 3-21 Western blot for AhR in insoluble bacterial extracts. BL21 (a control of extract from *Ecoli* bacteria only), G, GG, GGA and GGAG bacterial extracts were run on 10% SDS-PAGE then blotted to PVDF membrane. The PVDF was exposed to a mixture of 1:1000 mouse AhR primary antibody and a crude *E. coli* extract followed by 1:10,000 secondary antibody (Goat Anti-Rabbit TgG). Then detection reagents were added before expose PVDF to Kodak film. Finally, the film was developed in the dark room. G, GGA and GGAG bacterial extracts show bands at 84 and 109 kDa respectively.

```
                        1                                                  50
  GST from pET41b     (1) MSPILGYWKIKGLVQPTRLLLEYLEEKYEEHLYERDEGDKWRNKKFELGL
pRSETb Histag seq     (1) --------------------------------------------------
        Consensus     (1)
                       51                                                 100
  GST from pET41b    (51) EFPNLPYYIDGDVKLTQSMAIIRYIADKHNMLGGCPKERAEISMLEGAVL
pRSETb Histag seq     (1) --------------------------------------------------
        Consensus    (51)
                      101                                                 150
  GST from pET41b   (101) DIRYGVSRIAYSKDFETLKVDFLSKLPEMLKMFEDRLCHKTYLNGDHVTH
pRSETb Histag seq     (1) --------------------------------------------------
        Consensus   (101)
                      151                                                 200
  GST from pET41b   (151) PDFMLYDALDVVLYMDPMCLDAFPKLVCFKKRIEAIPQIDKYLKSSKYIA
pRSETb Histag seq     (1) --------------------------------------------------
        Consensus   (151)
                      201                                                 250
  GST from pET41b   (201) WPLQGWQATFGGGDHPPKSDGSTSGSGHHHHHHSAGLVPRGSTAIGMKET
pRSETb Histag seq     (1) ----------------------MRGSHHHHHHGMASMTGG---------
        Consensus   (201)                          HHHHHH       G
                      251                                                 300
  GST from pET41b   (251) AAAKFERQHMDSPDLGTGGGSGDDDDKSPMDIGDPNSVQALARLQASSVD
pRSETb Histag seq    (19) -------------QQMGRDLYDDDDKDPSSRSAAGTMEFEA--------
        Consensus   (251)                 G    DDDDK P            A
                      301         315
  GST from pET41b   (301) KLAAALEHHHHHHH
pRSETb Histag seq    (47) --------------
        Consensus   (301)
```

Figure 3-22 Alignment between the pET41b leader and the pRSETb leader. The upper sequence 'GST from pET41b' is a translation sequence of GST from pET41b vector and the lower sequence 'pRSET Histag seq' is a translation sequence of pRSET Histadine Tag sequence. The two matching areas appeared in grey colour.

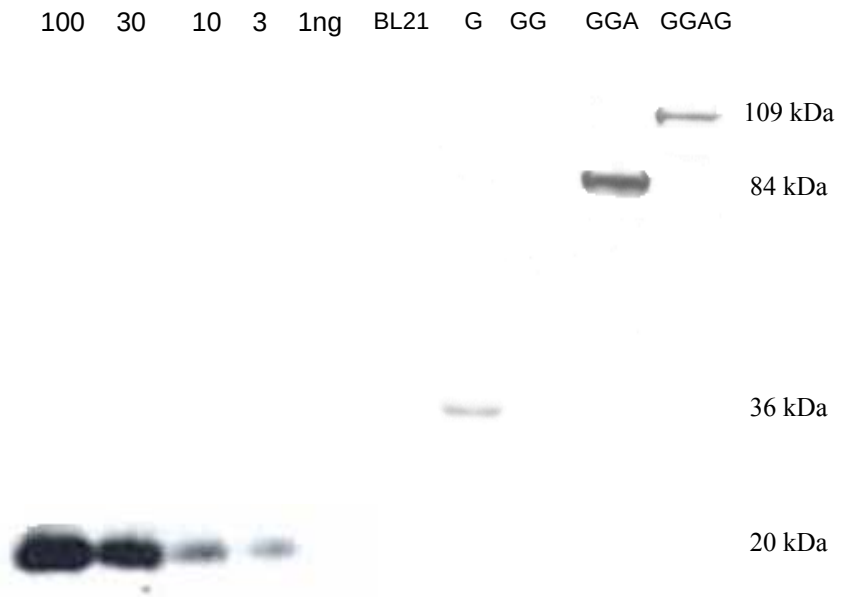

Figure 3-23 Western blot quantitation of recombinant AhR.LBD proteins. The indicated amounts (1, 3, 10, 30 and 100 ng) of just LBD of AhR protein and Induced BL21 cells, G, GG, GGA and GGAG bacterial extracts were run on 10% SDS-PAGE then blotted to PVDF membrane and developed as mention in Figure 3-21. Standard curve bands of AhR protein (the recombinant AhR antigen, containing amino acids 285-416 of the AhR) appear at 20 kDa. In addition of GGA and GGAG bacterial extracts show bands at 84 and 109 kDa respectively.

3.5.1.3 Purification of the G (GST) Recombinant Proteins

This protein purification method aimed to reduce the amount of contaminants eluting with the target protein. In order to optimise the purification of GST-fusion proteins, the G recombinant protein was used to optimise conditions for purification, prior to studies with other recombinant proteins (GG, GGA and GGAG). Several optimisation experiments were carried out using Bulk and MicroSpin GST purification modules. The protocol supplied by the manufacturer resulted in some contaminants such as glutathione and other low molecular weight proteins eluting with the target protein.

This purification experiment was performed in two ways. The first method was without using a 30 kDa Aminco Ultra-4 filter spin column whereas, the second was with the Ultra-4 filter spin filter column. 200 µg of the G bacterial extract fractions were filtered (0, 1, 2 or 3 times) with a 30 kDa Aminco Ultra-4 filter spin column. The fractions were filtered with a 30kDa molecular weight cut-off filter, to remove low molecular weight contaminants. The filtered G bacterial extract was added to 50 µl of a 50% slurry of glutathione beads. The beads were washed 1, 2 or 4 times with 1 ml of 1 x PBS in order to get the optimal number of washes, and eluted with 50 µl of GSH solution in an attempt to collect the maximum amount of purified protein. According to Figures 3-24 A and B there was no significant difference between using and not using the 30 kDa Aminco Ultra-4 filter spin column. Only slightly more yield can be seen

without using the Ultra-4 filter spin filter column (Figure 3-24A); the G protein was successfully purified from the bacterial protein extract by affinity chromatography using this method.

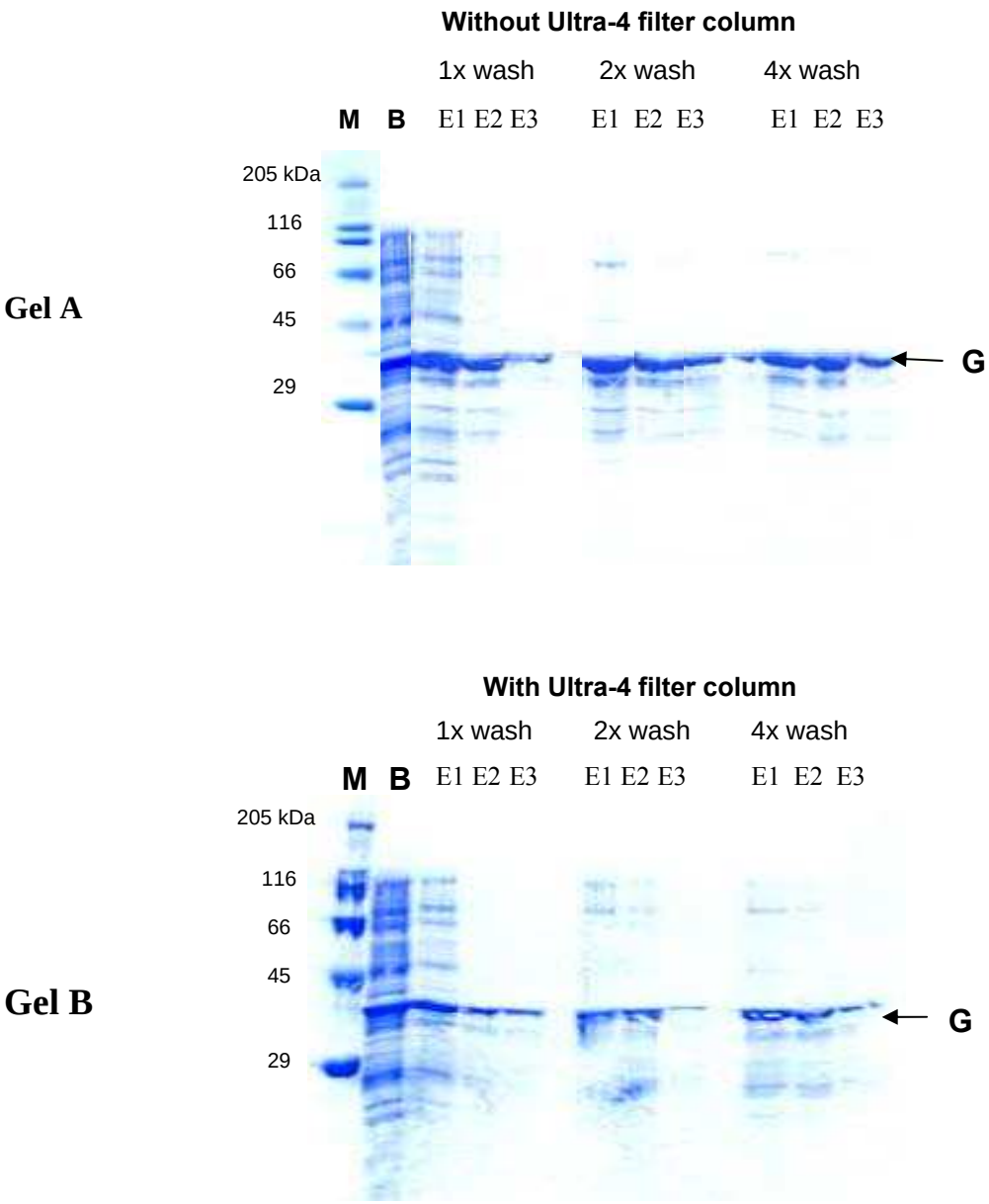

Figure 3-24A and B Purification optimisation of G bacterial extract using GST-affinity beads. The purified G bacterial extract was separated on 12% SDS-PAGE and detected by coomassie blue stain. Gel A shows the purification of G extract without using 30 kDa Aminco Ultra-4 filter spin column. The fractions were filtered 0, 1, 2 or 3 times as described in Materials and Methods section 2.2.3.10.1. Gel B shows the purification of G extract after using the spin column. Lane M in both Gels A and B contain the 6H marker. Positions of 29, 45, 66, 116 and 205 kDa for the marker are indicated to the left of each gel. Lane B in both Gels contains the protein sample before purification. Both gels show the effect of wash repetition 1, 2 and 4 times. Also, the gels show the effect of eluting three times on the yield of proteins.

3.5.1.4 Binding of Recombinant AhR to [^{3}H]-TCDD

As shown in Figures 3-20 and 3-21 the recombinant GGAG protein expressing in BL21(DE3)plysS bacteria was soluble, fluoresced and was the correct size. This was in contrast to the insolubility of the GGA protein, and was unexpected; however, it raised the possibility that the AhR LBD in the GGAG protein was correctly folded. Therefore, in order to test if the soluble AhR.LBD was functional, a [^{3}H]-TCDD binding assay experiment was carried out using rat liver cytosol as an AhR-containing positive control, G recombinant protein as a negative control and soluble GGAG recombinant protein. Figure 3-25 represent that rat liver cytosol (RLC) has approximately 10 fmols of AhR /mg cytosolic protein; this is specific binding which is saturated by excess AhR ligand, and demonstrates that the ligand binding assay is working. However no specific binding of the [^{3}H]-TCDD was detected for either the G or GGAG soluble recombinant extracts. That means the bacterial-expressed AhR.LBD in the soluble GGAG recombinant protein is not functional because we can detect ligand binding of the AhR in the rat liver cytosol, whereas no specific protein was binding to [^{3}H]-TCDD in the soluble GGAG protein samples.

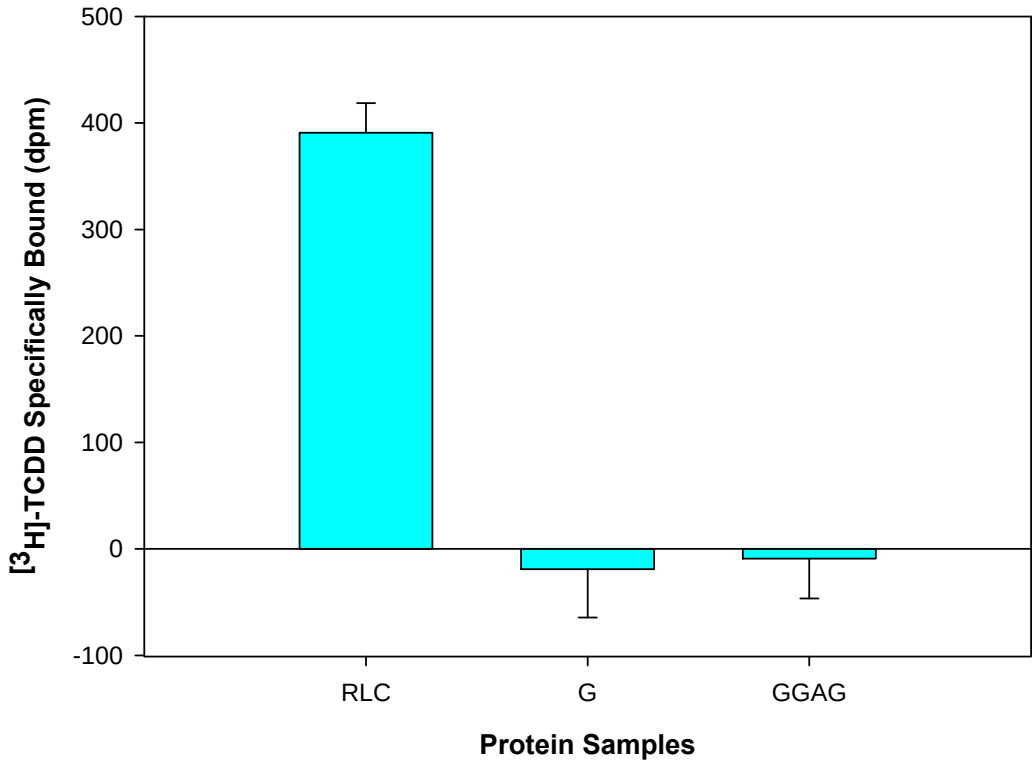

Figure 3-25 Specific binding of [^{3}H]-TCDD to bacterial-induced proteins. Rat liver cytosol (RLC) was used as a positive control, G recombinant protein as a negative control and GGAG recombinant AhR protein were bound to [^{3}H]-TCDD. Bound [^{3}H]-TCDD was separated from free [^{3}H]-TCDD by charcoal addition followed by centrifugation at 14,000 x g, and radioactivity determined in the supernatant, as described in section 2.2.3.12. Radioactivity in paired samples with excess competitor (TCAOB), was subtracted from the samples without added competitor, and the difference defines [^{3}H]-TCDD that is specifically bound. Each bar shows the average ± SD of triplicate samples.

3.5.2 Expression of Recombinant DNAs in Reticulocyte Lysate

3.5.2.1 Optimisation of Expression of the Recombinant DNAs in Reticulocyte Lysate System

To perform expression of GST constructs in the *In Vitro* Coupled Transcription and Translation rabbit reticulocyte lysate System, important parameters that can affect the efficiency of the experiment were optimised. The most important of these were found to be: the concentration of rabbit reticulocyte lysate in the reaction, the amount of DNA used, the length of exposure of the SDS-PAGE to the Imaging Plate (IP), the amount of [^{35}S]-methionine, and addition of RNase ribonuclease inhibitor and amino acid mixture, minus Leucine, (the use of a mixture of all amino acids, minus Leucine, as provided by Promega). All of these parameters were optimised using different ranges for each.

Figures 3-26 shows the result of an experiment that was carried out to optimize different parameters such as using 2 µg/ml of DNA instead of 1 µg/ml, 2 µl of [^{35}S]-methionine instead of 1µl and addition of RNase ribonuclease inhibitor. Also, in addition to the amino acid mixture minus Methionine, the amino acid mixture minus Leucine (at the beginning of incubation or after 60 minutes) was added or not to the reaction. The expressed proteins in each condition were separated on SDS-PAGE and autoradiographed. Moreover, S.Tag rapid assay was used in order to confirm the SDS-PAGE result (Figure 3-27).

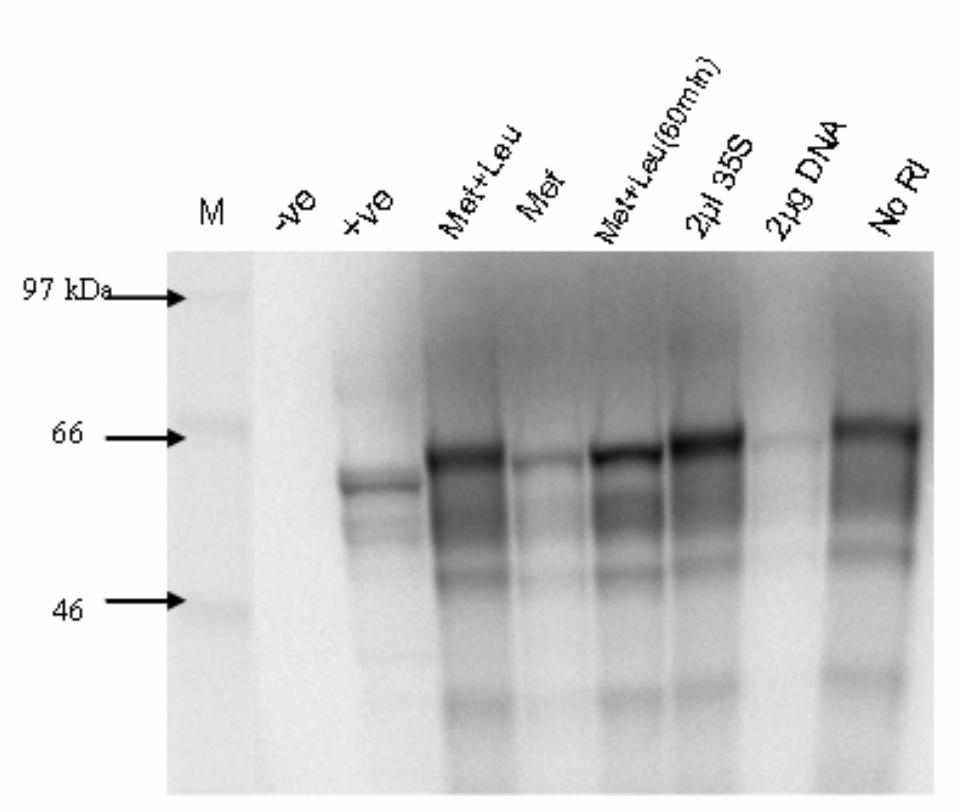

Figure 3-26 Optimaisation of experession of the GG recombinant DNA in reticuolocyte lysate. The experessed proteins in reticuolocyte lysate were separated on 4-12% SDS-PAGE and autoradiographed as described in section 2.2.3.4. Lane 1 contained the radioactive marker. Positions of 30, 46, 66 and 97 kDa for the marker are indicated on the left. Next lanes are a negative control (no DNA) and a firefly luciferase positive control. Then next lanes used abbreviations of (Met+Leu), is amino acid mixture, minus Methionine and Leucine; (Met), is amino acid mixture, minus Methionine only; (Met+Leu (60 minutes)), is amino acid mixture, minus Methionine and addition of minus Leucine after 60 minutes incubation; (2µl 35S), a mixture with 2µl of [^{35}S]-methionine; (2µg DNA), a mixture used 2µg/ml of DNA; and the last lane contained mixture without addition of RNase ribonuclease inhibitor (RI).

3.5.2.1.1 Measurement the Amount of Total Protein in Reticulocyte Lysate

The S.Tag rapid assay was described in section 2.2.3.9 as a protein tagging and detection system based on the interaction of the S.Tag peptide with ribonuclease S-protein. The S.Tag System was used for a direct measurement of the concentration of S.Tag fusion protein that provides by the assay of ribonuclease activity following the addition of purified S-protein. This detection procedure works well with the large quantities of protein produced in bacteria as well as with the small amounts of protein produced in reticulocyte lysate.

As can be seen in Figure 3-26 the GG was expressed in reticulocyte lysate using different conditions in order to optimise the expression of the four GST constructs in the rabbit reticulocyte lysate system. The intensity of expressed proteins in each condition was determined using the S.Tag rapid assay (Figure 3-27). From Figures 3-26 and 3-27, it can be said that using 1 µg /ml DNA, 2 µl of [^{35}S]-methionine, addition of amino acid mixture, minus Leucine, at the beginning of incubation and also using ribonuclease inhibitor are the optimal conditions to be used for further experiments.

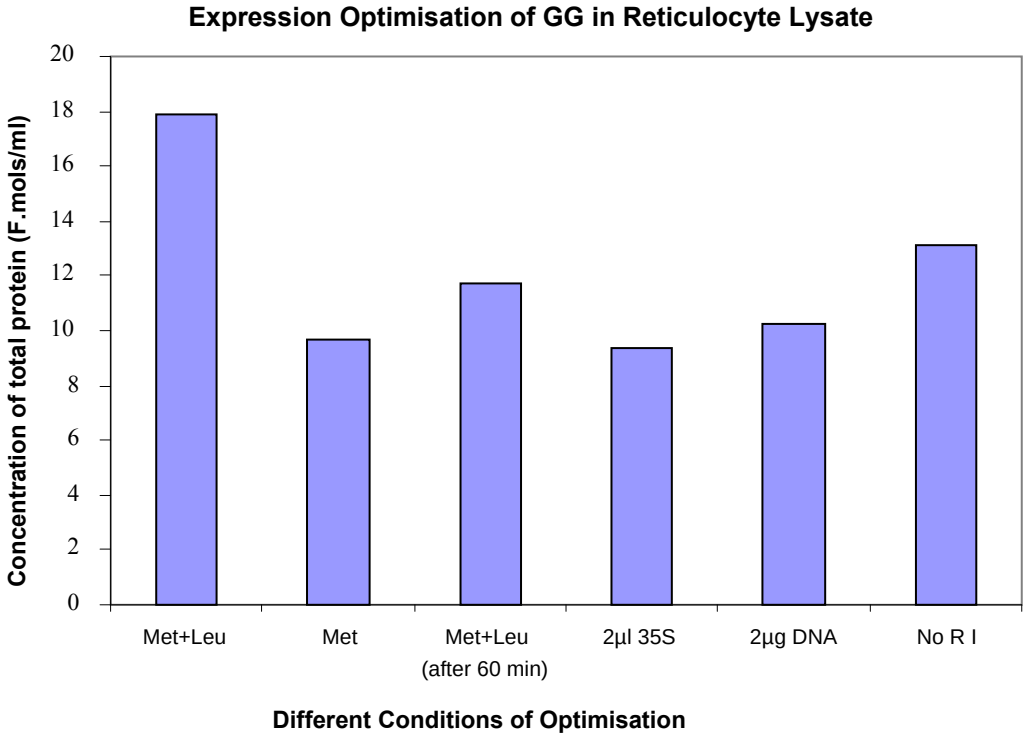

Figure 3-27 Concentration of total protein produced by expressed the GG in the reticulocyte lysate system. The expressed proteins in reticuolocyte lysate were calculated by S.Tag assay for the different conditions of optimization. The amount of total protein in each condition ((Met+Leu), is amino acid mixture, minus Methionine and minus Leucine; (Met), is amino acids mixture, minus Methionine only; (Met+Leu (60 minutes)), is amino acid mixture, minus Methionine and addition of minus Leucine after 60 minutes incubation; (2 µl ^{35}S), a mixture with 2 µl of [^{35}S]-methionine; (2 µg DNA), a mixture used 2 µg/ml of DNA; and the last lane contained mixture without addition of RNase ribonuclease inhibitor (RI)) was analysed by spreadsheet.

3.5.2.1.2 Effect of Rabbit Reticulocyte Lysate Concentration

In order to optimise the concentration of rabbit reticulocyte lysate in the reaction of *In Vitro* Coupled Transcription and Translation Reticulocyte Lysate System, experiment, consisting of two rabbit reticulocyte lysate concentrations can be used according to the manufacturer's instruction. These two concentrations are 25 µl (50%) and 27.5 µl (55%) of whole reaction of 50 µl was carried out using the GG recombinant DNA as a template. As can be seen from Figure 3-28 expression of the GG protein (as a template) shows higher result with the 50% of rabbit reticulocyte lysate concentration than in case of 55%.

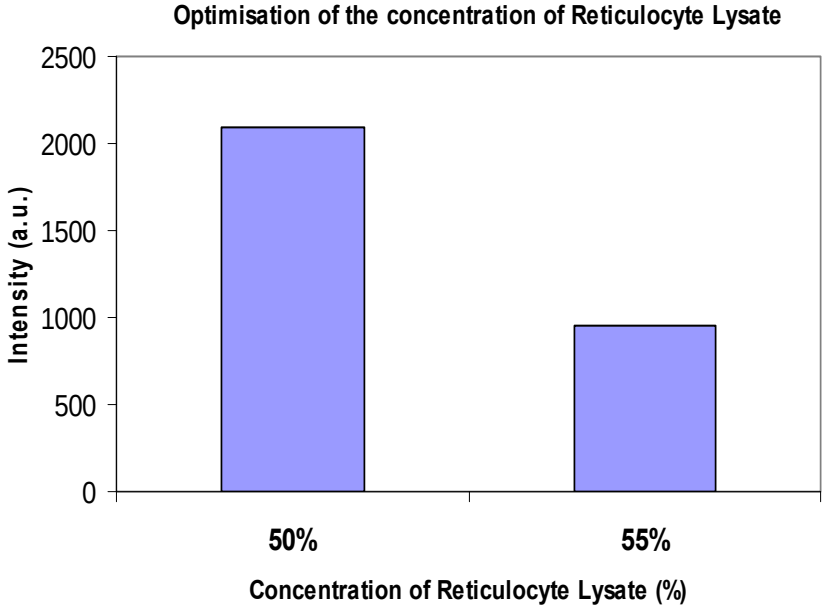

Figure 3-28 Effect of the amount of rabbit reticulocyte lysate in the reaction. The GG recombinant DNA was expressed in *In Vitro* Coupled Transcription and Translation Reticulocyte Lysate System using two different amounts of reticulocyte lysate, 50 and 55% of the whole reaction. The amounts of expressed proteins were then measured by phosphor imaging of gel separated proteins, specifically the labelled AhR protein; the experiment was repeated with consistent results.

3.5.2.1.3 Effect of Exposure Time of the SDS-PAGE to the Imaging Plate

The GST constructs were introduced into rabbit reticulocyte lysate System. The proteins were separated on SDS-PAGE followed by drying and exposure to imaging plate of phosphor imager machine. Toward optimise the length of exposure of SDS-PAGE to the imaging plate, SDS-PAGE in Figure 3-29 was exposed using a time course of 4, 24 and 72 hours. The integral reading as described in the legend of the figure shows the greatest intensity of the expressed proteins in case of the 24 hour exposure.

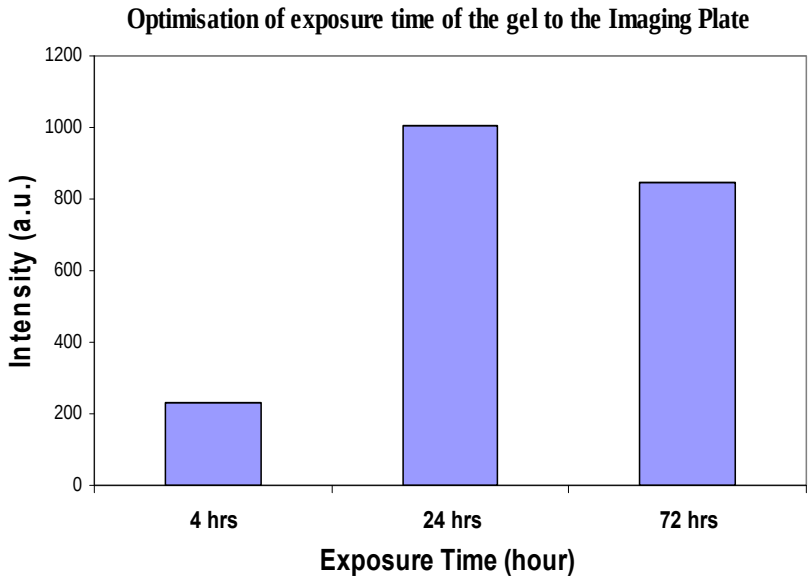

Figure 3-29 Time course of the exposure time of SDS-PAGE to the Imaging Plate. Time course of The GG recombinant DNA was expressed in *In Vitro* Couple Transcription and Translation Reticulocyte Lysate System. At the indicated number of hours exposure (4, 24 and 72 hours), bands intensity per square mm of the expressed proteins were then measured using AIDA software.

3.5.2.1.4 Effect of the Amount of DNA

The bacterial-expressed GGA recombinant DNA was used as a template to find the optimum amount of DNA used in *In Vitro* Coupled Transcription and Translation Reticulocyte Lysate System. The expressed proteins were then separated on 4-12% SDS-PAGE followed by autoradiograph. It can be seen in Figure 3-30 that serial amount (1, 2, 3 and 4 µg/ml) of the GGA recombinant DNA was introduced into rabbit reticulocyte lysate System. But the 1µg/ml concentration gave the highest result of the GGA expressed protein, whereas the 4 µg/ml shows the lowest expression.

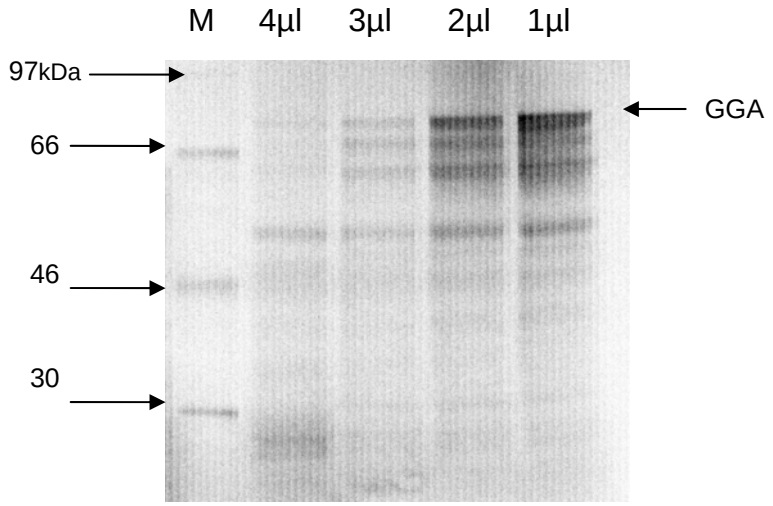

Figure 3-30 Effect of the concentration of DNA used. Serial amount of the GGA plasmid was introduced into reticulocyte lysate to produce proteins. The reaction is incubated at 30 ºC for 90 minutes. Then 5µl of the reaction separated on 4-12% SDS-PAGE and autoradiographed as described in section 2.2.3.4. Lane 1 contained the radioactive marker. Positions of 30, 46, 66 and 97 kDa for the marker are indicated on the left. The next four lanes contained different DNA concentration of GGA 4, 3, 2 and 1µg/ml respectively.

3.5.2.2 Optimal Expression of Recombinant Proteins in Reticulocyte Lysate

From the previous optimisation experiments, the expression of the four recombinant DNAs (G, GG, GGA and GGAG) in the *In Vitro* Coupled Transcription and Translation Reticulocyte Lysate System was optimal with 50% lysate concentration, amino acid mixture, minus Methionine (as provided by Promega) and minus Leucine, 2 µl of [^{35}S]-methionine, 1 µg/ ml of recombinant DNA, addition of RNase ribonuclease inhibitor and 24 hours exposure of SDS-PAGE to the imaging plates.

Figure 3-31 illustrates an phosphor image of translation of the four proteins using the above optimisation conditions. Fujifilm Fluorescent Image Analyzer FL-A-2000 and storage phosphor imager was used to analyse the four GST-fusion proteins and their expected size. All tracks show a fragment of the expected size, but smaller fragments are also present; these may be due to incomplete transcription or translation.

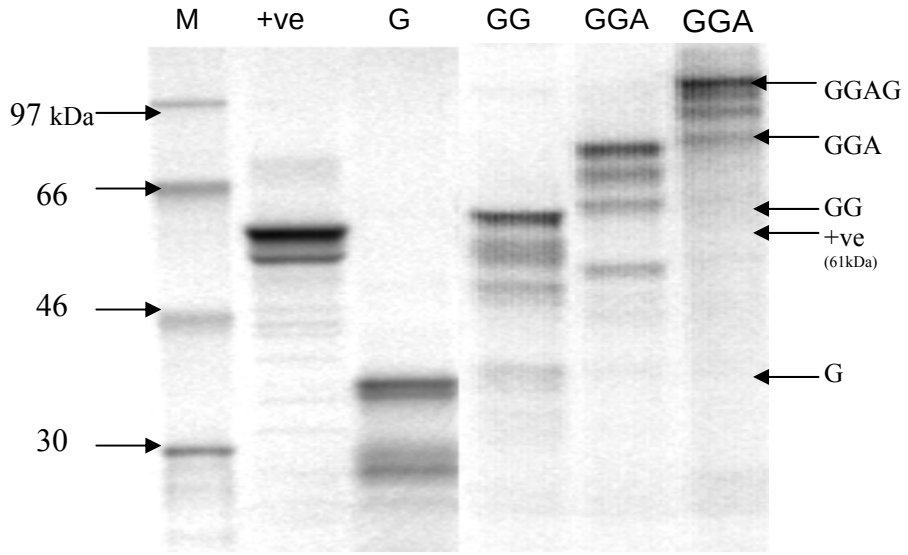

Figure 3-31 Optimal conditions to be used for expression of the GST constructs in reticuolocyte lysate. The expressed proteins in reticuolocyte lysate were separated on 4-12% SDS-PAGE and autoradiographed. Lane 1 contained the radioactive marker. Positions of 30, 46, 66 and 97 kDa for the marker are indicated on the left. Lane 2 contained firefly luciferase positive control that is approximately 61 kDa. The next four lanes contained expressed G, GG, GGA and GGAG proteins respectively.

3.5.2.3 Fluorescence Detection of Venus Protein

In this experiment purified Venus protein (Nagai *et al.* 2002) has been used as a control for estimating the lowest concentration of a yellow GFP that can be detected of yellow GFP in the rabbit reticulocyte lysate system. Serial dilutions of 20 and 200 pM and 2 nM of purified Venus protein in both water and reticulocyte lysate were added to a total volume of 500 µl distilled water. As can be seen from Figure 3-32A and B that Venus protein in water shows approximately three-fold higher intensity of fluorescence than this protein in rabbit reticulocyte lysate, and the reticulocyte lysate assay additionally has more fluctuation than when fluorescence was determined in water.

Chart A

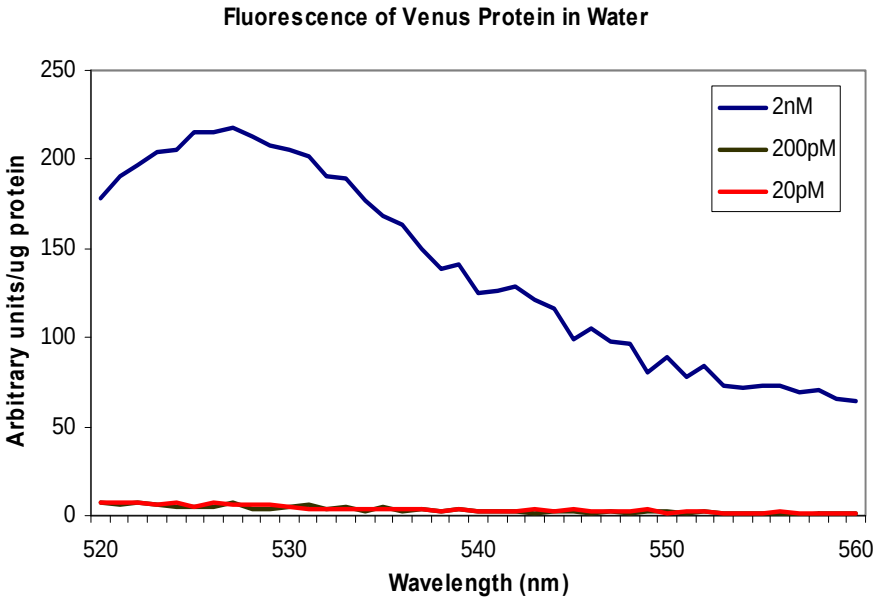

Chart B

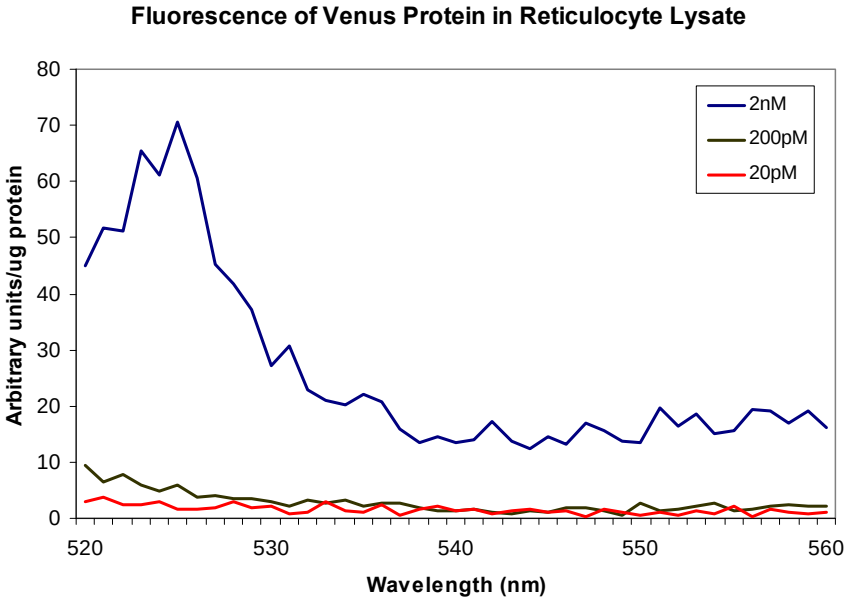

Figure 3-32A and B Charts illustrate fluorescence of the yellow Venus protein in water and reticulocyte lysate system. Chart A shows series dilution of 20 and 200 pM and 2 nM of purified Venus protein in reticulocyte lysate was added to the total volume of 500 µl distilled water. Chart B shows series dilution of 20 and 200 pM and 2 nM of purified Venus protein in 50 µl of reticulocyte lysate that added to the total volume of 500 µl distilled water. Fluorescence emission spectra were obtained with excitation at 485 nm.

3.5.2.4 Fluorescence Detection of EGFP in Reticulocyte Lysate

In order to measure the fluorescence in the translation reaction for the G, GG, GGA and GGAG proteins from reticulocyte lysate system, an emission scan was performed with excitation at 485 nm for EGFP, with an expected emission maximum at 509 nm. GG, GGA and GGAG proteins show peaks of fluorescence at about 509 nm, whereas G shows no peak (Figure 3-33). Therefore, the fluorescence that was detected from GG, GGA and GGAG proteins showed the presence of EGFP, whereas the fluorescence from G (GST only) is not showing EGFP fluorescence.

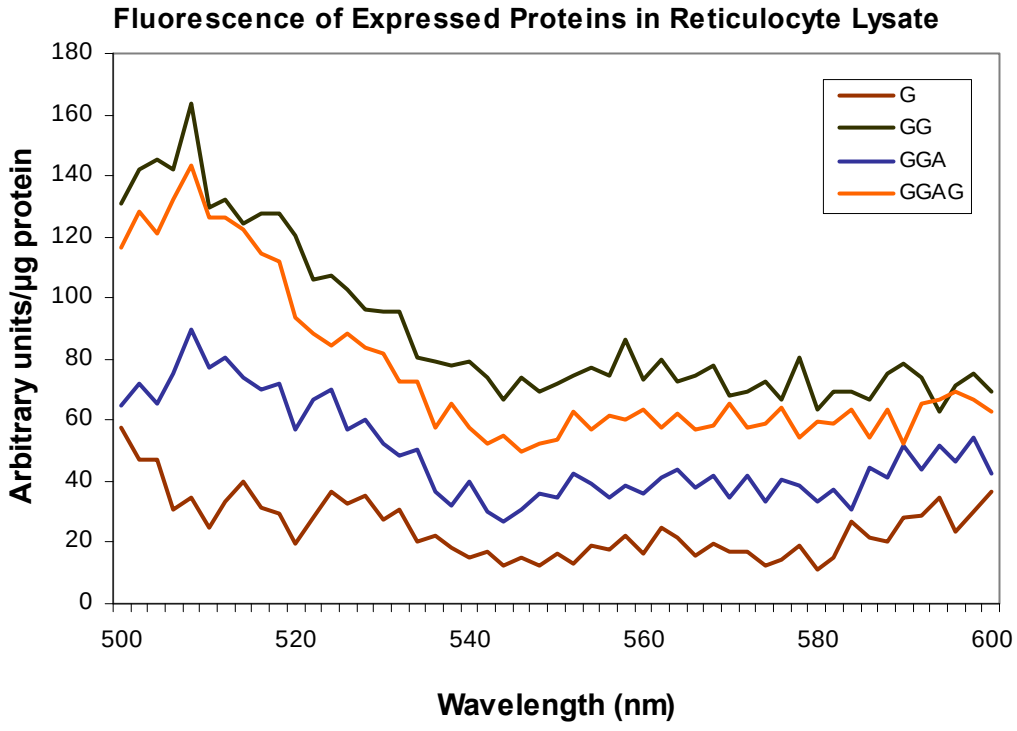

Figure 3-33 Charts illustrate fluorescence of the translated G, GG, GGA and GGAG proteins in reticulocyte lysate system. 2 nM of expressed protein in reticulocyte lysate was added to the total volume of 500 µl distilled water as described in section 2.2.3.8. Fluorescence emission spectra were obtained with excitation at 485 nm.

3.5.2.5 Binding of Recombinant AhR to [^{3}H]-TCDD

As shown in section 3.5.1.4 and Figure 3-25 soluble bacterial-expressed recombinant protein do not yield functional AhR. This is the result expected from AhR expression in bacteria but would it be the case for AhR in rabbit reticulocyte lysate system?

The GGA and GGAG proteins were expressed in *In Vitro* Coupled Transcription and Translation Rabbit Reticulocyte Lysate System. Binding assay experiment was carried out using rat liver cytosol (RLC) as an AhR-containing positive control, GG recombinant protein as a negative control and GGA and GGAG recombinant proteins. Radioactivity of [^{3}H]-TCDD was determined by liquid scintillation counting as described in section 2.2.3.12.3. Specific binding was defined as the difference between total and non-specific binding (Figure 3-34).

According to Figure 3-34 the rat liver cytosol (RLC) has approximately 28 fmols of AhR /mg of cytosolic protein, while, GGA and GGAG have approximately 20 and 19 fmols of AhR /mg of cytosolic protein. By comparing the results of the two AhR proteins GGA and GGAG with the results of positive (RLC) and negative (GG) controls, it can be said that the expression of AhR in reticulocyte lysate system produced functional protein as the AhR proteins bind to [^{3}H]-TCDD.

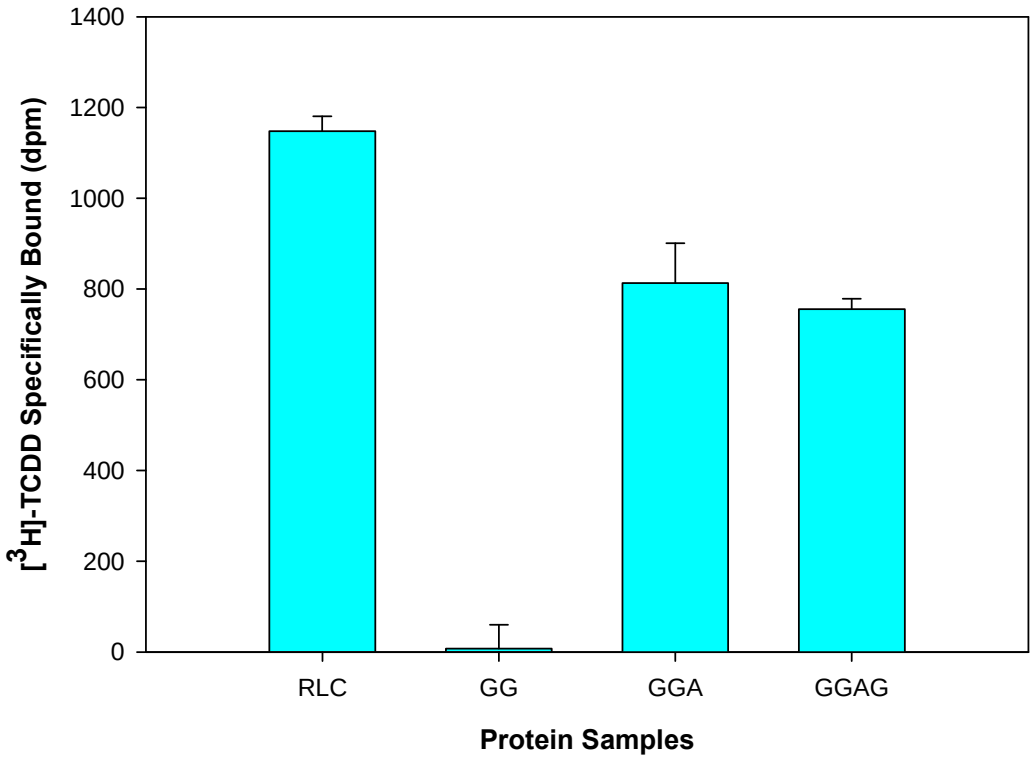

Figure 3-34 Specific binding of [^{3}H]-TCDD to recombinant AhR proteins expressed in reticuolocyte lysate. Rat liver cytosol (RLC) as a positive control, GG recombinant protein as a negative control and GGA and GGAG recombinant AhR proteins were bound to [^{3}H]-TCDD. Bound [^{3}H]-TCDD was separated from free [^{3}H]-TCDD by charcoal addition followed by centrifugation at 14,000 x g at. Then Radioactivity was determined total and non-specific binding. The substraction of the radioactivity corresponding at each non-specific binding from total binding defines [^{3}H]-TCDD specifically bound AhR. Each bar showed the average ± SD of triplicate samples.

3.5.2.6 Purification of Recombinant Proteins in Reticulocyte Lysate

The GST affinity purification method developed in section 3.5.1.3 was used to purify proteins from reticulocyte lysate. Although this purification procedure works well with the large quantities of protein produced in bacteria, purification was inadequate with the small amounts of protein produced in reticulocyte lysate (data not shown).

In order to purify the four GST-fusion proteins resulting from translation reaction of reticulocyte lysate system, Anti-GST MicroBeads Epitope Tag was used. 10 µl of G, GG, GGA and GGAG translation reactions were purified. Purified protein was eluted with 50 µl elution buffer. Only 20 µl of purified protein was separated on 4-12% SDS-PAGE. Figure 3-35 shows an autoradiograph picture of before and after purification of the G, GG, GGA and GGAG expressed proteins in reticulocyte lysate. The input and output proteins were calculated, and approximately 60 to 66% of input protein was purified.

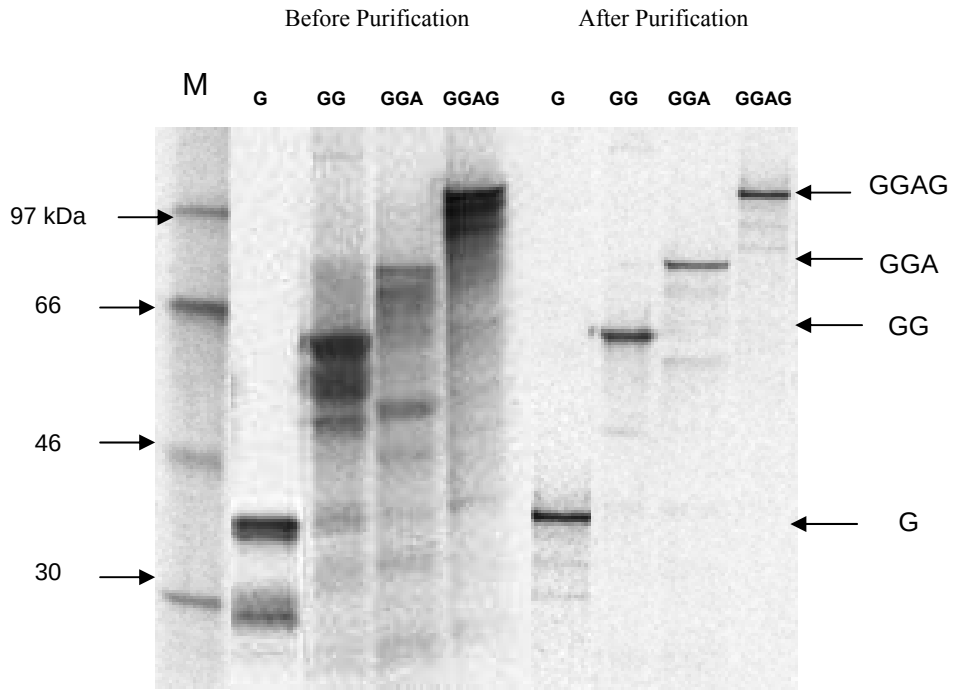

Figure 3-35 Expression and purification of the four GST-fusion proteins that expressed in reticuolocyte lysate. The four expressed proteins were purified with Anti-GST MicroBeads Apitope Tag kit, separated on 4-12% SDS-PAGE and autoradiographed as described in section 2.2.3.10.5. The first lane from the left (M) contained the radioactive marker. Positions of 30, 46, 66 and 97 kDa for the marker are indicated on the left. The next four lanes contained G, GG, GGA and GGAG proteins respectively before purification. Then the next four lanes contained G, GG, GGA and GGAG proteins respectively after purification.

3.6 Sensitivity of SYPRO Ruby Stain

One aim of this study was to see if we can detect any proteins (e.g. chaperones) bound to the AhR protein after purification from reticulocyte lysate. However, given the small amounts of protein synthesised in reticulocyte lysate, it was important to be able to detect small amounts of unlabelled protein, and this experiment set out to determine the sensitivity for detecting proteins with SYPRO ruby.

The SYPRO Ruby protein gel stain has two excitation maxima, one at ~280 nm and one at ~450 nm, and has an emission maximum near 610 nm. Proteins stained with the dye can be visualized using a 300 nm UV transilluminator. Long exposure time of the gel to the UV light during fluorescence determination might be improve the sensitivity of this stain (Smejkal *et al.* 2004). The SYPRO Ruby stain is more sensitive stain than Coomassie brillant blue stain. The amount of GST-fusion proteins produced from reticulocyte lysate is very little. Therefore, in order to determine the bottom limit for detecting GST-fusion protein, a serial concentration (1, 3, 10, 30, 100, 300 ng, and 1 and 3 μg) of the GG bacterial-expressed protein was separated on SDS-PAGE and detected by SYPRO Ruby stain. It can be seen from the Figure 3-36 that the minimum amount of GST-fusion protein can be detected was about 10 ng.

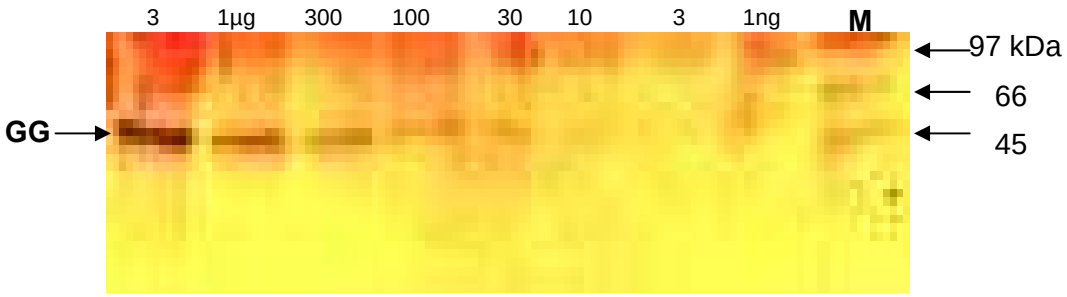

Figure 3-36 Electrophoresis of bacterially-induced GG construct. Plasmid was introduced into bacteria to produce protein. Bacteria were lysed and separated by centrifugation at 10000g for 20 minutes to yield supernatant fraction. The GG bacterial expressed protein was diluted (1, 3, 10, 30, 100, 300ng, and 1 and 3µg), separated on 16% SDS-PAGE and detected by SYPRO Ruby stain as described in section 2.2.3.6.3. The first lane from the right (M) contained 6H marker. Positions of 45, 66 and 97 kDa for the marker are indicated on the right. Other Lanes contained a serial concentration of GG proteins respectively from the right to the left.

CHAPTER 4

4. DISCUSSION

4.1 GST-fusion Protein

The Glutathione-S-Transferase (GST) gene binds specifically to immobilised glutathione, and hence allows for high affinity binding of a fusion protein for simple purification, coupled with selective elution using mild reagents (i.e. glutathione). This selective elution is highly desirable for studying protein-protein interactions. The constructs were designed using a computer application known as Vector NTI Suite 7, a software package used for *in silico* manipulation and creation of biological molecules.

Making GST constructs started when enhanced green fluorescent protein (EGFP) was coupled to the AhR.LBD, to enable fluorescence analytical techniques of ligand binding to the AhR.LBD. The resulting constructs contained EGFP-AhR.LBD and EGFP-AhR.LBD-EGFP fusions proteins, with EGFP as a control. It was routinely necessary to check the constructs by sequencing, as several constructs were found to have deletions or mutations (data not shown). In order to produce recombinant proteins these fragments were subcloned into the pET41b vector, developed for the cloning and

expression of recombinant proteins in *E. coli*. It is based on the T7 promoter-driven system originally constructed by Studier and colleagues (Moffatt 1986; Rosenberg *et al.* 1987; Studier *et al.* 1990). The pET41b vector contains the GST Tag protein (Figure 3-1). The GST constructs were made, initially verified by restriction mapping, and confirmed by sequencing to ensure the absence of aberrant constructs. This step was necessary, as aberrant constructs with e.g. frameshifts, were detected on sequencing of candidate clones (data not shown). These constructs were then to be introduced into reticulocyte lysate system that contains the cellular components necessary for protein synthesis and is known to produce functional AhR (Bell and Poland 2000; Kazlauskas *et al.* 1999). This will enable proteomic analysis of the proteins associated with the AhR.LBD.

4.2 Expression of GST-fusion Protein

4.2.1 Expression in *E. coli* BL21(DE3)pLysS

The GST-fusion proteins were expressed in *E. coli* BL21(DE3)pLysS cells as a positive control for expression, and for affinity-tag purification. At the same time, AhR expression in the BL21(DE3)pLysS cells was used to check if the GST constructs are correct or not before doing further expression in reticulocyte lysate system. Therefore, expression in the BL21(DE3)pLysS gives much larger protein yield than reticulocyte lysate system, and so it is easier and much cheaper to assay the products.

The GST constructs were induced with 1mM IPTG at 37 °C for one hour incubation, 30 °C for 3 hours or at 25 °C with overnight incubation. The time of induction is a variable in this experiment, but this is because the kinetics of bacterial growth and protein expression are markedly different at 25 and 37°C. It is not practical to use similar induction times for all three temperatures, since short times will yield inadequate production of protein at low temperature, and longer times will result in bacterial overgrowth by mutant bacteria which do not express the recombinant protein at higher temperatures.

By comparison with uninduced or IPTG-treated bacterial cultures, proteins of ~36, 66, 84 and 109 kDa were observed in induced cultures for G, GG, GGA and GGAG constructs, respectively (Figure 3.17, Figure 3.30). These were the expected size for the proteins predicted from *in silico* analysis, and confirm that the constructs had been correctly made, and were achieving induction of protein in the bacteria. Figures 3-17A and B, and 3-18 show that only the G protein was visible on SDS-PAGE in the soluble protein extract while, G, GG, GGA and GGAG proteins were visible as insoluble proteins.

Therefore, measuring the fluorescence (Figure 3-20A and B) was carried out as a sensitive method of confirming the presence of the fusion proteins that contain EGFP, i.e. GG, GGA and GGAG. The GGA construct yielded no soluble protein, as measured either by western blotting or fluorescence detection of EGFP. This insolubility was a consequence of the AhR.LBD

sequence, as the GG construct was soluble. Surprisingly, I found that the GGAG protein was soluble. This was not due to contamination of the supernatant, since the protocol for determining solubility required two sequential centrifugation steps, hence limiting the possibility that the supernatant could be contaminated by insoluble material. The second spin was in an ultracentrifuge, at 240,000 x g for 30 minutes, yielding a cytosol. This shows that the GGAG protein is indeed a soluble protein, and the efficacy of the centrifugation steps is confirmed by the fact that the GGA protein was entirely removed from the soluble fraction. The number of EGFP molecules was only the difference between the two fusion proteins. Therefore, the position of two molecules of EGFP might be affecting the folding of the AhR LBD domain in the GGAG fusion protein. Hung-Chun and his colleagues reported that the position of EGFP as the N or C-terminal fusion protein had no effect on protein solubility (Chang *et al.* 2005). In order to determine the concentration of the soluble GGAG protein in bacterial supernatants, a western blot standard curve that used serial amounts of AhR antigen (1, 3, 10, 30 and 100 ng) was performed. The concentration of AhR in the GGAG protein was estimated at approximately 0.6% of total protein (Figure 3-23).

Although the fluorescence assay specifically detected the presence of the folded EGFP domain, it was possible that the fluorescence results from proteolytic degradation of the GGAG protein, yielding a soluble EGFP, and insoluble AhR-containing protein. Because the GG, GGA and GGAG proteins might be present in the soluble fractions at low concentration, and as a result of

that SDS-PAGE may not be sensitive enough to detect these proteins. To address this problem western blot, which is a more sensitive technique, was used with an antibody raised against the mouse AhR.LBD from 285-416 amino acids. This protocol also serves to demonstrate that the expressed protein contain a sequence which is immunoreactive with the AhR Ligand-binding sequence from amino acids of 285-410 of the AhR, which was used as an antigen for raising the antiserum. Also, Figure 3-21 showed that western blot confirmed the presence of AhR protein in the AhR-constructs (GGA and GGAG) by showing clear bands of GGA and GGAG protein bacterial extracts of the expected molecular mass. This showed that the soluble AhR was full-length, and there was no evidence of degradation of the protein. Although this assay does not specifically exclude the possibility of a GFP-containing proteolysis product, the presence of a soluble protein of the correct size for GGAG provides a simple and sufficient explanation for the presence of the fluorescent signal for EGFP in the soluble bacterial extract.

It has been reported that expressed AhR in bacteria was totally insoluble, and non-functional. This could be due to failure to interact with Hsp90, leading to improper folding or aggregation of expressed AhR protein (Coumailleau *et al.* 1995). Thus the expression of soluble AhR-LBD containing protein was a surprise.

4.2.1.1 Functionality of Soluble AhR Protein Expression in Bacteria

In order to characterize further the soluble AhR LBD fusion protein expressed in bacteria, we examined its ability to bind [^{3}H]-TCDD. Rat liver cytosol was used as an AhR-containing positive control; it was found to bind approximately 10 fmols of [^{3}H]-TCDD/ mg of cytosolic protein, whereas G (not containing AhR) and GGAG protein extracts both have undetectable binding to TCDD. This is not due to inadequate amounts of soluble AhR protein in the assay; for example, rat liver has ~10-100 fmols of detectable AhR protein/ mg cytosol, whereas the bacterial GGAG extract had ~6 μg of AhR LBD per mg of total protein, or 50 pmols of AhR per mg of cytosolic protein. These results clearly indicate that the soluble GGAG protein bacterial extract shows no binding of ligand and so was not functional.

Fusion proteins are widely used as a method for improving the yield of soluble protein in bacteria (Esposito and Chatterjee 2006); however, the effectiveness of fusion proteins in enhancing solubility are accepted to be inconsistent between proteins. A systematic screen with fusing GFP to the N- or C-terminus of a variety of proteins (Dyson *et al.* 2004) showed that GFP was less effective at inducing solubility of fusion partner proteins. However, GFP is an effective reporter for protein solubility, since the solubility of GFP is required for folding, and fusion proteins that are folded at the N-terminus of GFP control its solubility and hence folding, resulting in a systematic screen for protein

solubility (Waldo *et al.* 1999). In the case of the GGA construct, the AhR LBD has conferred insolubility on the N-terminal GST and EGFP domains; this would be expected from the insolubility of the AhR LBD (Coumailleau *et al.* 1995); Dr. Tao Jiang, PhD thesis). However, in the case of the GGAG molecule, there is soluble fluorescent protein. This is likely to be the full-length GGAG protein, since this protein is detected at high level in a cytosol from induced cells, where the GGA protein is not detectable in a bacterial supernatant. There is no evidence for proteolysis in these samples, but our data do not rule out the possibility of proteolytically cleaved EGFP domains being present. The failure of the GGAG protein to bind TCDD is unlikely to be due to a failure of the experimental system, as the positive control assay detected specific binding in rat liver cytosol, demonstrating the assay to be robust. Moreover, the high levels of expression of soluble GGAG protein allowed assay of pmols of soluble GGAG protein, as compared to fmols of rat liver cytosol, and so insufficient protein binding to detect the activity is an unlikely explanation. It therefore appears that the GGAG protein is soluble, but that the LBD has not folded properly.

It would be of interest to determine if the AhR.LBD of the soluble GGAG can be folded correctly. One approach might be to coexpress chaperone proteins with this protein, to see if they could lead to folding and functionality of the protein. However, given the large number of chaperone proteins that AhR is predicted to interact with (Yao *et al.* 2004), and the uncertainties about the AhR folding pathway, it is not clear which chaperone proteins would have to

be coexpressed with this protein. An alternative possibility would be to add soluble GGAG protein to a system that is known to be capable of folding AhR to a functional form, such as a reticulocyte lysate.

4.2.1.2 Purification of Bacterial Extract Fractions

Before purification a 30 kDa Aminco Ultra-4 filter spin column was used to remove low molecular weight contaminants of bacterial extract fractions. The filtered bacterial extract was added to 50% slurry of glutathione beads. For comparison, another bacterial protein extract that was not filtered with the 30 kDa Aminco Ultra-4 filter was also added to 50% slurry of glutathione beads. Then same purification procedure was applied for both samples. Using this method the protein was successfully purified from bacterial protein extract. As can be seen in Figures 3-24A and B that only slightly more yield can be seen without using the 30 kDa Aminco Ultra-4 filter. But there was no significant difference between using and not using the 30 kDa Aminco Ultra-4 filter. These data confirm that the GST-tag system works successfully in affinity purification.

4.2.2 Expression in Rabbit Reticulocyte Lysate

4.2.2.1 Optimization of Expression of the Recombinant DNAs in Rabbit Reticulocyte Lysate

Different conditions have been used to optimise the expression of the four GST constructs in the rabbit reticulocyte lysate system (Figures 3-26 to 3-30). The amount of expressed proteins under each set of conditions was determined using the S.Tag rapid assay, as the pET41b constructs contains an S.Tag, which can be measured by a specific assay. Therefore, it can be shown that using 1 µg/ml DNA, 2 µl of [^{35}S]-methionine, addition of amino acid mixture of minus Leucine at the beginning of incubation and also using ribonuclease inhibitor, in a volume of 50 µl reaction that incubated at 30 °C for 90 minutes, are the best conditions that can be used for further experiments. We also observed that 50% of rabbit reticulocyte lysate in the *in vitro* coupled transcription and translation reaction gives better expression results than a reaction with 55% of rabbit reticulocyte lysate. Consequently, the recombinant proteins translation, which I have optimized here should become a useful tool to produce the G, GG, GGA and GGAG fusion proteins. In Figure 3-31 proteins of ~36, 66, 84 and 109 kDa were observed on autoradiogram for G, GG, GGA and GGAG constructs, respectively. Showing clear bands of GG, GGA and GGAG of the expected molecular weight is evidence of there being no proteolytic degradation of these proteins which contain EGFP, and that the proteins are of the expected molecular mass. My conclusion is that the induction of G, GG, GGA and

GGAG fusion proteins has been established in the rabbit reticulocyte lysate system.

It would be of interest to measure the fluorescence of the fusion proteins expressed in the rabbit reticulocyte lysate to confirm the presence of the fusion proteins, GG, GGA and GGAG, which contain EGFP. Venus protein has an emission in 528 nm that is not too far from EGFP in 509 nm. Therefore, yellow fluorescent Venus protein (as a control to measure the limit for detection of fluorescence) in water or reticulocyte lysate was measured using serial dilutions of 10 and 100 fmole and 1pmole. Charts A and B in Figure 3-32 show that 1 pmole of florescence protein was the limit that can be detected. Based on this result, 1pmole of each EGFP proteins (GG, GGA and GGAG) in reticulocyte lysate showed peaks at approximately 509 nm, whereas G does not because it does not contain EGFP (Figure 3-33).

4.2.2.2 Fluorescence Detection of EGFP Protein Expression in Reticulocyte Lysate

Although we detected fluorescence from EGFP-fusion proteins using fluorometer, the EGFP fluorescence for these EGFP expression proteins in reticulocyte lysate was faint compared with those proteins expressed in bacteria (Figure 3-20A and B). And Figure 3-32A and B (intensity of fluorescence protein in water was approximately 220 a.u./µg protein, whereas in reticulocyte lysate was only about 70) also can confirm that. The reason behind that may be

reticulocyte lysate (with red colour) absorbed the colour of EGFP. Another possibility would be due to a delay in experiment processing. Khan reported that fluorescence was stable for at least 3 days at 4°C (Khan *et al.* 2003). Moreover, the fluorescence charts in reticulocyte lysate situation have more fluctuation than those in case of water. This could be due to reticulocyte lysate has more proteins than bacteria.

4.2.2.3 Functionality of AhR Protein

Dioxins (e.g. 2,3,7,8-tetrachlorodibenzo-p-dioxin) are highly hydrophobic chemicals and their solubility in water is poor (approximately 0.008 ng/ml) (Adams and Blaine 1986). However, in the presence of protein, solubility of the dioxins can reach as high as 0.29 ng/ml (Poland and Glover 1976). It was therefore necessary to control for protein concentration in binding assays, as this can affect the solubility of TCDD. In this study, the recombinant AhR proteins were synthesized by *in vitro* transcription and translation in rabbit reteculocyte lysate system. The labelling of translation products with [^{35}S]-methionine yielded too much cross-talk with the [^{3}H]-channel when these samples were used for binding assay with [^{3}H]-TCDD. It has been established by several studies that 5 µl (Ducancelle *et al.* 2005) and 30 µl (Jensen and Hahn 2001) of cold transcription/ translation products (without [^{35}S]-methionine) could be used for binding with [^{3}H]-TCDD to AhR. Therefore, I performed parallel translations with and without the presence of [^{35}S]-methionine; the translations with [^{35}S]-methionine were used to check that the

reaction had been successful, and the reaction without [^{35}S]-methionine was then used for binding assays with [^{3}H]-TCDD. In this thesis 2, 5, 10 and 20 µl of cold transcription/ translation products were used for binding assay experiment. Only 20 µl showed significant specific binding of AhR protein to [^{3}H]-TCDD, whereas the 2, 5 and 10 µl reactions showed that no significant binding was detected.

Binding assay experiment was carried out as previously described in section 3.5.2.5, using rat liver cytosol as a positive control and GG protein expression in rabbit reticulocyte lysate as a negative control. When the GGA and GGAG proteins were expressed in rabbit reticulocyte lysate, they showed specific binding of approximately 20 and 19 fmols of [^{3}H]-TCDD/ mg of protein respectively (Figure 3.34). That was significantly greater than the negative control (GG) that gave undetectable binding to [^{3}H]-TCDD; the positive control also showed specific binding to TCDD. These results have established that GGA and GGAG proteins produced functional proteins, as the AhR protein bind [^{3}H]-TCDD.

It is possible to obtain quantitative results on the amount and affinity of AhR proteins (Poland *et al.* 1994), but these authors did not quantify how much of the recombinant AhR protein was functional. Although the data shows significant binding to TCDD of GGA/ GGAG proteins expressed in reticulocyte lysate, the amount of protein calculated by S.Tag rapid assay and by binding to [^{3}H]-TCDD were different. It is necessary to be clear that the

amount of [^{3}H]-TCDD added to the binding assay was in excess, and is present at a concentration ~ 3-fold greater than Kd; hence the amount of binding of [^{3}H]-TCDD should reflect the amount of functional AhR LBD present. In the case of reticulocyte lysate, the specific binding was approximately 5% of the protein concentration determined by the S.Tag rapid assay. There are numerous explanations for this discrepancy. Firstly, it is possible that there are partial length proteins produced in the reticulocyte lysate system, and that these incomplete proteins retain S.Tag activity, but not AhR functionality. Figure 3-31 (inter alia) confirms that there are incomplete translation products produced, but this data does not suggest that incomplete products account for >95% of the translated proteins. Rough estimation of the full-length proteins from Figure 3-31 suggests that the full-length constructs are >25% of the translation product. An alternative explanation is that not all of the translation products fold correctly to yield functional AhR protein; given the difficulty of obtaining high yields of functional AhR from baculovirus expression in insect cells (Dr. Tao Jiang, PhD thesis and Dr. MingQi Fan, unpublished data), this is a plausible explanation. However, it entails that less than 20%, and possibly as little as 5%, of the AhR folds correctly in a reticulocyte lysate system. Since the GGA and GGAG systems yield equivalent levels of specific binding to TCDD (Figure 3-34), it appears that C-terminal fusion of EGFP to the AhR LBD does not adversely affect folding efficiency. However, it remains possible that the N-terminal fusion of EGFP to the AhR LBD has decreased the efficiency of AhR LBD folding, either through the juxtaposition of the domains, or removal of other domains of the AhR which aid the folding of the LBD.

4.2.2.4 Purification of Reticulocyte Lysate Expressed Protein

The four GST-fusion proteins were expressed in reticulocyte lysate and were purified using GST affinity tag. Initially, the protein purification did not work well, and we proposed that this was because the reticulocyte lysate has high concentrations of glutathione, which would therefore inhibit binding of GST proteins to glutathione beads. Therefore, a buffer (50 mM KCl, 10 mM Tris (pH 7.5), 5 mM $MgCl_2$, 2 mM ATP and 10 mM sodium molybdate (pH 7.5)) was used, to get rid of the glutathione and the other low molecular weight protein by diafiltration, However, the filtration experiment failed because filter membranes blocked with the reticulocyte lysate mixture.

Under no circumstances, Bulk GST purification, Microspin GST purification and Nickel affinity chromatography methods were shown very poor yield of purified protein that was between 8 to 16 %. However using Anti-GST Microbeads Apitope Tag kit, a better yield of purified protein was obtained between 60 to 66 % of input protein purified (Figure 3-35).

4.3 Sensitivity of Protein Detection Reagent

Serial dilution of GST protein (from expression in bacteria) was separated on SDS-PAGE and detected by SYPRO Ruby protein gel stain. SYPRO Ruby stain is a fluorescent stain that more sensitive (sensitive to 1 ng of protein) than

Coomassie brilliant blue stain (to 5 ng of protein). SYPRO Ruby stain was used in this project to determine the bottom limit of concentration detecting GST-fusion proteins produced from rabbit reticulocyte lysate. This stain also can use to identify associated protein to AhR. Comparing which proteins are bound to the AhR before and after ligand-binding may identify those chaperones required for the functionality of the AhR (e.g. folding of the ligand-binding form, transport of the ligand-bound form from the cytoplasm to nucleus, etc).

Based on the results of Figure 3-36 we found that the limit for detection of the GST-fusion proteins was approximately 10 ng, this experiment need to be repeated with more precautions. For example, presence of about 68 kDa band in all lanes is a result of contamination with keratin from skin or hair. In the same time, to avoid dye cross-contamination or other artefacts and get a better result, staining containers should be thoroughly clean by rinse them with ethanol and then ultra-pure water before use. Keep containers covered all time. It is better to use polypropylene or polycarbonate containers and class dishes are not recommended.

Finally, this study has not established yet the identification and characterisation the AhR associated chaperones, because of insufficient time to complete the research. Mass spectrometry (MS method) is a powerful analytical technique that could be used to identify the AhR associated chaperones and to elucidate the structure and chemical properties of these chaperones. This can be

performed by separating the lysed cells on SDS-PAGE. The associated protein bands on the gel will be excised and sent for MS-MS sequencing. While, characterisation of ligand-binding domain may need to use new fluorescence techniques such as Fluorescence Correlation Spectroscopy (FCS) and FRET (Fluorescence Resonance Energy Transfer). FRET can be used for a double GFP construct (GGAG) to determine the polarizations of the two GFP molecules using conventional fluorescence.

CHAPTER 5

5. REFERENCES

Adams, W. J., and Blaine, K. M. (1986). A water solubility determination of 2,3,7,8-TCDD. *Chemosphere* **15**, 1397-1400.

Baxevanis, B. F., and Ouellette, F. (1998). *Bioinformatics: A Practical Guide to the Analysis of Genes and Proteins.* John Wiley and Sons, Interscience, New York.

Bayney, R. M., Morton, M. R., Favreau, L. V., and Pickett, C. B. (1989). Rat liver NAD(P)H: Quinone reductase. Regulation of quinone reductase gene expression by planar aromatic compounds and determination of the exon structure of the quinone reductase structural gene. *Journal of Biological Chemistry* **264**, 21793-7.

Bedouelle, H., and Duplay, P. (1988). Production in Escherichia coli and one-step purification of bifunctional hybrid proteins which bind maltose. Export of the Klenow polymerase into the periplasmic space. *European Journal of Biochemistry* **171**, 541-9.

Bell, D. R., and Poland, A. (2000). Binding of aryl hydrocarbon receptor (AhR) to AhR-interacting protein. The role of hsp90. *J Biol Chem* **275**, 36407-14.

Bergander, L., Wahlstrom, N., Alsberg, T., Bergman, J., Rannug, A., and Rannug, U. (2003). Characterization of *in vitro* metabolites of the aryl hydrocarbon receptor ligand 6-formylindolo[3,2-*b*]carbazole by liquid chromatography-mass spectrometry and NMR. *Drug Metab. Dispos.* **31**, 233-241.

Bigelow, S. W., Zijlstra, J. A., Vogel, E. W., and Nebert, D. W. (1985). Measurements of the cytosolic Ah receptor among four strains of Drosophila melanogaster. *Arch Toxicol* **56**, 219-25.

Birdsall, N. J., and Lazareno, S. (1997). To what extent can binding studies allow the quantification of affinity and efficacy? *Annals of the New York Academy of Sciences* **812**, 41-7.

Birnbaum, L. S. (1994). The mechanism of dioxin toxicity: relationship to risk assessment. *Environmental Health Perspectives* **102 Suppl 9**, 157-67.

Blagosklonny, M. V., Toretsky, J., Bohen, S., and Neckers, L. (1996). Mutant conformation of p53 translated *in vitro* or in vivo requires functional HSP90.

Proceedings of the National Academy of Sciences of the United States of America **93**, 8379-83.

Bose, S., T. Weikl, H. Bügl, and J. Buchner, (1996). Chaperone function of Hsp90-associated proteins. *Science* **247**, 1715-17.

Bradford, M. M., and Williams, W. L. (1976). New, Rapid, Sensitive Method For Protein Determination. **35**, 274-274.

Brejc, K., Sixma, T. K., Kitts, P. A., Kain, S. R., Tsien, R. Y., Ormo, M., and Remington, S. J. (1997). Structural basis for dual excitation and photoisomerization of the Aequorea victoria green fluorescent protein. *Proceedings of the National Academy of Sciences of the United States of America* **94**, 2306-11.

Bresnick, E. H., Dalman, F. C., and Pratt, W. B. (1990). Direct stoichiometric evidence that the untransformed Mr 300,000, 9S, glucocorticoid receptor is a core unit derived from a larger heteromeric complex. *Biochemistry* **29**, 520-7.

Bruce, A., Johnson, A., Lewis, J., Raff, M., Roberts, K., and Walters, P. (2002). *"The Shape and Structure of Proteins". Molecular Biology of the Cell;* New York and London: Garland Science.

Buchner, J. (1999). Hsp90 & Co. - a holding for folding. *Trends in Biochemical Sciences* **24**, 136-41.

Buckingham, J. C. (2006). Glucocorticoids: exemplars of multi-tasking. *British Journal of Pharmacology* **147**, S258-268.

Bukau, B., and Horwich, A. L. (1998). The Hsp70 and Hsp60 chaperone machines. *Cell* **92**, 351-66.

Burbach, K. M., Poland, A., and Bradfield, C. A. (1992). Cloning of the Ah-receptor cDNA reveals a distinctive ligand-activated transcription factor. *Proceedings of the National Academy of Sciences of the United States of America* **89**, 8185-9.

Carlstedt-Duke, J. M., Elfstrom, G., Hogberg, B., and Gustafsson, J. A. (1979). Ontogeny of the rat hepatic receptor for 2,3,7,8-tetrachlorodibenzo-p-dioxin and its endocrine indepence. *Cancer Res* **39**, 4653-6.

Carver, L. A., and Bradfield, C. A. (1997). Ligand-dependent interaction of the aryl hydrocarbon receptor with a novel immunophilin homolog in vivo. *J Biol Chem* **272**, 11452-56.

Carver, L. A., LaPres, J. J., Jain, S., Dunham, E. E., and Bradfield, C. A. (1998). Characterization of the Ah receptor-associated protein, ARA9. *J Biol Chem* **273**, 33580-7.

Chadli, A. (2000). Dimerization and n-terminal domain proximity underlie the function of the molecular chaperone heat shock protein 90. *Proc Natl Acad Sci* **A 97**, 12524-9.

Chalfie, M., and Kain, S. R. (1998). *Green Fluorescent Protein: Properties, Applications, and Protocols*. Hoboken, N.J Wiley-Liss, New York.

Chalfie, M., Tu, Y., Euskirchen, G., Ward, W., and Prasher, D. (1994). Green fluorescent protein as a marker for gene expression. *Science* **263**, 802-5.

Chan, W. K., Chu, R., Jain, S., Reddy, J. K., and Bradford, C. A. (1994). Baculovirus expression of the Ah receptor and Ah receptor nuclear translocater. Evidence for additional dioxin responsive element-binding species and factors required for signaling. *J Biol Chem.* **269**, 26464-71.

Chang, H. C., Kaiser, C. M., Hartl, F. U., and Barral, J. M. (2005). De novo folding of GFP fusion proteins: high efficiency in eukaryotes but not in bacteria. *Journal of Molecular Biology* **353**, 397-409.

Chaudhary, J., and Skinner, M. K. (1999). Basic helix-loop-helix proteins can act at the E-box within the serum response element of the c-fos promoter to influence hormone-induced promoter activation in Sertoli cells. *Molecular Endocrinology* **13**, 774-86.

Chen, H. S., and Perdew, G. H. (1994). Subunit composition of the heteromeric cytosolic aryl hydrocarbon receptor complex. *Journal of Biological Chemistry* **269**, 27554-8.

Cody, C. W., Prasher, D. C., Westler, W. M., Prendergast, F. G., and Ward, W. W. (1993). Chemical structure of the hexapeptide chromophore of the Aequorea green-fluorescent protein. *Biochemistry* **32**, 1212-18.

Coumailleau, P., Poellinger, L., Gustafsson, J. A., and Whitelaw, M. L. (1995). Definition of a minimal domain of the dioxin receptor that is associated with Hsp90 and maintains wild type ligand binding affinity and specificity. *J Biol Chem* **270**, 25291-300.

Cox, M. B., and Miller, C. A. (2002). The p23 co-chaperone facilitates dioxin receptor signaling in a yeast model system. *Toxicol Lett* **129**, 13-21.

Cox, M. B., and Miller, C. A. (2003). Pharmacological and genetic analysis of 90-kda heat shock isoprotein-aryl hydrocarbon receptor complexes. *Mol Pharmaco* **164**, 1549-56.

Crameri, A., Whitehorn, E. A., Tate, E., and Stemmer, W. P. (1996). Improved green fluorescent protein by molecular evolution using DNA shuffling. *Nature Biotechnology* **14**, 315-9.

Crews, S. T., Thomas, J. B., and Goodman, C. S. (1988). The Drosophila single-minded gene encodes a nuclear protein with sequence similarity to the per gene product. *Cell* **52**, 143-51.

Csermely, P., Schnaider, T., Soti, C., Prohaszka, Z., and Nardai, G. (1998). The 90-kDa molecular chaperone family: structure, function, and clinical applications. A comprehensive review. *Pharmacology & Therapeutics* **79**, 129-68.

Davenport, D., and Nicol, J. A. C. (1955). Luminescence of hydromedusae. *Pro. R. Soc. London Ser. B.* **144**, 399-411.

Denison, M. S., Pandini, A., Nagy, S. R., Baldwin, E. P., and Bonati, L. (2002). Ligand binding and activation of the Ah receptor. *Chem Biol Interact* **141**, 3-24.

Di Guan, C., Li, P., Riggs, P. D., and Inouye, H. (1988). Vectors that facilitate the expression and purification of foreign peptides in Escherichia coli by fusion to maltose-binding protein. *Gene* **67**, 21-30.

Dittmar, K. D., Hutchison, K. A., Owens-Grillo, J. K., and Pratt, W. B. (1996). Reconstitution of the steroid receptor.hsp90 heterocomplex assembly system of rabbit reticulocyte lysate. *Journal of Biological Chemistry* **271**, 12833-9.

Dolwick, K. M., Schmidt, J. V., Carver, L. A., Swanson, H. I., and Bradfield, C. A. (1993b). Cloning and expression of a human Ah receptor cDNA. *Mol Pharmacol* **44**, 911-7.

Dolwick, K. M., Swanson, H. I., and Bradfield, C. A. (1993a). *In vitro* analysis of Ah receptor domains involved in ligand-activated DNA recognition. *Proceedings of the National Academy of Sciences of the United States of America* **90**, 8566-70.

Ducancelle, A., Gravisse, J., Alain, S., Fillet, A. M., Petit, F., Pors, M. J., and Mazeron, M. C. (2005). Phenotypic characterisation of cytomegalovirus DNA polymerase: a method to study cytomegalovirus isolates resistant to foscarnet. *Journal of Virological Methods* **125**, 145-51.

Dyson, M. R., Shadbolt, S. P., Vincent, K. J., Perera, R. L., and McCafferty, J. (2004). Production of soluble mammalian proteins in Escherichia coli: identification of protein features that correlate with successful expression. *BMC Biotechnology* **4**, 32.

Emmons, R. B., Duncan, D., Estes, P. A., Kiefel, P., Mosher, J. T., Sonnenfeld, M., Ward, M. P., Duncan, I., and Crews, S. T. (1999). The spineless-aristapedia and tango bHLH-PAS proteins interact to control antennal and tarsal development in Drosophila. *Development* **126**, 3937-45.

Esposito, D., and Chatterjee, D. K. (2006). Enhancement of soluble protein expression through the use of fusion tags. *Current Opinion in Biotechnology* **17**, 353-8.

Fang, Y., Fliss, A. E., Rao, J., and Caplan, A. J. (1998). SBA1 encodes a yeast hsp90 cochaperone that is homologous to vertebrate p23 proteins. *Mol Cell Biol* **18**, 3727-34.

Freeman, B. C., Toft, D. O., and Morimoto, R. I. (1996). Molecular chaperone machines: chaperone activities of the cyclophilin Cyp-40 and the steroid aporeceptor-associated protein p23.[see comment]. *Science* **274**, 1718-20.

Freeman, B. C., Felts, S. J., Toft, D. O., and Yamamoto, K. R. (2000). The p23 molecular chaperones act at a late step in intracellular receptor action to differentially affect ligand efficacies. *Genes Dev* **14**, 422-34.

Fukunaga, B. N., Probst, M. R., Reisz-Porszasz, S., and Hankinson, O. (1995). Identification of functional domains of the aryl hydrocarbon receptor. *Journal of Biological Chemistry* **270**, 29270-8.

Garret, E. R., and Johnson, J. L. (1962). Selection, evaluation, and control of the assay of the pharmaceutical product. III. Statistical and economic evaluation of the three-component infrared spectrophotometric assay of aspirin anhydride. *Journal of Pharmaceutical Sciences* **51**, 767-70.

Gerner, E. W., and Schneider, M. J. (1975). Induced thermal resistance in HeLa cells. *Nature (Lond.)* **256**, 500-02.

Gething, M. (1997). *Guidebook to Molecular Chaperones and Protein-Folding Catalysts*. Oxford University Press, Oxford.

Geyer, H. J., Schramm, K. W., Feicht, E. A., Behechti, A., Steinberg, C., Bruggemann, R., Poiger, Henkelmann, and Kettrup (2002). Half-lives of tetra-, penta-, hexa-, hepta-, and octachlorodibenzo-p-dioxin in rats, monkeys, and humans-a critical review. *Chemosphere* **48**, 631-44.

Gibson, G. G., and Skett, P. (1994). *Introduction to drug metabolism*. Blackie Acad. & Prof., London.

Gonzalez, F. J., and Fernandez-Salguero, P. (1998). The aryl hydrocarbon receptor: studies using the AHR-null mice. *Drug Metabolism & Disposition* **26**, 1194-8.

Gram, T. E. (1994). *Metabolism of drugs*. Little, Brown, Boston.

Gu, Y. Z., Hogenesch, J. B., and Bradfield, C. A. (2000). The PAS superfamily: sensors of environmental and developmental signals. *Annu Rev Pharmacol Toxicol* **40**, 519-61.

Hahn, M., E., S., Karchner, S. I., Shapiro, M. A., and Perera, S. A. (1997). Molecular evolution of two vertebrate aryl hydrocarbon (dioxin) receptors (AHR1 and AHR2) and the PAS family. *Proceedings of the National Academy of Sciences of the United States of America* **94**, 13743-8.

Hahn, M. E. (1998). The aryl hydrocarbon receptor: a comparative perspective. *Comparative Biochemistry & Physiology Part C Pharmacology, Toxicology, Endocrinology* **121**, 23-53.

Hahn, M. E. (2002). Aryl Hydrocarbon Receptors: Diversity and Evolution. *Chemico-Biological Interactions* **141**, 131-160.

Hankinson, O. (1995). The aryl hydrocarbon receptor complex. *Annu Rev Pharmacol Toxicol* **35**, 307-40.

Hartl, F. (1996). Molecular chaperones in cellular protein folding. *Nature (Lond.)* **381**, 571-80.

Hayashi, R., Wada, H., Ito, K., and Adcock, I. M. (2004). Effects of glucocorticoids on gene transcription. *European Journal of Pharmacology* **500**, 51-62.

Heminger, K. A., Hartson, S. D., Rogers, J., and Matts, R. L. (1997). Cisplatin inhibits protein synthesis in rabbit reticulocyte lysate by causing an arrest in elongation. *Archives of Biochemistry & Biophysics* **344**, 200-07.

Hoffman, E. C., Reyes, H., Chu, F. F., Sander, F., Conley, L. H., Brooks, B. A., and Hankinson, O. (1991). Cloning of a factor required for activity of the Ah (dioxin) receptor. *Science* **252**, 954-8.

Holloway, M. (1994). Dioxin indictment. A growing body of research links the compound to cancer. *Scientific American* **270**, 25.

Hulme, E. C., and Birdsall, N. J. M. (1992). *Strategy and tactics in receptor binding studies, in Receptor Ligand Interactions: A Practical Approach*. Oxford University Press, New York.

Hutzinger, O., Choudhry, G. G., Chittim, B. G., and Johnston, L. E. (1985). Formation of polychlorinated dibenzofurans and dioxins during combustion, electrical equipment fires and PCB incineration. *Environmental Health Perspectives* **60**, 3-9.

Ingemar, K. (1963). *In Vitro* Diagnosis of Pregnancy. an Agglutination-Inhibition Test For Demonstration of Human Chorionic Gonadotropins Used In A Series of Patients. *Nordisk Medicin* **70**, 1289-92.

Inouye, S., and Tsuji, F. (1994). Aequorea green fluorescent protein. Expression of the gene and fluorescence characteristics of the recombinant protein. *FEBS Lett* **341**, 277-80.

Jain, S., Dolwick, K. M., Schmidt, J. V., and Bradfield, C. A. (1994). Potent transactivation domains of the Ah receptor and the Ah receptor nuclear translocator map to their carboxyl termini. *Journal of Biological Chemistry* **269**, 31518-24.

Jakob, U., and Buchner, J. (1994). Assisting spontaneity: the role of Hsp90 and small Hsps as molecular chaperones. *Trends in Biochemical Sciences* **19**, 205-11.

Jensen, B. A., and Hahn, M. E. (2001). cDNA cloning and characterization of a high affinity aryl hydrocarbon receptor in a cetacean, the beluga, Delphinapterus leucas. *Toxicological Sciences* **64**, 41-56.

Jeremy, M. B., John, L. T., and Lubert, S. (2002). *"3. Protein Structure and Function". Biochemistry*. San Francisco: W.H. Freeman.

Johnson, J. L., and Toft, D. O. (1994). A novel chaperone complex for steroid receptors involving heat shock proteins, immunophilins and p23. *J. Biol. Chem.* **269**, 24989-93.

Kahn, T. W., Beachy, R. N., and Falk, M. M. (1997). Cell-free expression of a GFP fusion protein allows quantitation *in vitro* and in vivo. *Current Biology* **7**, R207-208.

Kazlauskas, A., Poellinger, L., and Pongratz, I. (1999). Evidence that the co-chaperone p23 regulates ligand responsiveness of the dioxin (Aryl hydrocarbon) receptor. *J Biol Chem* **274**, 13519-24.

Kazlauskas, A., Poellinger, L., and Pongratz, I. (2000). The immunophilin-like protein XAP2 regulates ubiquitination and subcellular localization of the dioxin receptor. *Journal of Biological Chemistry* **275**, 41317-24.

Kazlauskas, A., Sundstrom, S., Poellinger, L., and Pongratz, I. (2001). The hsp90 chaperone complex regulates intracellular localization of the dioxin receptor. *Mol Cell Biol.* **7**, 2594-607.

Khan, F., Stott, K., and Jackson, S. (2003). 1H, 15N and 13C backbone assignment of the green fluorescent protein (GFP). *Journal of Biomolecular NMR* **26**, 281-82.

Kim, J. S., and Raines, R. T. (1993). Ribonuclease S-peptide as a carrier in fusion proteins. *Protein Science* **2**, 348-56.

Kimura, S., Kozak, C. A., and Gonzalez, F. J. (1989). Identification of a novel P450 expressed in rat lung: cDNA cloning and sequence, chromosome mapping, and induction by 3-methylcholanthrene. *Biochemistry* **28**, 3798-803.

Korkalainen, M., Tuomisto, J., and Pohjanvirta, R. (2004). Primary Structure and Inducibility by 2,3,7,8- Tetrachlorodibenzo-p-Dioxin (TCDD) of Aryl hydrocarbon Receptor Repressor in A TCDD-Sensitive and A TCDD-Resistant Rat Strain. *Biochem. Biophys. Res. Commun.* **315**, 123-31.

Kumar, M. B., Ramadoss, P., Reen, R. K., Vanden Heuvel, J. P., and Perdew, G. H. (2001). The Q-rich subdomain of the human Ah receptor transactivation domain is required for dioxin-mediated transcriptional activity. *Journal of Biological Chemistry* **276**, 42302-10.

Kuzhandaivelu, N., Cong, Y. S., Inouye, C., Yang, W. M., and Seto, E. (1996). XAP2, a novel hepatitis B virus X-associated protein that inhibits X transactivation. *Nucleic Acids Res* **24**, 4741-50.

Lai, B.-T., N. W. Chin, A. E. Stanek, W. Keh, and K. W. Lanks (1984). Quantitation and intracellular localization of the 85K heat shock protein by using monoclonal and polyclonal antibodies. *Mol. Cell. Biol.* **4**, 2802-10.

Landers, J. P., and Bunce, N. J. (1991). The Ah receptor and the mechanism of dioxin toxicity. *Biochem J* **276 (Pt 2)**, 273-87.

LaPres, J. J., Glover, E., Dunham, E. E., Bunger, M. K., and Bradfield, C. A. (2000a). ARA9 modifies agonist signaling through an increase in cytosolic aryl hydrocarbon receptor. *Journal of Biological Chemistry* **275**, 6153-9.

LaPres, J. J., Glover, E., Dunham, E. E., Bunger, M. K., and Bradfield, C. A. (2000b). ARA9 modifies agonist signaling through an increase in cytosolic aryl hydrocarbon receptor. *J Biol Chem* **275**, 6153-9.

Lindquist, S., and Kim, G. (1996). Heat-shock protein 104 expression is sufficient for thermotolerance in yeast. *Proc Natl Acad Sci.* **93**, 5301-06.

Lodish, H. F. (2004). *Molecular Cell Biology*. W H Freeman & Co (Sd).

Lucier, G. W., Portier, C. J., and Gallo, M.A (1993). Receptor mechanisms and dose response models for the effects of dioxins. *Env. Health Pers.* **101**, 36-44.

Ma, Q., and Whitlock, J. P., Jr. (1997). A novel cytoplasmic protein that interacts with the Ah receptor, contains tetratricopeptide repeat motifs, and

augments the transcriptional response to 2,3,7,8-tetrachlorodibenzo-p-dioxin. *J Biol Chem* **272**, 8878-84.

Marcus, J. R. (1990). *The Jew in the Medieval World: A Source Book*. Cincinnati, Ohio: Hebrew Union College Press.

Meyer, B. K., Pray-Grant, M. G., Vanden Heuvel, J. P., and Perdew, G. H. (1998). Hepatitis B virus X-associated protein 2 is a subunit of the unliganded aryl hydrocarbon receptor core complex and exhibits transcriptional enhancer activity. *Molecular & Cellular Biology* **18**, 978-88.

Meyer, B. K., and Perdew, G. H. (1999). Characterization of the ahr-hsp90-xap2 core complex and the role of the immunophilin-related protein xap2 in ahr stabilization. *Biochemistry* **38**, 8907-17.

Meyer, B. K., Petrulis, J. R., and Perdew, G. H. (2000). Aryl hydrocarbon (Ah) receptor levels are selectively modulated by hsp90-associated immunophilin homolog XAP2. *Cell Stress & Chaperones* **5**, 243-54.

Miller, C. A. (2002). Anticholinergics: the good and the bad. *Geriatric Nursing* **23**, 286-7.

Mimura, J., and Fujii-Kuriyama, Y. (2005). Molecular mechanisms of AhR functions in the regulation of cytochrome P450 genes. *Biochem. Biophys. Res. Commun.* **338**, 311-17.

Moffatt, B. A. a. S., F.W. (1986). Use of bacteriophage T7 RNA polymerase to direct selective high-level expression of cloned genes. *J. Mol. Biol.* **189**, 113-130.

Morise, H., Shimomura, O., Johnson, F., and Winant, J. (1974). Intermolecular energy transfer in the bioluminescent system of Aequorea. *Biochemistry* **13**, 2656-62.

Mullis, K., Faloona, F., Scharf, S., Saiki, R., Horn, G., and Erlich, H. (1986). Specific enzymatic amplification of DNA in vitro: the polymerase chain reaction. *Cold Spring Harbor Symposia on Quantitative Biology* **51 Pt 1**, 263-73.

Murphy, P. J., Morishima, Y., Chen, H., Galigniana, M. D., Mansfield, J. F., Simons, S. S., Jr., and Pratt, W. B. (2003). Visualization and mechanism of assembly of a glucocorticoid receptor.Hsp70 complex that is primed for subsequent Hsp90-dependent opening of the steroid binding cleft. *Journal of Biological Chemistry* **278**, 34764-73.

Nagai, T., Ibata, K., Park, E. S., Kubota, M., Mikoshiba, K., and Miyawaki, A. (2002). A variant of yellow fluorescent protein with fast and efficient maturation for cell-biological applications.[see comment]. *Nature Biotechnology* **20**, 87-90.

Nair, S. C., Rimerman, R. A., Toran, E. J., Chen, S., Prapapanich, V., Butts, R. N., and Smith, D. F. (1997). Molecular cloning of human FKBP51 and comparisons of immunophilin interactions with Hsp90 and progesterone receptor. *Molecular & Cellular Biology* **17**, 594-603.

Nebert, D. W., Puga, A., and Vasiliou, V. (1993). Role of the Ah receptor and the dioxin-inducible [Ah] gene battery in toxicity, cancer, and signal transduction. *Annals of the New York Academy of Sciences* **685**, 624-640.

Nilsson, B., Moks, T., Jansson, B., Abrahmsen, L., Elmblad, A., Holmgren, E., Henrichson, C., Jones, T. A., and Uhlen, M. (1987). A synthetic IgG-binding domain based on staphylococcal protein A. *Protein Engineering* **1**, 107-13.

Ormo, M., Cubitt, A. B., Kallio, K., Gross, L. A., Tsien, R. Y., and Remington, S. J. (1996). Crystal structure of the Aequorea victoria green fluorescent protein.[see comment]. *Science* **273**, 1392-5.

Owens-Grillo, J. K., Hoffmann, K., Hutchison, K. A., Yem, A. W., Deibel, M. R., Jr., Handschumacher, R. E., and Pratt, W. B. (1995). The cyclosporin A-

binding immunophilin CyP-40 and the FK506-binding immunophilin hsp56 bind to a common site on hsp90 and exist in independent cytosolic heterocomplexes with the untransformed glucocorticoid receptor. *Journal of Biological Chemistry* **270**, 20479-84.

Owens-Grillo, J. K., Czar, M. J., Hutchison, K. A., Hoffmann, K., Perdew, G. H., and Pratt, W. B. (1996). A model of protein targeting mediated by immunophilins and other proteins that bind to hsp90 via tetratricopeptide repeat domains. *Journal of Biological Chemistry* **271**, 13468-75.

Palm, G. J., Zdanov, A., Gaitanaris, G. A., Stauber, R., Pavlakis, G. N., and Wlodawer, A. (1997). The structural basis for spectral variations in green fluorescent protein. *Nature Structural Biology* **4**, 361-5.

Pedelacq, J.-D., Cabantous, S., Tran, T., Terwilliger, T. C., and Waldo, G. S. (2006). Engineering and characterization of a superfolder green fluorescent protein.[erratum appears in Nat Biotechnol. 2006 Sep;24(9):1170]. *Nature Biotechnology* **24**, 79-88.

Perdew, G. H., and Bradfield, C. A. (1996). Mapping the 90 kda heat shock protein binding region of the ah receptor. *Biochem Mol Biol Int* **39**, 589-93.

Perdew, G. H., and Poland, A. (1988). Purification of the Ah receptor from C57BL/6J mouse liver. *J Biol Chem* **263**, 9848-52.

Perozzo, M. A., Ward, K. B., Thompson, R. B., and Ward, W. W. (1988). X-ray diffraction and time-resolved fluorescence analyses of Aequorea green fluorescent protein crystals. *Journal of Biological Chemistry* **263**, 7713-6.

Peterson, R. E., Theobald, H. M., and Kimmel, G. L. (1993). Developmental and reproductive toxicity of dioxins and related compounds: cross-species comparisons. *Critical Review in Toxicology* **23**, 283-335.

Pitot, H. C., Goldsworthy, T., Campbell, H. A., and Poland, A. (1980). Quantitative evaluation of the promotion by 2,3,7,8-tetrachlorodibenzo-p-dioxin of hepatocarcinogenesis from diethylnitrosamine. *Cancer Res* **40**, 3616-20.

Poland, A., and Glover, E. (1976). Stereospecific, High Binding Affinity of 2,3,7,7-Tetrachlorodibenzo-p-dioxin by Hepatic Cytosol. *J.Biol.Chem* **251**, 4936-46.

Poland, A., and Glover, E. (1979). An estimate of the maximum in vivo covalent binding of 2,3,7,8-tetrachlorodibenzo-p-dioxin to rat liver protein, ribosomal RNA, and DNA. *Cancer Research* **39**, 3341-4.

Poland, A., Glover, E., Ebetino, F. H., and Kende, A. S. (1986). Photoaffinity labeling of the Ah receptor. *J. Biol. Chem.* **261**, 6352-65.

Poland, A., Glover, E., and Taylor, B. A. (1987). The murine Ah locus: a new allele and mapping to chromosome 12. *Molecular Pharmacology* **32**, 471-8.

Poland, A., and Knutson, J. C. (1982). 2,3,7,8-tetrachlorodibenzo-p-dioxin and related halogenated aromatic hydrocarbons: examination of the mechanism of toxicity. *Annu. Rev. Pharmacol. Toxicol.* **22**, 517-54.

Poland, A., Palen, D., and Glover, E. (1994). Analysis of the four alleles of the murine aryl hydrocarbon receptor. *Molecular Pharmacology* **46**, 915-21.

Pongratz, I., Mason, G. G., and Poellinger, L. (1992). Dual roles of the 90-kDa heat shock protein hsp90 in modulating functional activities of the dioxin receptor. Evidence that the dioxin receptor functionally belongs to a subclass of nuclear receptors which require hsp90 both for ligand binding activity and repression of intrinsic DNA binding activity. *J Biol Chem.* **267**, 13728-34.

Powell-Coffman, J. A., Bradfield, C. A., and Wood, W. B. (1998). Caenorhabditis elegans orthologs of the aryl hydrocarbon receptor and its heterodimerization partner the aryl hydrocarbon receptor nuclear translocator. *Proceedings of the National Academy of Sciences of the United States of America* **95**, 2844-9.

Pratt, W. B., Galigniana, M. D., Morishima, Y., and Murphy, P. J. (2004). Role of molecular chaperones in steroid receptor action. *Essays Biochem* **40**, 41-58.

Pratt, W. B., Morishima, Y., Murphy, M., and Harrell, M. (2006). Chaperoning of glucocorticoid receptors. *Handbook of Experimental Pharmacology*, 111-38.

Pratt, W. B., and Toft, D. O. (1997). Steroid receptor interactions with heat shock protein and immunophilin chaperones. *Endocr Rev* **18**, 306-60.

Pratt, W. B., and Toft, D. O. (2003). Regulation of signaling protein function and trafficking by the hsp90/hsp70-based chaperone machinery. *Exp Biol Med (Maywood)* **228**, 111-33.

Prokipcak, R. D., Faber, L. E., and Okey, A. B. (1989). Characterization of the Ah receptor for 2,3,7,8-tetrachlorodibenzo-p-dioxin: use of chemical crosslinking and a monoclonal antibody directed against a 59-kDa protein associated with steroid receptors. *Archives of Biochemistry & Biophysics* **274**, 648-58.

Radanyi, C., Chambraud, B., and Baulieu, E. E. (1994). The ability of the immunophilin FKBP59-HBI to interact with the 90-kDa heat shock protein is encoded by its tetratricopeptide repeat domain. *Proceedings of the National Academy of Sciences of the United States of America* **91**, 11197-201.

Ratajczak, T., Carrello, A., Mark, P. J., Warner, B. J., Simpson, R. J., Moritz, R. L., and House, A. K. (1993). The cyclophilin component of the unactivated estrogen receptor contains a tetratricopeptide repeat domain and shares identity with p59 (FKBP59). *Journal of Biological Chemistry* **268**, 13187-92.

Rexin, M., Busch, W., Segnitz, B., and Gehring, U. (1988). Tetrameric structure of the nonactivated glucocorticoid receptor in cell extracts and intact cells. *FEBS Letters* **241**, 234-8.

Richter, K., and Buchner, J. (2001). Hsp90: chaperoning signal transduction. *J Cell Physiol* **188**, 281-90.

Rosenberg, A. H., Lade, B. N., Chui, D. S., Lin, S. W., Dunn, J. J., and Studier, F. W. (1987). Vectors for selective expression of cloned DNAs by T7 RNA polymerase. *Gene* **56**, 125-35.

Rowlands, J. C., and Gustafsson, J. A. (1997). Aryl hydrocarbon receptor-mediated signal transduction. *Crit Rev Toxicol* **27**, 109-34.

Safe, S. H. (1986). Comparative toxicology and mechanism of action of polychlorinated dibenzo-p-dioxin and dibenzofurans. *Ann. Rev. Pharm. Tox.* **26**, 371-99.

Sanger, F., Nicklen, S., and Coulson, A. R. (1977). DNA sequencing with chain-terminating inhibitors. *Proceedings of the National Academy of Sciences of the United States of America* **74**, 5463-7.

Schmidt, J. V., and Bradfield, C. A. (1996). Ah receptor signaling pathways. *Annu. Rev. Cell Dev. Biol.* **12**, 55-89.

Schwetz, B. A., Norris, J. M., Sparschu, G. L., Rowe, U. K., Gehring, P. J., Emerson, J. L., and Gerbig, C. G. (1973). Toxicology of chlorinated dibenzo-p-dioxins. *Environ Health Perspect* **5**, 87-99.

Shimada, T., Hayes, C. L., Yamazaki, H., Amin, S., Hecht, S. S., Guengerich, F. P., and Sutter, T. R. (1996). Activation of chemically diverse procarcinogens by human cytochrome P-450 1B1. *Cancer Res.* **56**, 2979-84.

Shimomura, O., Johnson, F. H., and Saiga, Y. (1961). Purification and properties of Cypridina luciferase. *Journal of Cellular & Comparative Physiology* **58**, 113-23.

Siemering, K. R., Golbik, R., Sever, R., and Haseloff, J. (1996). Mutations that suppress the thermosensitivity of green fluorescent protein. *Current Biology* **6**, 1653-63.

Smejkal, G. B., Robinson, M. H., and Lazarev, A. (2004). Comparison of fluorescent stains: relative photostability and differential staining of proteins in two-dimensional gels. *Electrophoresis* **25**, 2511-9.

Smith, A. H., Matheson, D. P., and Fisher, D. O. (1981). Preliminary report of reproductive outcomes among pesticide applicators using 2,4,5-T. *NZ Med J.* **93**, 177-79.

Smith, D. B., and Johnson, K. S. (1988). Single-step purification of polypeptides expressed in Escherichia coli as fusions with glutathione S-transferase. *Gene* **67**, 31-40.

Smith, D. F., Faber, L. E., and Toft, D. O. (1990). Purification of unactivated progesterone receptor and identification of novel receptor-associated proteins. *J. Biol. Chem.* **265**, 3996-4003.

Smith, G. E., Ju, G., Ericson, B. L., Moschera, J., Lahm, H. W., Chizzonite, R., and Summers, M. D. (1985). Modification and secretion of human interleukin 2 produced in insect cells by a baculovirus expression vector. *Proc. Nat. Acad. Sci., USA.* **82**, 8404-8.

Studier, F. W., Rosenberg, A. H., Dunn, J. J., and Dubendorff, J. W. (1990). Use of T7 RNA polymerase to direct expression of cloned genes. *Methods in Enzymology* **185**, 60-89.

Sullivan, W., Stensgard, B., Caucutt, G., Bartha, B., McMahon, N., Alnemri, E. S., Litwack, G., and Toft, D. (1997a). Nucleotides and two functional states of hsp90. *J Biol Chem* **272**, 8007-12.

Sullivan, W., Stensgard, B., Caucutt, G., Bartha, B., McMahon, N., Alnemri, E. S., Litwack, G., and Toft, D. (1997b). Nucleotides and two functional states of hsp90. *J Biol Chem* **272**, 8007-12.

Tai, P. K., Albers, M. W., Chang, H., Faber, L. E., and Schreiber, S. L. (1992). Association of a 59-kilodalton immunophilin with the glucocorticoid receptor complex. *Science* **256**, 1315-8.

Tatemichi, M., Nomura, S., Ogura, T., Sone, H., Nagata, H., and Esum, H. (1999). Mutagenic activation of environmental carcinogens by microsomes of gastric mucosa with intestinal metaplasia. *Cancer Res.* **59**, 3893-98.

Townsend, J. C., Bodner, K. M., Van Peenen, P. F., Olson, R. D., and Cook, R. R. (1982). Survey of reproductive events of wives of employees exposed to chlorinated dioxins. *American Journal of Epidemiology* **115**, 695-713.

Tschirley, F. H. (1986). Dioxin. *Scientific American* **254**, 29-35.

Tsien, R. Y., and Prasher, D. C. (1997). *In GFP: Green Fluorescent Protein Strategies and Applications*. M Chalfie, S Kain, Wiley & Sons, New York.

Vanden Berg, M., Birnbaum, L. S., Denison, M., De Vito, M., Farland, W., Feeley, M., Fiedler, H., Hakansson, H., Hanberg, A., Haws, L., Martin Rose, L., Safe, S., Schrenk, D., Tohyama, C., Tritscher, A., Tuomisto, J., Tysklind, M., Walker, N., E., R., and Peterson, E. (2006). The 2005 World Health Organization Reevaluation of Human and Mammalian Toxic Equivalency Factors for Dioxins and Dioxin-Like Compounds. *Toxicology Science* **93**, 223-241.

Vanden Heuvel, J. P., and Lucier, G. (1993). Environmental toxicology of polychlorinated dibenzo-p-dioxins and polychlorinated dibenzofurans. *Environ Health Perspect.*, 189-200.

Vaughn, J. L., Goodwin, R. H., Tompkins, G. J., and McCawley, P. (1977). The establishment of two cell lines from the insect Spodoptera frugiperda (Lepidoptera; Noctuidae). *In Vitro* **13**, 213-7.

Waldo, G. S., Standish, B. M., Berendzen, J., and Terwilliger, T. C. (1999). Rapid protein-folding assay using green fluorescent protein.[see comment]. *Nature Biotechnology* **17**, 691-5.

Walker, C. H. (2001). *Major organic pollutants Organic pollutants, an ecotoxicological perspective.* Taylor & Francis, London.

Warner, B. J., and McArthur, G. A. (2001). Cancer and the genetic revolution. *Australian Family Physician* **30**, 933-6.

Welch, W. J., and Brown, C. R. (1996). Influence of molecular and chemical chaperones on protein folding.[see comment][erratum appears in Cell Stress Chaperones 1996 Sep;1(3):207]. *Cell Stress & Chaperones* **1**, 109-15.

Whitelaw, M. L., McGuire, J., Picard, D., Gustafsson, J. A., and Poellinger, L. (1995). Heat shock protein hsp90 regulates dioxin receptor function in vivo. *Proc Natl Acad Sci U S A* **92**, 4437-41.

Whitlock, J. P., Jr., Okino, S. T., Dong, L., Ko, H. P., Clarke-Katzenberg, R., Ma, Q., and Li, H. (1996). Cytochromes P450 5: induction of cytochrome P4501A1: a model for analyzing mammalian gene transcription. *FASEB Journal* **10**, 809-18.

Yao, G., Craven, M., Drinkwater, N., and Bradfield, C. A. (2004). Interaction networks in yeast define and enumerate the signaling steps of the vertebrate aryl hydrocarbon receptor. *Plos Biology* **2**, E65.

Zhang, G., Gurtu, V., and Kain, S. R. (1996). An Enhanced Green Fluorescent Protein Allows Sensitive Detection of Gene Transfer in Mammalian Cells. *Biochemical and Biophysical Research Communications* **227**, 707-11.

Zimmer, M. (2002). Green fluorescent protein (GFP): applications, structure, and related photophysical behavior. *Chemical Reviews* **102**, 759-81.

http://en.wikipedia.org/wiki/Aryl_hydrocarbon_receptor

http://www.ejnet.org/dioxin/

https://www.asms.org/whatisms/index.html